University of Alberta

FINITE-AMPLITUDE INSTABILITY OF TIME-VARYING FRONTAL GEOSTROPHIC CURRENTS

by

Mattea R. Turnbull 

A thesis submitted to the Faculty of Graduate Studies and Research
in partial fulfillment of the requirements for the degree of
Master of Science

in

Applied Mathematics

Department of Mathematical and Statistical Sciences
Edmonton, Alberta
Fall 2006

Your file Votre référence
ISBN: 978-0-494-22391-8
Our file Notre référence
ISBN: 978-0-494-22391-8

ABSTRACT

A weakly nonlinear theory is developed for marginally stable or unstable, time varying frontal geostrophic currents on sloping topography with dissipation. The evolution of frontal geostrophic currents is modelled by the use of the two layer system of coupled differential equations derived in Swaters (1993). This model allows us to account for the large amplitude variations in the upper layer fluid thickness. Linear stability theory is used to generate two marginal stability curves. Following this, we include nonlinear terms and study the evolution of a weakly unstable, time varying, wedge front. Dissipation terms are then introduced. Upon expanding our equations asymptotically, we introduce slow time and large space parameters, and derive an amplitude equation describing the slow time evolution of the amplitude of the normal mode perturbations. The resulting equation is then solved numerically for a selection of parameter values.

ACKNOWLEDGEMENT

First and foremost I would like to thank my supervisor, Dr. Gordon Swaters, for his direction and support during the completion of my calculations and the production of this manuscript.

I would also like to thank my mother and father, Geraldine and John Mitchell, and my in-laws, Carmen and Richard Turnbull, for their support and encouragement throughout the completion of this thesis. I would like to thank fellow graduate students Seung Ji Ha and Mika Kashiwagi for our discussions of GFD, and most importantly, for their friendship and company.

Last, but not least, I have to thank my husband, Joe, for his encouragement, patience and understanding - and for his love.

Table of Contents

List of Tables

List of Figures

Chapter 1

Introduction

Fronts play an important role in ocean circulation, acting to hinder horizontal heat and momentum transfer, while aiding vertical transfer (Cushman-Roisin, 1986). As well, they are a significant source of *available potential energy* (the portion of the total potential energy which is available for transformation to kinetic energy), which may be released in the form of eddies and rings (Cushman-Roisin, 1986). Fronts are geostrophic, ie., the leading order velocity is determined by a balance between pressure gradients and the Coriolis effect (Robinson, 1983). In addition, fronts are defined as regions having large horizontal density gradients. These gradients are so large that often the depth variation of an *isopycnic* (a surface of constant density) will be of the order of the isopycnic depth (Roden, 1975). Thus, one is not able to apply the classic quasigeostrophic model (as in Pedlosky (1987, §3)) which requires the assumption of small isopycnal deflections.

There are two approaches that may be taken when dealing large horizontal density gradients. The first approach is to analyse the full primitive equations (see, for example, Griffiths et al. (1982); Killworth (1983); Paldor (1983a,b); Killworth et al. (1984); Paldor and Killworth (1987); Paldor and Ghil (1990)). There are drawbacks to this approach, one of these stemming from the difficulty in generalizing the primitive equation solutions to large scale open ocean fronts (as discussed in Karsten and Swaters (2000); Benilov

and Reznik (1996)). In fact, such models neglect the β-effect, which plays a significant role in frontal evolution (Rhines, 1975). It is valuable to fully understand such effects in the context of our simplified models as a means of enriching our understanding of what is seen when dealing with the more complex fully ageostrophic models. This brings us to the second approach.

In the second approach, we make note of the fact that the flows can be geostrophic with large amplitude if their length scales are larger than the Rossby radius of deformation (Phillips, 1963). Such flows are called *large amplitude geostrophic* (LAG) flows. As noted in Karsten and Swaters (2000), there are many examples of ocean fronts and motions for which length scales exceed the Rossby deformation radius, including Rossby waves (Chelton and Schlax, 1996), mesoscale ocean eddies (Olson et al., 1985), and various North Pacific fronts (Roden, 1975; Ikeda and Emery, 1984; Ikeda et al., 1984).

The simplest frontal model is the reduced gravity model with an outcropping interface (as described in Cushman-Roisin (1986)). In this model, only the top layer is taken to be active, with surface and interface boundaries intersecting along one or more lines. These lines are termed *outcrop lines*, with each outcrop line representing a surface front. A drawback of this model was demonstrated by Killworth et al. (1984) who showed that, if there is motion introduced in a second layer, the stability properties of the front are significantly changed.

Cushman-Roisin (1986) applied this reduced gravity model to a monotonic front with spatially varying potential vorticity. Solving the linear stability problem, while keeping only leading order ageostrophic terms, they showed the front to be unconditionally linearly stable. This leads us to conclude that baroclinic processes and/or higher order ageostrophic effects may need to be added into the model in order for instabilities to be generated. This has been noted by Benilov (1992, 1995), Benilov and Cushman-Roisin (1994), and, Slomp and Swaters (1997).

Swaters (1993) extended the Cushman-Roisin (1986) model by the inclusion of baroclinic processes and a sloping bottom. Quasigeostrophic methods

were used to model the dynamics of the underlying slope water, which take into account a background vorticity gradient due to the sloping bottom. Here, Swaters (1993) deals with LAG flows. There is a coupling of the two layers via the process of baroclinic vortex-tube stretching of the perturbed density driven current. They were able to show that, in the barotropic limit of the linear stability problem, all fronts are linearly stable in the sense of Liapunov. Thus, the instabilities of the baroclinic model are not simply baroclinically modified versions of previously derived modes, but instead they represent a new class of instabilities not previously discussed (Swaters, 1993).

Reszka (1997) and Reszka and Swaters (1999), used the Swaters (1993) model to study the baroclinic dynamics of buoyancy driven surface flows over a sloping bottom. The authors derived an amplitude equation which was used to examine the growth of perturbations in an idealized, marginally unstable steady, parallel shear flow. They found that the perturbations oscillate in time as a result of the interaction between linear and nonlinear terms, and found conditions for which the flow exhibits explosive growth. The authors then introduced slow time and large space parameters, which lead to a space dependent amplitude equation, which was solved, providing an analytical nonlinear wave-packet stability theory for a marginally unstable flow.

The purpose of this thesis is to establish a weakly nonlinear theory for a marginally stable or unstable, *time varying* frontal geostrophic current on sloping topography with *dissipation.* We extend the research of Reszka (1997) and Reszka and Swaters (1999) by the inclusion of time variability and dissipation terms, using the methods described in Pedlosky and Thomson (2003). The model used in this thesis is a two-layer system of LAG surface currents over a sloping bottom. An amplitude equation analogous to that of Reszka (1997) and Reszka and Swaters (1999) is derived. This amplitude equation is seen to have the same form as that derived for the Phillips model by Pedlosky and Thomson (2003).

This thesis is outlined as follows. In Chapter 2, we derive the governing equations for a two layer shallow water system. The fluid is taken to be in-

compressible and inviscid, and we are working in a rotating reference frame. We will perform a scale analysis, which will allow us to apply the hydrostatic relation, and remedy the problem of geostrophic degeneracy. Upon simplifying the resulting equations in the one layer case, with use of the hydrostatic relation, we will expand our system to two layers, each having a different density. This will provide us with mass conservation and continuity equations for each layer, as well as a reduced gravity equation, which relates the two pressures.

Next, we nondimensionalize our equations using the scalings of Swaters (1993). After asymptotically expanding our variables about a small scaled slope parameter, we will match terms having the same magnitude, which gives us a series of equations. After performing some algebraic manipulations, we will arrive at the governing equations of the Swaters (1993) model. We will also repeat the calculation starting with the equations of conservation for potential vorticity in each layer, obtaining the same result.

In Chapter 3, we derive the linear stability equations. These are derived by writing the height and pressure variables as a mean part plus a perturbation part. We then set the mean flow in the lower layer to be zero in order to prevent barotropic shear instabilities, which enables us to focus on the pure baroclinic problem. Also, we assume the steady solution for the upper layer thickness to be of the form of a simple wedge. We then obtain stability conditions by examining the averaged-energy form of the linearized upper layer equation, following the derivation from Swaters (1993). This allows us to find a necessary condition for perturbation growth, and a sufficient condition to inhibit that growth.

Next, we perform a normal mode analysis by first assuming that the perturbation field is a superposition of waves. It is known that an instability in the flow arises when a perturbation grows in time. We will determine when instability occurs by noting that the perturbations will grow in time if the imaginary part of the complex-valued phase velocity is positive. We substitute our normal mode equations into the linear stability equations, perform an order analysis, and neglect all terms above a particular order. This leads

us to a pair of coupled ordinary differential equations for our perturbation amplitudes. After subsequent calculations, we arrive at a dispersion relation. We then establish a sufficient condition for stability, and therefore, a necessary condition for instability. We then determine equations for the marginal stability curves, which are curves lying on the boundary between stability and instability. We note that there are two curves in our case, which we call the Upper and Lower Branches of the Marginal Stability Curve (MSC). Having these two marginal stability curves results in a unique critical slope and phase velocity value for each of the Upper and Lower Branches. We also determine a high frequency cutoff, which is a cutoff of the total wavenumber above which the flow is always stable.

In Chapter 4, we will study the evolution of a wedge front which is weakly unstable, ie. the nonlinear terms are small but nonnegligible. By assuming that the perturbation is initially small, and expanding our equations asymptotically, we are able to derive an amplitude equation describing the slow time evolution of the perturbation. In deriving our amplitude equation, we will follow Pedlosky (1987).

First, we begin by adding in dissipation terms, which are chosen to be proportional to the perturbation potential vorticity. This form for the dissipation, first introduced by Klein and Pedlosky (1992), is a purely heuristic choice that assumes that smaller scale turbulence acts directly to degrade the larger scale potential vorticity (Klein and Pedlosky, 1992).

We next add in a wedge front and scale our variables by the wedge slope parameter. We then introduce a perturbation into the critical slope parameter. Depending on the sign of this perturbation term, we will either have a sub- or a super- criticality. In the region of supercriticality, the critical slope parameter is perturbed from the marginal stability curve into the unstable region, giving us marginally unstable solutions, while, in the region of subcriticality, it is perturbed into the stable region, giving us marginally stable solutions. In the case where the sign of the perturbation term is both positive and negative, we have regions of super- and sub- criticality: that is, regions of marginal

instability with regions of marginal stability.

This follows the calculations of Reszka (1997), however, here we introduce a time variability parameter into the critical slope perturbation. We then rederive the dispersion relation with our new slope parameter. A scale analysis on the complex part of the slope parameter gives us the order of our growth rate. We introduce slow time and large space parameters, and expand our perturbation functions in asymptotic series. We then derive the the $O(1)$, $O(s)$, and $O(s^2)$ equations from this expansion. This leads us to our amplitude equation, which is a coupled set of ordinary differential equations.

Then, we will derive the Lorenz equivalent of our amplitude equation in the case where there is no time variability in the perturbations and the perturbation amplitude is real-valued. This will allow us to show that the observation of nontrivial time dependence in our solutions is due to the presence of the time-varying component of the perturbations.

The slow space term is dropped in Chapter 5. After first deriving the Reszka (1997) solution, we obtain solutions on the Lower Branch with the addition of either a sub- or super- criticality and time variability, while keeping dissipation zero. We then examine plots of these solutions and discuss their properties. Next, we choose five cases to explore with dissipation included, representing a selection of curve shapes. We discuss the magnitude of dissipation required for each curve shape in order to observe significant damping.

In Chapter 6, we summarize and analyse our results; as well as making concluding remarks, and suggestions for further research.

Chapter 2

Derivation of the Governing Equations

2.1 Introduction

In this chapter, we will derive the governing equations for a two layer shallow water system. The fluid is taken to be incompressible and inviscid, and we are working in a rotating reference frame. In the leading order problem, we will see that the curl of the pressure gradient is zero, and the curl of the Coriolis acceleration is the divergence of the geostrophic velocity, which is almost zero. Thus, when we take the curl of the equations of motion, the problem is trivially satisfied to leading order. This is called *geostrophic degeneracy* (Pedlosky, 1987, §2.10).

Due to geostrophic degeneracy, we will see that there are more unknowns than there are equations in the leading order problem. To deal with this, we will perform a scale analysis which will allow us to apply the hydrostatic relation. In addition, we will apply the *rigid lid approximation.* The rigid lid approximation is used where surface displacements are small compared to interface displacements; it approximates the free surface as being fixed (Gill, 1982, §6.3). Upon simplifying the resulting equations in the one layer case with use of the hydrostatic relation, we expand our system to two layers,

each having different density. This gives us mass conservation and continuity equations for each layer, as well as a reduced gravity equation which relates the two pressures.

Next, we nondimensionalize our equations using the scalings of Swaters (1993). After asymptotically expanding our variables about some small parameter, we match terms having the same magnitude, which gives us a series of equations. These equations are evaluated up to the point where we are able to determine the leading order behaviour of our unknown quantities. Performing some algebraic manipulations, we arrive at the governing equations of the Swaters (1993) model. We also repeat the calculation starting with the equations of conservation for potential vorticity in each layer, obtaining the same result.

2.2 The Two-Layer Shallow Water Equations

Starting with the inviscid, incompressible Navier-Stokes equations for a constant density fluid, we will derive the shallow water equations upon which our model is based. We start by deriving equations for the one layer model, and then expand the system to two layers of differing density. In the case of the one layer model, we examine a channel of fluid bounded between walls at $y = 0$ and $y = L$, unbounded in the x-direction, and with depth $h(x, y, t)$ (as seen in Figure 2.1). That is, x is the along channel coordinate, y is the across channel coordinate, and z the vertical height.

The Navier-Stokes equations for conservation of momentum and mass take the form

$$\mathbf{u}_t + (\mathbf{u} \cdot \boldsymbol{\nabla})\mathbf{u} + f(\mathbf{k} \times \mathbf{u}) = -\frac{1}{\rho}\boldsymbol{\nabla} p - \mathbf{k}g, \tag{2.1}$$

$$\boldsymbol{\nabla} \cdot \mathbf{u} = 0. \tag{2.2}$$

where we have the fluid velocity, $\mathbf{u}(x, y, z, t) = (u, v, w)$, with u, v, and w representing the along-channel, cross-channel and vertical velocity components respectively, ρ the fluid density, $p(x, y, z, t)$ the total pressure, $\boldsymbol{\nabla} = (\partial_x, \partial_y, \partial_z)$ the gradient operator, and $\mathbf{k}$ the unit vector normal to the earth's surface.

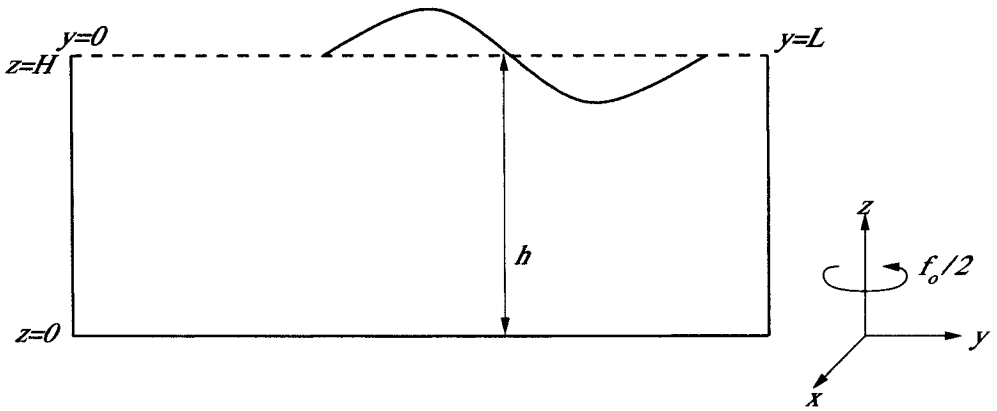

Figure 2.1: Model geometry for the one-layer model.

We take into account the rotation of the earth by the inclusion of the Coriolis parameter f. We will assume that our phenomena occur over a region with small enough spatial extent such that f will not vary significantly from its value at a mean latitude, θ_0. Therefore, we apply the f-plane approximation, defining f to be $f_0 = 2\Omega\sin(\theta_0)$, where $\Omega = 2\pi$ radians/day. In the oceans, the f-plane approximation is considered appropriate if the horizontal length scale is less than 100 km (Pond and Pickard, 1983), which is the case here.

It will be more convenient in our derivations to work with the component forms of (2.1) and (2.2),

$$u_t + uu_x + vu_y + wu_z - fv = -\frac{1}{\rho}p_x, \tag{2.3}$$

$$v_t + uv_x + vv_y + wv_z + fu = -\frac{1}{\rho}p_y, \tag{2.4}$$

$$w_t + uw_x + vw_y + ww_z = -\frac{1}{\rho}p_z - g, \tag{2.5}$$

$$u_x + v_y + w_z = 0. \tag{2.6}$$

To simplify our calculations, we introduce scalings for all of the variables. We represent our horizontal and vertical length scales by H and L, respectively. For example, for the Gulf Stream, L is of order 100 km and H is of order 1

km (Pond and Pickard, 1983). The aspect ratio, A_r, is then given by $A_r = \frac{H}{L}$, where $A_r << 1$ on the scales given above.

We scale the horizontal velocities by U and the vertical velocity by W. We note that, in the Gulf Stream, U is of order 1 m s^{-1} (Pond and Pickard, 1983). Writing the continuity equation (2.2) with scalings underneath, we get

$$u_x + v_y + w_z = 0. \tag{2.7}$$

$$\frac{U}{L} \quad \frac{U}{L} \quad \frac{W}{H}$$

Taking w_z to scale like u_x and v_y, we see that

$$W = \frac{UH}{L} = A_r U. \tag{2.8}$$

Applying our scalings to the vertical momentum equation, we obtain

$$w_t + uw_x + vw_y + ww_z = -\frac{1}{\rho}p_z - g, \tag{2.9}$$

$$\frac{W}{T} \quad \frac{UW}{L} \quad \frac{UW}{L} \quad \frac{WW}{H}$$

where T is taken to be the advective time scale, $T = \frac{L}{U}$. There are two natural time scales in the governing equations - the inertial time scale, f^{-1}, and the advective time scale, $\frac{L}{U}$. In the theory we develop here, it is assumed that $T = \frac{L}{U} << f^{-1}$.

All of the terms on the left hand side of equation (2.9) scale as $O\left(\frac{HU^2}{L^2}\right)$, implying the relation

$$-\frac{1}{\rho}p_z - g = O\left(\frac{HU^2}{L^2}\right). \tag{2.10}$$

Taking our rough ocean values for H,U, and L from above gives us a value for $\frac{HU^2}{L^2}$ of order 10^{-7} m/s^2. Noting that the gravitational acceleration, g, is of order 10 m/s^2, the pressure gradient term must balance with the gravitational term, giving us the hydrostatic relation,

$$p_z = -\rho g. \tag{2.11}$$

Integrating this relation with respect to z, and applying the boundary condition $p(x, y, h, t) = p_o$, where p_o is a constant, gives us

$$p = \rho g(h - z) + p_o. \tag{2.12}$$

Thus, the horizontal gradient of p takes the form

$$\nabla_H p = \rho g(h_x, h_y), \tag{2.13}$$

where ∇_H is used to denote the horizontal gradient. We see that the horizontal pressure gradient is independent of z. This suggests that, if u and v are initially independent of z, they may stay independent of z, ie. $u_z = v_z = 0$ for all $t \geq 0$.

Next, we consider a two layer model with each model layer having a different density, as shown in Figure 2.2. We denote the upper layer thickness by $h(x, y, t)$, and the two-layer thickness by H. In addition, we introduce a deformation of the fluid surface, denoted by $\eta(x, y, t)$, and a sloping bottom, with slope $-s$. The labels '1' and '2' denote the upper layer and the lower layer, respectively. We assume each layer to have constant density, and that the pressure must be continuous across the interface, ie. $p_1 = p_2$ at $z = H - h$. This allows us to form pressure equations by use of (2.11). The pressures in the upper and lower layers are given by

$$p_1 = \rho_1 g(H + \eta - z), \tag{2.14}$$

$$p_2 = \rho_1 g(h + \eta) + \rho_2 g(H - h - z). \tag{2.15}$$

We now develop the continuity equation for our two layer shallow water model. We will use the notation ∇ to denote the horizontal gradient operator, (∂_x, ∂_y), and $D/Dt = \partial_t + \mathbf{u} \cdot \nabla$ to denote the total derivative with respect to time of any property following individual fluid elements, where $\mathbf{u}$ represents the velocity in the layer under consideration. We require that fluid parcels on the surface, and on the interface between layers, remain there for all time. This provides us with the following kinematic conditions for layer 1

$$w_1 = \frac{D}{Dt}(H + \eta) \text{ on } z = H + \eta, \tag{2.16}$$

$$w_1 = \frac{D}{Dt}(H - h) \text{ on } z = H - h.$$

Since $\eta << H$ in our investigations, we will impose the rigid lid approximation by approximating $H + \eta$ by H. This reduces (2.16) to

$$w_1 = 0 \text{ on } z = H. \tag{2.17}$$

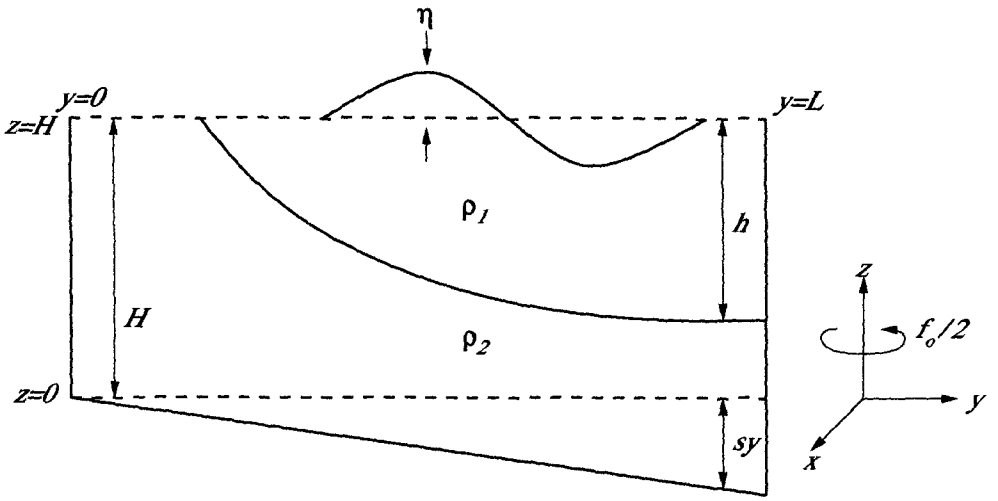

Figure 2.2: Model geometry for the two-layer model.

Next, we integrate the continuity equation (2.2), with respect to z, over the upper layer,

$$\int_{H-h}^{H} u_{1x} + v_{1y} + w_{1z}\, dz = 0, \tag{2.18}$$

which yields the equation,

$$(u_{1x} + v_{1y})(H - (H - h)) + w_1(x, y, H, t) - w_1(x, y, H - h, t) = 0. \tag{2.19}$$

Applying equation (2.16) gives us

$$(u_{1x} + v_{1y})h + \frac{D}{Dt}h = 0. \tag{2.20}$$

Simplifying gives us our kinematic condition for the upper layer,

$$h_t + \nabla \cdot (\mathbf{u}_1 h) = 0. \tag{2.21}$$

The kinematic condition for the lower layer is obtained similarly. We note that the upper and lower boundaries of the abyssal layer are at $z = H - h$ and $z = -sy$, respectively. Since the flow component perpendicular to the bottom must be zero, we have

$$sv_2 + w_2 = 0 \text{ on } z = -sy. \tag{2.22}$$

For our second equation, we will again have

$$w_2 = \frac{D}{Dt}(H-h) \text{ on } z = H-h. \tag{2.23}$$

Integrating the continuity equation (2.2), with respect to z, over the lower layer, we get

$$\int_{-sy}^{H-h} u_{2x} + v_{2y} + w_{2z}\, dz = 0, \tag{2.24}$$

which evaluates to,

$$(u_{2x} + v_{2y})(H - h - (-sy)) + w_2(x, y, H-h, t) - w_2(x, y, -sy, t) = 0. \tag{2.25}$$

Applying equations (2.22) and (2.23) gives us

$$(u_{2x} + v_{2y})(H - h + sy) + \partial_t(H-h) + \mathbf{u}_2 \cdot \boldsymbol{\nabla}(H-h) + sv_2 = 0, \tag{2.26}$$

or equivalently,

$$\boldsymbol{\nabla} \cdot \mathbf{u}_2(H - h + sy) - \partial_t h - \mathbf{u}_2 \cdot \boldsymbol{\nabla} h + sv_2 = 0. \tag{2.27}$$

Simplifying gives us our kinematic condition for the lower layer,

$$h_t + \boldsymbol{\nabla} \cdot [\mathbf{u}_2(h - sy - H)] = 0. \tag{2.28}$$

We will now summarize our derivations. Asterisks are introduced to denote dimensional variables. The momentum equations and kinematic conditions for our two layer model are

$$\mathbf{u}_{1t}^* + (\mathbf{u}_1^* \cdot \boldsymbol{\nabla}^*)\mathbf{u}_1^* + f_o(\mathbf{k} \times \mathbf{u}_1^*) = -g\boldsymbol{\nabla}^*\eta^*, \tag{2.29}$$

$$h_t^* + \boldsymbol{\nabla}^* \cdot (\mathbf{u}_1^* h^*) = 0, \tag{2.30}$$

$$\mathbf{u}_{2t}^* + (\mathbf{u}_2^* \cdot \boldsymbol{\nabla}^*)\mathbf{u}_2^* + f_o(\mathbf{k} \times \mathbf{u}_2^*) = -\frac{1}{\rho_2}\boldsymbol{\nabla}^*\tilde{p_2}^*, \tag{2.31}$$

$$h_t^* + \boldsymbol{\nabla}^* \cdot [\mathbf{u}_2^*(h^* - s^*y^* - H)] = 0, \tag{2.32}$$

where

$$\tilde{p_2}^* = \rho_1 g\eta^* - \rho_2 g' h^*, \tag{2.33}$$

and g' is the reduced gravity $g(\rho_2 - \rho_1)/\rho_2 > 0$.

2.3 Scalings for the Two Layer Shallow Water Equations

We now scale our dimensional variables to obtain the Swaters (1993) model. Henceforth, all non-asterisked variables will be nondimensional. First, we define the parameter δ as

$$\delta = \frac{\bar{h}}{H}, \tag{2.34}$$

where $\bar{h}$ is a representative thickness of the upper layer and H is a scale for the total fluid depth. Qualitatively, δ is measure of the magnitude of vortex tube stretching in the lower layer, which is caused by a perturbed upper layer (Swaters, 1993). We now scale our horizontal spatial coordinates by

$$(x^*, y^*) = L(x, y), \tag{2.35}$$

where $L = \delta^{-1/4}R$, and $R = \sqrt{g'\bar{h}}/f_o$ is the internal *Rossby radius of deformation* for the upper layer. The Rossby radius of deformation is the horizontal scale for which rotation effects balance buoyancy effects (Gill, 1982, §7.5). This scaling acts to ensure we achieve a balance between the Coriolis and pressure gradient terms in our final equations.

We take a subinertial time scale,

$$t^* = \frac{t}{f_o\delta}, \tag{2.36}$$

since the processes under consideration occur on a time scale for which the rotation of the earth is important (ie. the time scale will be much longer than the period of the rotation of the earth). We scale the upper layer thickness as

$$h^* = \bar{h}h, \tag{2.37}$$

where $\bar{h} = \delta H$.

Next we will derive the scaling for $\mathbf{u_2}$. *Vortex tube stretching* is the dominant process driving lower layer dynamics. The magnitude of vorticity production from vortex tube stretching is δf_o (Swaters, 1993). The relative vorticity

of layer two, $v^*_{x^*} - u^*_{y^*}$, must balance the production of vorticity from vortex tube stretching. Since relative vorticity scales as U/L, we must have U/L balancing with δf_o. Solving for the velocity scale, U, gives us

$$\mathbf{u}^*_2 = \delta f_o L \mathbf{u}_2. \tag{2.38}$$

The upper layer scaling is taken to be,

$$\mathbf{u}^*_1 = \delta^{\frac{1}{2}} f_o L \mathbf{u}_1. \tag{2.39}$$

As discussed in Swaters (1993), these scalings are required as a result of the isopycnal deflections being $O(1)$.

Requiring the flow to be geostrophic to leading order causes η and p to scale as

$$\eta^* = \delta^{\frac{1}{2}} \frac{(f_o L)^2}{g} \eta, \tag{2.40}$$

$$\tilde{p}^*_2 = \rho_2 \delta (f_o L)^2 p. \tag{2.41}$$

Finally, we scale the slope parameter,

$$s^* = \frac{\bar{h}}{L} s. \tag{2.42}$$

As will be seen further on, this results in the bottom slope parameter being of the same order of magnitude as the relative vorticity.

2.4 Governing Equations

Applying the scalings derived in §2.3 to equations (2.29) through (2.33), we get the nondimensional two layer shallow water equations,

$$\delta \mathbf{u}_{1t} + \delta^{\frac{1}{2}}(\mathbf{u}_1 \cdot \boldsymbol{\nabla})\mathbf{u}_1 + \mathbf{k} \times \mathbf{u}_1 + \boldsymbol{\nabla}\eta = \mathbf{0}, \tag{2.43}$$

$$\delta^{\frac{1}{2}} h_t + \boldsymbol{\nabla} \cdot (\mathbf{u}_1 h) = 0, \tag{2.44}$$

$$\delta \mathbf{u}_{2t} + \delta(\mathbf{u}_2 \cdot \boldsymbol{\nabla})\mathbf{u}_2 + \mathbf{k} \times \mathbf{u}_2 + \boldsymbol{\nabla} p = \mathbf{0}, \tag{2.45}$$

$$\boldsymbol{\nabla} \cdot \mathbf{u}_2 = \delta h_t + \delta \boldsymbol{\nabla} \cdot [\mathbf{u}_2(h - sy)], \tag{2.46}$$

$$\eta = h + \delta^{\frac{1}{2}} p, \tag{2.47}$$

where terms of order g'/g have been neglected in (2.47) since we are assuming that $\rho_2 - \rho_1$ is small when compared to ρ_2. This is consistent with the rigid lid approximation. We assume an asymptotic expansion of the form

$$(\mathbf{u}_1, \mathbf{u}_2, h, p, \eta) = (\mathbf{u}_1, \mathbf{u}_2, h, p, \eta)^{(0)} + \delta^{\frac{1}{2}}(\mathbf{u}_1, \mathbf{u}_2, h, p, \eta)^{(1)} + O(\delta), \tag{2.48}$$

and substitute it into equations (2.43) through (2.47). We will start by developing our lower layer governing equations.

Expanding the variables in (2.45) gives us the leading order equation,

$$\mathbf{k} \times \mathbf{u}_2^{(0)} + \boldsymbol{\nabla} p^{(0)} = \mathbf{0}, \tag{2.49}$$

or, equivalently,

$$\mathbf{u}_2^{(0)} = \mathbf{k} \times \boldsymbol{\nabla} p^{(0)} = (-p_y^{(0)}, p_x^{(0)}). \tag{2.50}$$

Thus, to leading order, the lower layer velocity is geostrophically determined.

In order to develop an equation for the time evolution of p, we start by writing down (2.45) in its component form,

$$\delta(u_{2t} + u_2 u_{2x} + v_2 u_{2y}) - v_2 + p_x = 0, \tag{2.51}$$

$$\delta(v_{2t} + u_2 v_{2x} + v_2 v_{2y}) + u_2 + p_y = 0. \tag{2.52}$$

Taking the curl (ie. $-\frac{\partial}{\partial y}(2.51) + \frac{\partial}{\partial x}(2.52)$) we get,

$$\begin{aligned} &\delta(v_{2x} - u_{2y})_t + \delta(u_{2x}v_{2x} + u_2 v_{2xx} - u_{2y}u_{2x} - u_2 u_{2xy} \\ &+ v_{2x}v_{2y} + v_2 v_{2xy} - v_{2y}u_{2y} - v_2 u_{2yy}) + u_{2x} + v_{2y} = 0. \end{aligned} \tag{2.53}$$

By defining a new variable, $\xi = v_{2x} - u_{2y}$, where ξ is the relative vorticity for the lower layer, this can be rewritten as,

$$\delta\xi_t + \delta(u_2\xi_x + v_2\xi_y + u_{2x}\xi + v_{2y}\xi) + u_{2x} + v_{2y} = 0. \tag{2.54}$$

This expression can be compacted further by employing the total derivative notation,

$$\delta\frac{D\xi}{Dt} + (1 + \delta\xi)\nabla \cdot \mathbf{u}_2 = 0. \tag{2.55}$$

Isolating for the divergence of $\mathbf{u}_2$ in the mass conservation equation (2.46) gives us

$$\nabla \cdot \mathbf{u}_2 = \delta h_t + \delta\nabla \cdot [\mathbf{u}_2(h - sy)], \tag{2.56}$$

which is then substituted into (2.55) to get

$$\delta\frac{D\xi}{Dt} + (1 + \delta\xi)(\delta h_t + \delta\nabla \cdot [\mathbf{u}_2(h - sy)]) = 0. \tag{2.57}$$

Now, we expand the variables using (2.48), and divide through by δ,

$$\frac{D\xi^{(0)}}{Dt} + (1 + \delta\xi^{(0)})\Big(h_t^{(0)} + \nabla \cdot \mathbf{u}_2^{(0)}h^{(0)} + \mathbf{u}_2^{(0)} \cdot \nabla(h^{(0)} - sy)\Big) = 0, \tag{2.58}$$

where $\xi^{(0)} = v_{2x}^{(0)} - u_{2y}^{(0)}$, which becomes

$$\xi^{(0)} = \Delta p^{(0)}, \tag{2.59}$$

after applying $(u_2^{(0)}, v_2^{(0)}) = (-p_y^{(0)}, p_x^{(0)})$, where we have used the Laplacian operator $\Delta = \partial_{xx} + \partial_{yy}$. Note that we have restricted ourselves to writing the first term of each expansion, as this will be sufficient. The $O(1)$ problem is given by

$$\frac{D}{Dt}\Delta p^{(0)} + h_t^{(0)} + \nabla \cdot \mathbf{u}_2^{(0)}h^{(0)} + \mathbf{u}_2^{(0)} \cdot \nabla(h^{(0)} - sy) = 0, \tag{2.60}$$

where $D/Dt = \partial_t + \mathbf{u}^{(0)} \cdot \nabla$. We note that, since sy is independent of time, we can write $(h^{(0)} - sy)_t$ instead of $h_t^{(0)}$. Also, the third term drops out, since $\nabla \cdot \mathbf{u}_2^{(0)} = -p_{yx}^{(0)} + p_{xy}^{(0)} = 0$. Thus, (2.60) reduces to

$$\frac{D}{Dt}(\Delta p^{(0)} + h^{(0)} - sy) = 0. \tag{2.61}$$

We now make use of the Jacobian operator,

$$J(A,B) = A_x B_y - A_y B_x, \tag{2.62}$$

to write our governing equation for layer 2 as

$$(\Delta p^{(0)} + h^{(0)})_t + J(p^{(0)}, \Delta p^{(0)} + h^{(0)} - sy) = 0. \tag{2.63}$$

Now we will derive our governing equation for the upper layer. Upon expanding the variables in the momentum equation (2.43), and applying (2.47), we get the $O(1)$ equation

$$\mathbf{u}_1^{(0)} = \mathbf{k} \times \boldsymbol{\nabla} h^{(0)}, \tag{2.64}$$

which tells us that the leading order velocity is geostrophic. To derive an equation for the time evolution of h, we again start by writing down the momentum equation (2.43) in component form,

$$\delta u_{1t} + \delta^{\frac{1}{2}}(u_1 u_{1x} + v_1 u_{1y}) - v_1 + \eta_x = 0, \tag{2.65}$$

$$\delta v_{1t} + \delta^{\frac{1}{2}}(u_1 v_{1x} + v_1 v_{1y}) + u_1 + \eta_y = 0. \tag{2.66}$$

Taking the curl, and setting $\zeta = v_{1x} - u_{1y}$,

$$\delta \zeta_t + \delta^{\frac{1}{2}}(u_1 \zeta_x + v_1 \zeta_y + u_{1x}\zeta + v_{1y}\zeta) + u_{1x} + v_{1y} = 0, \tag{2.67}$$

which then simplifies to

$$\delta \zeta_t + \delta^{\frac{1}{2}} \mathbf{u}_1 \cdot \boldsymbol{\nabla} \zeta + (1 + \delta^{\frac{1}{2}}\zeta) \boldsymbol{\nabla} \cdot \mathbf{u}_1 = 0. \tag{2.68}$$

Rearranging the continuity equation (2.44) gives us

$$\boldsymbol{\nabla} \cdot \mathbf{u}_1 = -\delta^{\frac{1}{2}} \frac{h_t}{h} - \frac{1}{h} \mathbf{u}_1 \cdot \boldsymbol{\nabla} h. \tag{2.69}$$

Substituting this into (2.68),

$$\delta \zeta_t + \delta^{\frac{1}{2}} \mathbf{u}_1 \cdot \boldsymbol{\nabla} \zeta - (1 + \delta^{\frac{1}{2}}\zeta) \frac{1}{h} (\delta^{\frac{1}{2}} h_t + \mathbf{u}_1 \cdot \boldsymbol{\nabla} h) = 0. \tag{2.70}$$

After expanding the variables using (2.48), we get the $O(1)$ problem,

$$\mathbf{u}_1^{(0)} \cdot \boldsymbol{\nabla} h^{(0)} = 0. \tag{2.71}$$

If we substitute (2.64) into the above equation, we will see that it is satisfied trivially. Thus, the leading order problem provides us with no new information regarding $h^{(0)}$. We next take the hydrostatic relation (2.47), and expand its variables in an asymptotic series which gives us,

$$\eta^{(0)} = h^{(0)}, \tag{2.72}$$

which again is not helpful in determining $h^{(0)}$.

Thus, we continue with the next highest order approximation, $O(\delta^{\frac{1}{2}})$, for (2.43), (2.44), and (2.47).

$$\mathbf{k} \times \mathbf{u}_1^{(1)} + \nabla\eta^{(1)} = -(\mathbf{u}_1^{(0)} \cdot \nabla)\mathbf{u}_1^{(0)}, \tag{2.73}$$

$$h_t^{(0)} + \nabla \cdot (\mathbf{u}_1^{(0)} h^{(1)} + \mathbf{u}_1^{(1)} h^{(0)}) = 0, \tag{2.74}$$

$$\eta^{(1)} = h^{(1)} + p^{(0)}. \tag{2.75}$$

Solving for $\mathbf{u}_1^{(1)}$ and $h^{(1)}$ in (2.73) and (2.75) respectively,

$$\mathbf{u}_1^{(1)} = \mathbf{k} \times \nabla\eta^{(1)} + J(\nabla h^{(0)}, h^{(0)}), \tag{2.76}$$

$$h^{(1)} = \eta^{(1)} - p^{(0)}. \tag{2.77}$$

Extracting the $O(\delta^{\frac{1}{2}})$ problem from (2.70), and making use of (2.77),

$$\begin{aligned} &- h_t^{(0)} + h^{(0)}\mathbf{u}_1^{(0)} \cdot \nabla\zeta^{(0)} - \zeta^{(0)}\mathbf{u}_1^{(0)} \cdot \nabla h^{(0)} \\ &- \mathbf{u}_1^{(0)} \cdot \nabla(\eta^{(1)} - p^{(0)}) - \mathbf{u}_1^{(1)} \cdot \nabla h^{(0)} = 0. \end{aligned} \tag{2.78}$$

Substituting in equations (2.64) and (2.76) for $\mathbf{u}_1^{(0)}$ and $\mathbf{u}_1^{(1)}$ respectively,

$$\begin{aligned} &h_t^{(0)} + h^{(0)} J(\Delta h^{(0)}, h^{(0)}) + \Delta h^{(0)} J(h^{(0)}, h^{(0)}) \\ &+ (-h_y^{(0)}, h_x^{(0)}) \cdot (\eta_x^{(1)}, \eta_y^{(1)}) + J(p^{(0)}, h^{(0)}) \\ &+ (-\eta_y^{(1)}, \eta_x^{(1)}) \cdot (h_x^{(0)}, h_y^{(0)}) + J(\nabla h^{(0)}, h^{(0)}) \cdot \nabla h^{(0)} = 0. \end{aligned} \tag{2.79}$$

Simplifying provides us with our upper layer governing equation,

$$h_t^{(0)} + J\left(p^{(0)} + h^{(0)}\Delta h^{(0)} + \frac{1}{2}\nabla h^{(0)} \cdot \nabla h^{(0)}, h^{(0)}\right) = 0. \tag{2.80}$$

2.5 Derivation from Potential Vorticity

Equations (2.80) and (2.63) can also be derived by making use of potential vorticity conservation. We note that for the shallow water model under consideration, potential vorticity (PV) is defined as,

$$PV = \frac{\text{relative + planetary vorticity}}{\text{thickness of layer}}, \tag{2.81}$$

where PV is conserved following the flow, ie.

$$\frac{D}{Dt}(PV) = 0. \tag{2.82}$$

For the lower layer, in dimensional variables, (2.82) is given by

$$\frac{D^*}{Dt}\left(\frac{v^*_{2x*} - u^*_{2y*} + f_o}{H - h^* + s^*y^*}\right) = 0, \tag{2.83}$$

where D^*/Dt represents the total derivative in dimensional variables. Making use of our scalings we get

$$(\delta f_o \partial_t + \delta f_o \mathbf{u_2} \cdot \boldsymbol{\nabla})\left(\frac{\delta f_o(v_{2x} - u_{2y}) + f_o}{H - \delta H h + \delta H s y}\right) = 0. \tag{2.84}$$

Simplifying and applying the quotient rule,

$$\begin{aligned}(1 - \delta h + \delta s y)\frac{D}{Dt}(\delta(v_{2x} - u_{2y}) + 1) \\ -(\delta(v_{2x} - u_{2y}) + 1)\frac{D}{Dt}(1 - \delta h + \delta s y) = 0.\end{aligned} \tag{2.85}$$

Expanding the variables in an asymptotic series gives us the $O(1)$ problem:

$$\frac{D}{Dt}(v^{(0)}_{2x} - u^{(0)}_{2y} + h^{(0)} - sy) = 0. \tag{2.86}$$

Recalling that, to first order, $\xi = v^{(0)}_{2x} - u^{(0)}_{2y} = \Delta p^{(0)}$, this becomes

$$\frac{D}{Dt}(\Delta p^{(0)} + h^{(0)} - sy) = 0, \tag{2.87}$$

which is identical to (2.61), and thus our governing equation simplifies to

$$(\Delta p^{(0)} + h^{(0)})_t + J(p^{(0)}, \Delta p^{(0)} + h^{(0)} - sy) = 0, \tag{2.88}$$

as before.

We now use the same technique to derive the upper layer governing equation. Conservation of potential vorticity for the upper layer is defined by

$$\frac{D^*}{Dt}\left(\frac{v^*_{1x^*} - u^*_{1y^*} + f_o}{h^*}\right) = 0. \tag{2.89}$$

Applying our scalings, we get the nondimensional form:

$$(\delta f_o \partial_t + \delta^{\frac{1}{2}} f_o \mathbf{u}_1 \cdot \boldsymbol{\nabla})\left(\frac{\delta^{\frac{1}{2}} f_o (v_{1x} - u_{1y}) + f_o}{\delta H h}\right). \tag{2.90}$$

Simplifying and applying the quotient rule,

$$\delta h(v_{1x}-u_{1y})_t+\delta^{\frac{1}{2}} h\mathbf{u}_1\cdot\boldsymbol{\nabla}(v_{1x}-u_{1y})[\delta^{\frac{1}{2}}(v_{1x}-u_{1y})+1][\delta^{\frac{1}{2}} h_t+\mathbf{u}_1\cdot\boldsymbol{\nabla}h] = 0. \tag{2.91}$$

Expanding the variables in an asymptotic series, we obtain the $O(1)$ problem

$$\mathbf{u}_1^{(0)} \cdot \boldsymbol{\nabla} h^{(0)} = 0, \tag{2.92}$$

which is again trivial, prompting us to seek the next higher order problem which takes the form,

$$h^{(0)}\mathbf{u}_1^{(0)}\cdot\boldsymbol{\nabla}(\Delta h^{(0)})-\Delta h^{(0)}\mathbf{u}_1^{(0)}\cdot\boldsymbol{\nabla}h^{(0)}-h_t^{(0)}-\mathbf{u}_1^{(0)}\cdot\boldsymbol{\nabla}h^{(1)}-\mathbf{u}_1^{(1)}\cdot\boldsymbol{\nabla}h^{(0)} = 0. \tag{2.93}$$

Expanding, applying (2.92), and substituting (2.77) and (2.76) for $h^{(1)}$ and $\mathbf{u}_1^{(1)}$ respectively gives us

$$h_t^{(0)} + J\left(p^{(0)} + h^{(0)}\Delta h^{(0)} + \frac{1}{2}\boldsymbol{\nabla}h^{(0)} \cdot \boldsymbol{\nabla}h^{(0)}, h^{(0)}\right) = 0, \tag{2.94}$$

the same as before.

We conclude the chapter by summarizing our governing equations. We will drop the subscript notation to maintain a cleaner appearance, however, we must remember that we are still dealing with the leading order variables $h^{(0)}$ and $p^{(0)}$. Thus we represent our upper and lower layer equations as

$$h_t + J\left(p + h\Delta h + \frac{1}{2}\boldsymbol{\nabla}h \cdot \boldsymbol{\nabla}h, h\right) = 0, \text{ and} \tag{2.95}$$

$$(\Delta p + h)_t + J(p, \Delta p + h - sy) = 0, \tag{2.96}$$

respectively.

Chapter 3

The Linear Stability Problem

3.1 The Linear Stability Equations

To derive the linear stability equations, we first note that the substitution of time independent solutions, $h = h_o(y)$ and $p = p_o(y)$, into (2.95) and (2.96) causes them to be trivially satisfied, since $h_{ot}(y) = 0$, $p_{ot}(y) = 0$, $h_{ox}(y) = 0$, and $p_{ox}(y) = 0$. Now, we may represent h and p by a time independent part which represents the exact solutions to (2.95) and (2.96), plus a small perturbation (where we use prime to denote a perturbation term),

$$h = h_o(y) + h'(x, y, t), \tag{3.1}$$

$$p = p_o(y) + p'(x, y, t). \tag{3.2}$$

Substituting (3.1) and (3.2) into (2.95) and (2.96), neglecting all nonlinear terms in the perturbations, and dropping the primes, gives us

$$h_t + h_{oy}p_x + [U_o + h_{oy}h_o\Delta + (h_{oy})^2\partial_y - (h_o h_{oyy})_y]h_x = 0, \tag{3.3}$$

$$(\partial_t + U_o\partial_x)(\Delta p + h) + (h_{oy} - U_{oyy} - s)p_x = 0, \tag{3.4}$$

in a channel with $0 < y < L$, where $U_o = -p_{oy}$ is the mean flow in the lower layer.

We will set the mean flow in the lower layer, U_o, to be zero in order to prevent barotropic shear instabilities, which enables us to focus on the pure

baroclinic problem (Swaters, 1993). We assume the steady solution for the upper layer thickness to be of the form of a simple wedge,

$$h_o(y) = 1 + \alpha\left(y - \frac{L}{2}\right), \tag{3.5}$$

where α represents the slope of the interface in the cross channel direction of the interface between the two layers. In dimensional variables, the slope is given by

$$\alpha^* = \frac{\bar{h}}{L}\alpha. \tag{3.6}$$

Thus, the linear stability equations for our model take the form

$$h_t + \alpha p_x + \alpha\left(1 + \alpha\left(y - \frac{L}{2}\right)\right)\Delta h_x + \alpha^2 h_{xy} = 0, \tag{3.7}$$

$$(\Delta p + h)_t + (\alpha - s)p_x = 0. \tag{3.8}$$

3.2 Perturbation Energetics

We can obtain stability conditions by examining the averaged-energy form of the linearized upper layer equation. We will follow the derivation from Swaters (1993). First, we assume that the cross channel width of the upper layer is equal to the channel width, L. We define an operator

$$\langle(\ldots)\rangle = \int_{-x_1}^{x_1} (\ldots) dx. \tag{3.9}$$

The averaged energy form of the linearized upper layer equation is obtained by multiplying (3.7) by the perturbation amplitude, $h(x, y, t)$, integrating over y from 0 to L, and then integrating over the length of the channel from $-x_1$ to x_1, where x_1 is constant, which gives us:

$$\int_0^L \left\langle hh_t + h_{oy} + h_{oy}hp_x + h_{oy}h_o h\Delta h_x + (h_{oy})^2 hh_{xy} - (h_o h_{oyy})_y hh_x \right\rangle dy = 0. \tag{3.10}$$

Noting that h_o is independent of x, we split up the $\langle(\ldots)\rangle$ term into a sum of terms, with the h_o parts taken out of the x-integral, so that (3.10) becomes:

$$\int_0^L \left(\left\langle \frac{1}{2}(h^2)_t + h_{oy}hp_x \right\rangle + h_{oy}h_o \langle hh_{xxx}\rangle + h_{oy}h_o \langle hh_{xyy}\rangle \right. \tag{3.11}$$

$$\left. + (h_{oy})^2 \langle hh_{xy}\rangle - (h_o h_{oyy})_y \langle hh_x\rangle \right) dy = 0.$$

We integrate each term by parts in order to simplify the expression. The second and last terms vanish through integration by parts, when we take into account the periodicity condition at $-x_1$ and x_1, ie.

$$\begin{aligned} \int_{-x_1}^{x_1} hh_{xxx} dx &= [h_x h_{xx}]_{-x_1}^{x_1} - \frac{1}{2}\int_{-x_1}^{x_1} ((h_x)^2)_x dx \qquad (3.12) \\ &= 0 - \frac{1}{2}[(h_x)^2]_{-x_1}^{x_1} \\ &= 0, \end{aligned}$$

$$\begin{aligned} \int_{-x_1}^{x_1} hh_x dx &= \frac{1}{2}\int_{-x_1}^{x_1} (h^2)_x dx \qquad (3.13) \\ &= \frac{1}{2}[h^2]_{-x_1}^{x_1} \\ &= 0. \end{aligned}$$

Next, we combine the third and fourth integrals, and simplify

$$\begin{aligned} & h_{oy}h_o\langle hh_{xyy}\rangle + (h_{oy})^2\langle hh_{xy}\rangle \qquad (3.14)\\ &= h_{oy}[h_o\langle hh_{xyy}\rangle + h_{oy}\langle hh_{xy}\rangle]\\ &= h_{oy}\langle h[h_oh_{xyy} + h_{oy}h_{xy}]\rangle\\ &= h_{oy}\langle h(h_oh_{xy})_y\rangle\\ &= \langle h_{oy}h(h_oh_{xy})_y\rangle\,. \end{aligned}$$

Then we integrate by parts,

$$\begin{aligned} & \int_0^L \langle h_{oy}h(h_oh_{xy})_y\rangle\, dy \qquad (3.15)\\ &= \int_{-x_1}^{x_1}[h_{oy}hh_oh_{xy}]_0^L dx - \int_{-x_1}^{x_1}\int_0^L h_oh_{xy}(h_{oy}h)_y dydx\\ &= \left[[h_oh_{oy}hh_y]_0^L\right]_{-x_1}^{x_1} - \int_{-x_1}^{x_1}[h_oh_{oy}h_xh_y]_0^L dx\\ &\quad - \int_{-x_1}^{x_1}\int_0^L h_oh_{xy}(h_{oyy}h + h_{oy}h_y)dydx. \end{aligned}$$

The first integral will vanish due to the periodicity, the second will vanish due to the condition of having no normal flow at the boundaries (ie. $h_x = 0$ at $y = 0, L$).This leaves us to work on the third integral,

$$\begin{aligned} & -\int_{-x_1}^{x_1}\int_0^L h_oh_{xy}(h_{oyy}h + h_{oy}h_y)dydx \qquad (3.16)\\ &= -\int_0^L\int_{-x_1}^{x_1} h_oh_{oyy}hh_{xy}dxdy - \frac{1}{2}\int_0^L\int_{-x_1}^{x_1} h_oh_{oy}((h_y)^2)_x dxdy\\ &= -\int_0^L [h_0h_{oyy}hh_y]_{-x_1}^{x_1}dy + \int_0^L\int_{-x_1}^{x_1} h_oh_{oyy}h_xh_y dxdy\\ &\quad -\frac{1}{2}\int_0^L [h_oh_{oy}(h_y)^2]_{-x_1}^{x_1}dy\\ &= \int_{-x_1}^{x_1}\int_0^L h_oh_{oyy}h_xh_y dydx, \end{aligned}$$

where we have again used the periodicity property of h and h_y with respect to x.

Now we substitute our wedge front form of h_o, and see that $h_{oyy} = 0$, causing the middle integrals to evaluate to zero as well. We are left with only the first term in (3.11), which simplifies to

$$\frac{1}{2}\frac{\partial}{\partial t}\int_0^L \langle h^2 \rangle \, dy = -\int_0^L \langle \alpha h p_x \rangle \, dy. \tag{3.17}$$

Thus, it is a necessary condition for perturbation growth that $\alpha h p_x$ is negative somewhere in the flow. On the other hand, it is sufficient that $\alpha h p_x$ be everywhere positive to inhibit the perturbation growth. In addition, (3.17) shows that no instability will occur in the case where $p = 0$ unless we introduce *baroclinic coupling*, ie. a second layer is required (this was also shown by Swaters (1993) and Reszka and Swaters (1999)).

3.3 Normal Mode Analysis

Each perturbation field is assumed to be a superposition of waves. Thus, we take p and h to be of the form,

$$p(x,y,t) = \tilde{p}(y)\exp[ik(x-ct)] + c.c., \tag{3.18}$$

$$h(x,y,t) = \tilde{h}(y)\exp[ik(x-ct)] + c.c., \tag{3.19}$$

where $c.c.$ denotes the complex conjugate, k is the real-valued along-channel wavenumber, and c is the along-channel complex phase velocity. An instability in the flow arises when a perturbation grows in time. We will determine when instability will occur using the following analysis. We note that p and h will grow in time if the imaginary part of the phase velocity is positive.

Substituting (3.18) and (3.19) into (3.7) and (3.8) gives us

$$\left(1+\alpha\left(y-\frac{L}{2}\right)\right)[\partial_{yy}-k^2]\tilde{h} + \alpha\tilde{h}_y - \frac{c}{\alpha}\tilde{h} + \tilde{p} = 0, \tag{3.20}$$

$$[\partial_{yy}-k^2]\tilde{p} + \frac{s-\alpha}{c}\tilde{p} + \tilde{h} = 0. \tag{3.21}$$

The fluid must satisfy the condition of having no normal flow at the channel walls. Thus, h_x and p_x must vanish at $y = 0, L$. However, because we have taken h and p to have the exponential forms (3.18) and (3.19), the boundary conditions reduce to (if $k \neq 0$)

$$\tilde{p} = \tilde{h} = 0 \text{ on } y = 0, L. \tag{3.22}$$

Examining equations (3.20) and (3.21), we see that these are not easily solved analytically. We will take α to be small, and s, the bottom slope, to be $O(\alpha)$. As will be shown later, this will cause c to be $O(\alpha)$ as well, permitting us to neglect all $O(\alpha)$ terms, while retaining terms of order $\frac{c}{\alpha}$ and $\frac{s}{c}$. We note that the assumption of α to be small is in effect taking our wedge to have a gentle slope. Dropping the tildes, and applying our assumptions, leads us to a pair of coupled ordinary differential equations,

$$h'' - \left(\frac{c}{\alpha} + k^2\right)h + p = 0, \tag{3.23}$$

$$p'' - \left(\frac{\alpha - s}{c} + k^2\right)p + h = 0, \tag{3.24}$$

where primes refer to derivatives with respect to y, and the boundary conditions at the channel walls are given by

$$p(0) = p(L) = h(0) = h(L) = 0. \tag{3.25}$$

Thus, the normal mode solutions are of the form

$$p(y) = A\sin(ly), \tag{3.26}$$

$$h(y) = B\sin(ly), \tag{3.27}$$

where A and B are constants, and l is the cross channel wavenumber, which is given by

$$l = \frac{n\pi}{L},\ n \in \{1, 2, 3, \dots\}. \tag{3.28}$$

Thus, our normal mode perturbation solutions take the form,

$$p(x, y, t) = A\sin(ly)\exp[ik(x - ct)] + c.c., \tag{3.29}$$

$$h(x, y, t) = B\sin(ly)\exp[ik(x - ct)] + c.c. \tag{3.30}$$

Applying our solutions to (3.23) and (3.24), and writing them in matrix form,

$$\begin{bmatrix} K^2 + \frac{\alpha - s}{c} & -1 \\ -1 & K^2 + \frac{c}{\alpha} \end{bmatrix} \begin{bmatrix} A \\ B \end{bmatrix} = \begin{bmatrix} 0 \\ 0 \end{bmatrix}, \tag{3.31}$$

where we have let $K^2 = k^2 + l^2$, the total wavenumber squared. The linear system given above puts a constraint on A and B, that they must be linearly dependent. Thus, in order for the problem to have nontrivial solutions, we need the determinant of the coefficient matrix to be zero, ie.

$$(cK^2 + \alpha - s)(\alpha K^2 + c) - \alpha c = 0. \tag{3.32}$$

Applying the quadratic formula yields the dispersion relation

$$c = \frac{s - \alpha K^4 \pm [(\alpha K^4 - s)^2 - 4\alpha(\alpha - s)K^4]^{\frac{1}{2}}}{2K^2}. \tag{3.33}$$

For $K^2 \sim O(1)$, $c \sim O(\alpha)$ as we required previously, we see that c will be complex wherever the discriminant is negative. Thus, there are two complex

phase velocities, with one being the complex conjugate of the other. If we represent c as a real part plus an imaginary part, ie.

$$c = c_R + ic_I, \tag{3.34}$$

then, for $c_I \neq 0$, we must have $c_I < 0$ for one of our two complex phase velocities, ie. there is an instability.

We now establish a sufficient condition for stability. Note that the system is stable whenever c is real, which happens when the discriminant is positive, ie.

$$(\alpha K^4 - s)^2 - 4\alpha(\alpha - s)K^4 > 0. \tag{3.35}$$

Expanding the quadratic, dividing by α^2 and rearranging gives us

$$\left(\frac{s}{\alpha}\right)^2 + 2K^4\frac{s}{\alpha} + K^8 > 4K^4, \tag{3.36}$$

which collapses down to

$$\left(\frac{s}{\alpha} + K^4\right)^2 > 4K^4, \tag{3.37}$$

or, equivalently,

$$\frac{s}{\alpha} + K^4 > 2K^2, \tag{3.38}$$

$$\frac{s}{\alpha} + K^4 < -2K^2. \tag{3.39}$$

Isolating these inequalities for $\frac{s}{\alpha}$, and rearranging, gives us

$$\frac{s}{\alpha} > K^2(2 - K^2), \tag{3.40}$$

$$\frac{s}{\alpha} < -K^2(2 + K^2), \tag{3.41}$$

which are sufficient conditions for stability. Thus, a necessary condition for instability is

$$-K^2(2 + K^2) < \frac{s}{\alpha} < K^2(2 - K^2). \tag{3.42}$$

We define *marginal stability curves* as curves which lie on the boundary between stability and instability, ie. where the discriminant is zero,

$$(\alpha K^4 - s)^2 = 4\alpha(\alpha - s)K^4. \tag{3.43}$$

Solving for $\frac{s}{\alpha}$, we obtain the marginal stability curves,

$$\frac{s}{\alpha} = K^2(2 - K^2) \text{ and,} \tag{3.44}$$

$$\frac{s}{\alpha} = -K^2(2 + K^2). \tag{3.45}$$

From now on, we will refer to (3.44) and (3.45) as the *Upper* and *Lower Branches* of the *Marginal Stability Curve (MSC)* respectively - see Figures 3.1 and 3.2. The *point of marginal stability* is defined as the point below which there exists wavenumbers for which the flow is unstable. On the Upper Branch, the point of marginal stability occurs at $(\frac{s}{\alpha}, K^2) = (1, 1)$. The model also exhibits a *high frequency cutoff*, defined as the K^2 value above which the flow is guaranteed to be stable, which occurs on the Upper Branch of the MSC when $K^2 > 1$. The high frequency cutoff was found by solving (3.44) for K^2 and taking the larger root, ie.

$$K^2_{\text{cutoff}} = 1 + \sqrt{1 - \frac{s}{\alpha}} \text{ for } \frac{s}{\alpha} < 1. \tag{3.46}$$

We note that $\frac{s}{\alpha}$ is necessarily $O(1)$ since we previously assumed s to be $O(\alpha)$.

We define a new variable α_c to be the critical slope which satisfies one of (3.44) or (3.45), for a given s, ie.

$$\alpha_c = \frac{s}{K^2(2 - K^2)} \text{ on the Upper Branch and,} \tag{3.47}$$

$$\alpha_c = \frac{-s}{K^2(2 + K^2)} \text{ on the Lower Branch.} \tag{3.48}$$

Substituting α_c into (3.31), we find that on the Lower Branch, $A = -B$, and on the Upper Branch, $A = B$. The first case, where the two solutions (h and p) are in phase, is known as the *barotropic mode*, while the second case, where the two solutions are 180 degrees out of phase, is called the *baroclinic mode.*

Substituting α_c into the dispersion relation gives us the real valued phase velocities as shown in Figures 3.3 and 3.4,

$$c = \frac{s(1 - K^2)}{K^2(2 - K^2)}, \text{ on the Upper Branch and,} \tag{3.49}$$

$$c = \frac{s(K^2 + 1)}{K^2(K^2 + 2)} \text{ on the Lower Branch.} \tag{3.50}$$

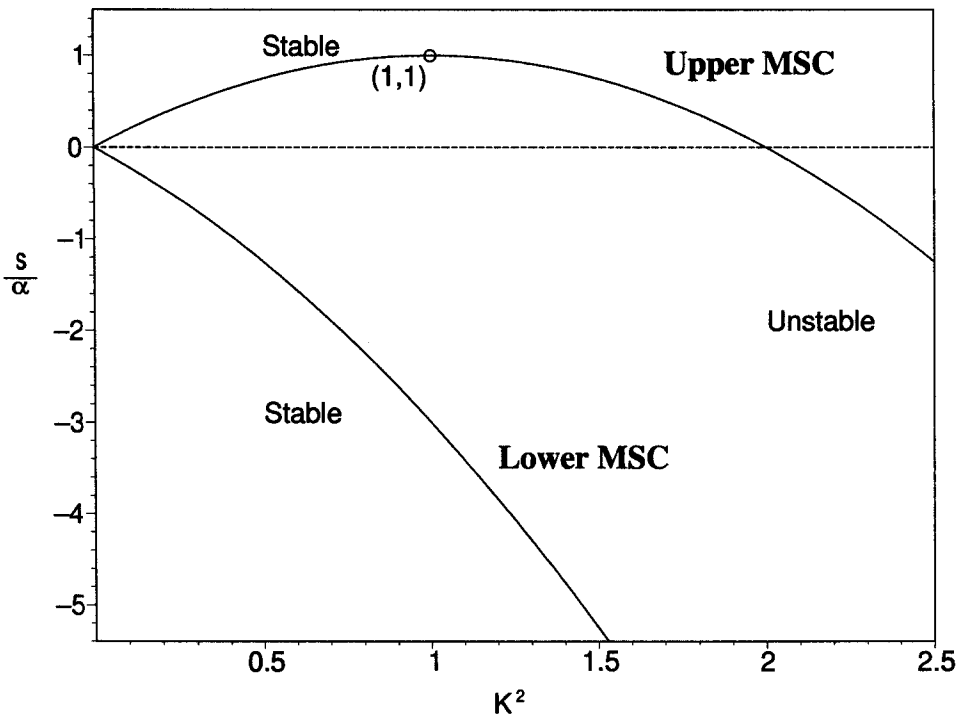

Figure 3.1: Marginal Stability Curves versus K^2.

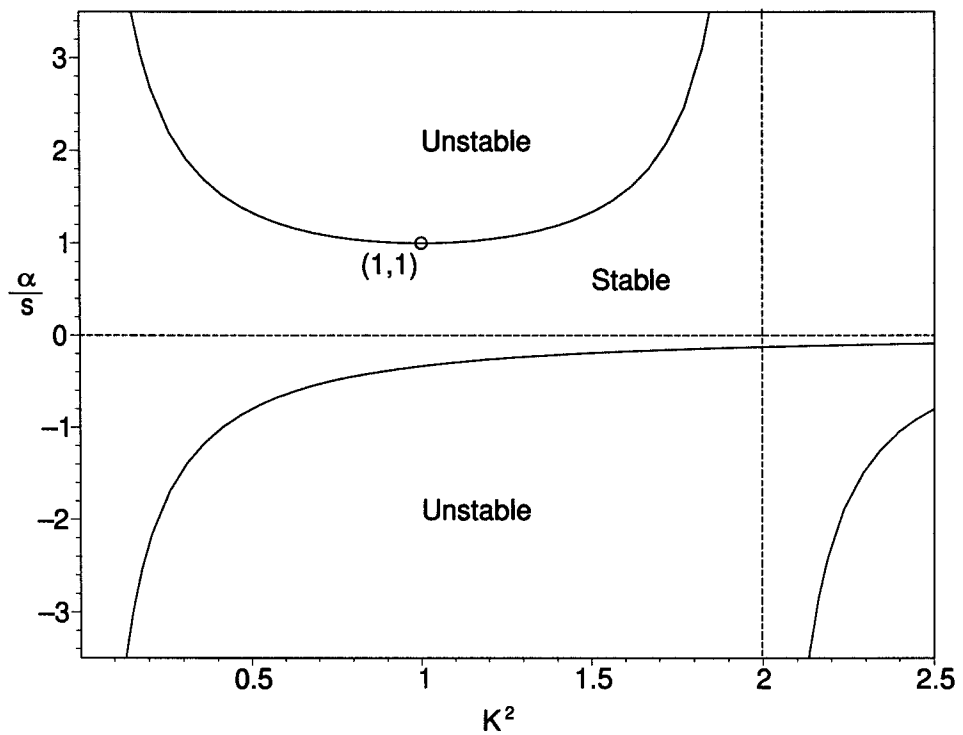

Figure 3.2: Marginal Stability Curves versus K^2 from another perspective.

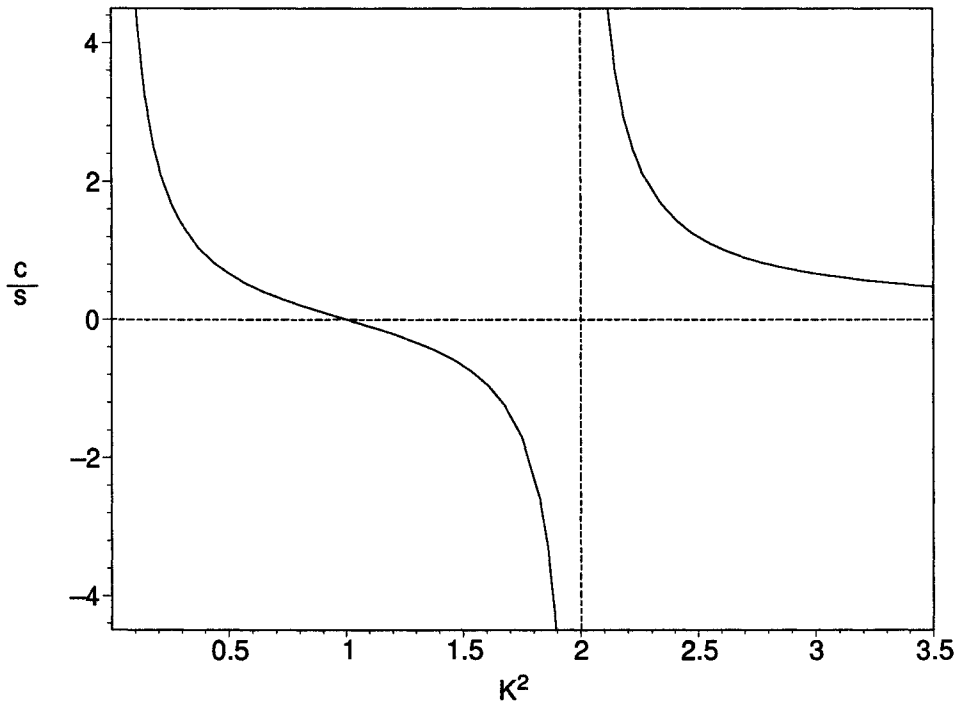

Figure 3.3: Phase velocity versus K^2 for the Upper Branch of the MSC.

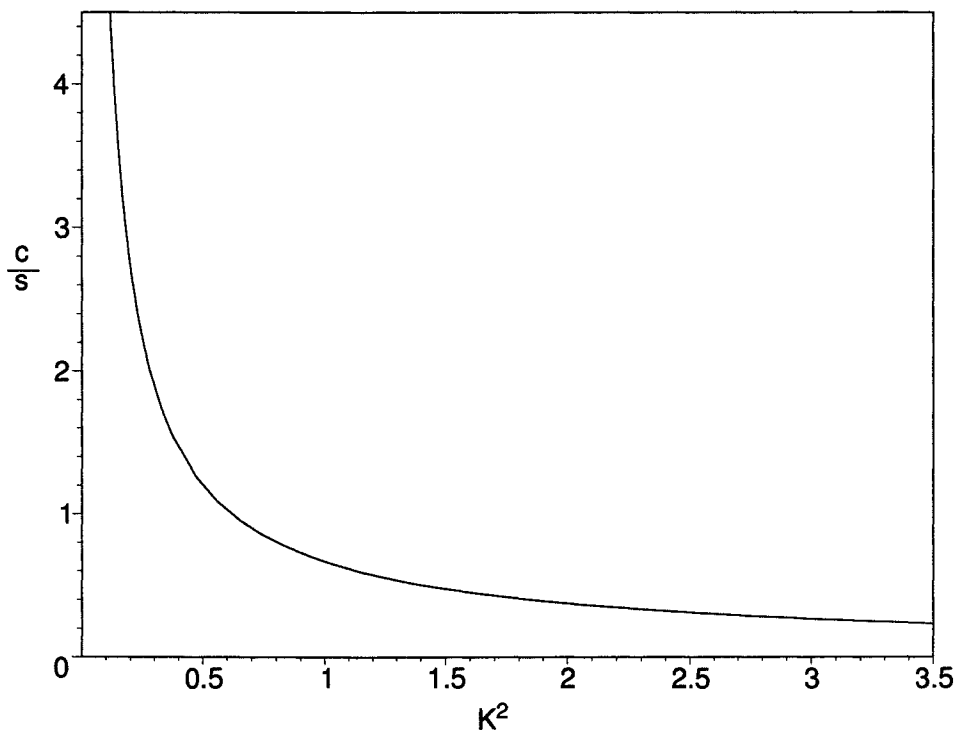

Figure 3.4: Phase velocity versus K^2 for the Lower Branch of the MSC.

Chapter 4

The Weakly Nonlinear Case

4.1 Introduction

We have solved for h and p, as well as the marginal stability curves, for the linear stability problem. These solutions are adequate when the nonlinear terms are negligible. However, as our perturbations become larger, the nonlinear terms become increasingly important. Since we are unable analytically to solve the fully nonlinear equations, we will study the evolution of a wedge front which is *weakly unstable*, ie. the nonlinear terms are small yet play a cumulatively important role. Assuming that the perturbation is initially small, and expanding our equations asymptotically, enables us to form an amplitude equation describing the slow time evolution of the leading order perturbation amplitude.

While using a wedge profile without isopycnal outcroppings is a highly idealized configuration, it allows us to analytically fully investigate available potential energy release and nonlinear interactions which will inhibit the growth predicted by our linear analysis. The wedge profile was first used by Griffiths and Linden (1981) who were able to recreate the instability characteristics observed in their laboratory. In deriving our amplitude equation, we will follow Pedlosky (1987) and Reszka (1997).

Following this, we will derive the Lorenz equivalent of our amplitude equa-

tion in the case where there is no time variability in the perturbations and the perturbation amplitude is real-valued. This will allow us to show that the observation of nontrivial time dependence in our solutions is due to the presence of the time-varying component of the perturbations.

4.2 Nonlinear Perturbation Equations

Adding dissipation terms to the governing equations, we have

$$h_t + J\left(p + h\Delta h + \frac{1}{2}\nabla h \cdot \nabla h, h\right) = -\nu h, \tag{4.1}$$

$$(\Delta p + h)_t + J(p, \Delta p + h - sy) = -\nu(\Delta p + h), \tag{4.2}$$

where we have chosen our dissipation terms to be proportional to the potential vorticity. This form of the dissipation, first introduced by Klein and Pedlosky (1992), is a purely heuristic choice that assumes that smaller scale turbulence acts directly to degrade the larger scale potential vorticity (Klein and Pedlosky, 1992).

As in chapter 3, we introduce perturbations h' and p',

$$h = h_o(y) + h'(x, y, t), \tag{4.3}$$

$$p = p_o(y) + p'(x, y, t). \tag{4.4}$$

Substituting these into (4.1) and (4.2), and again setting the mean flow in the lower layer to zero (ie. $p_o(y) = 0$), we arrive at the nonlinear perturbation equations:

$$\begin{aligned} h_t + h_{oy}h_o\Delta h_x + (h_{oy})^2 h_{xy} - (h_o h_{oyy})_y + h_{oy}p_x + h_o J(\Delta h, h) \\ + h_{oy}[h\Delta h_x + 2h_y h_{xy} - h_x h_{yy} + h_x h_{xx}] - h_{oyy}h_x h_y \\ - h_{oyyy}hh_x + J(p, h) = -\nu h, \end{aligned} \tag{4.5}$$

$$(\Delta p + h)_t + (h_{oy} - s)p_x + J(p, \Delta p + h) = -\nu(\Delta p + h), \tag{4.6}$$

where we have dropped primes and are no longer neglecting nonlinear terms.

As before, we let

$$h_o = 1 + \alpha\left(y - \frac{L}{2}\right), \alpha << 1, \tag{4.7}$$

a gently sloping wedge front. We now rescale α and t by taking

$$\alpha = s\tilde{\alpha}, \tag{4.8}$$

$$t = \frac{\tilde{t}}{s}, \tag{4.9}$$

which implies that phase velocity c will scale as

$$c = s\tilde{c}. \tag{4.10}$$

Now we will drop tildes on these new variables.

Defining

$$\mu = \pm 1, \tag{4.11}$$

where the plus sign gives the Upper Branch equations, and the minus sign the Lower Branch equations; our new critical slope, α_c, and phase velocity, c, are:

$$\alpha_c = \frac{\mu}{K^2(2-\mu K^2)}, \tag{4.12}$$

and

$$c = \frac{1-\mu K^2}{K^2(2-\mu K^2)}. \tag{4.13}$$

In order to discern the appropriate balance in which nonlinearity and dissipation arise at the same order, we rescale our perturbation quantities and our dissipative term by s^2:

$$h = s^2\tilde{h}, \tag{4.14}$$

$$p = s^2\tilde{p}, \tag{4.15}$$

$$\nu = s^2\tilde{\nu}. \tag{4.16}$$

Substituting these into (4.5) and (4.6), dividing by s^2, and dropping the tildes, we obtain

$$\begin{aligned} h_t + \alpha\Delta h_x + \alpha p_x = &-s\alpha^2 h_{xy} - s\alpha^2\left(y-\frac{L}{2}\right)\Delta h_x \\ &-sJ(\Delta h + p, h) - s^2\alpha\left(y-\frac{L}{2}\right)J(\Delta h, h) \\ &-s^2\alpha[h\Delta h_x + 2h_y h_{xy} - h_x h_{yy} + h_x h_{xx}] + s\nu h, \end{aligned} \tag{4.17}$$

$$(\Delta p + h)_t + (\alpha - 1)p_x = s[J(\Delta p + h, p) - \nu(\Delta p + h)], \tag{4.18}$$

where we have left off terms of $O(s^3)$ and higher, since these do not appear later, and we assume that α and ν are $O(1)$ parameters.

4.2.1 Multiple Scales

We introduce a small perturbation into α by setting

$$\alpha = \alpha_c + \mu(\tau_o + \tau(st))\Delta, \tag{4.19}$$

where Δ is initially only defined to be a positive, small quantity, and we recall that $\mu = 1$ on the upper branch and $\mu = -1$ on the lower branch. Also, we let $\tau_o + \tau(st)$ be $O(1)$ with $\tau_o = \pm 1$. The $\tau(st)$ parameter introduces time variability. If $\tau_o + \tau(st)$ is always positive, we will have a *supercriticality*, and if it is always negative, we will have a *subcriticality*. In the region of supercriticality, we are perturbing α from the MSC into the unstable region, giving us marginally unstable solutions, while, in the region of subcriticality, we perturb into the stable region, giving us marginally stable solutions. In the case where $\tau_o + \tau(st)$ is both positive and negative, we have regions of super- and sub- criticality: that is, regions of marginal instability with regions of marginal stability.

We note that, given the form of (4.19),

$$\begin{aligned} h = h_o &= 1 + \alpha\left(y - \frac{L}{2}\right), \\ y = y_o &= 0, \end{aligned} \tag{4.20}$$

is no longer an exact solution to the homogeneous part of (4.1) and (4.2). In order for $h_o(y,T)$ to be a solution to the governing equations, as in Ha and Swaters (2006), we must introduce a forcing term on the right hand side of (4.2) given by $F = h_{ot} + \nu h_o$. However, the forcing term does not appear in perturbation equations (4.5) and (4.6).

Applying scalings (4.8) through (4.10) to our dispersion relation (3.33), transforms c such that its imaginary part has the form, upon taking the positive root,

$$c_I = \frac{1}{2K^2}[4\alpha(\alpha-1)K^4 - (\alpha K^4 - 1)^{\frac{1}{2}}]^{\frac{1}{2}}, \tag{4.21}$$

noting that c_I is the same, independent of whether μ is plus or minus one.

Substituting in (4.19), we obtain

$$\frac{\Delta^{\frac{1}{2}}}{2K}[4-\Delta K^2(K^4-4)]^{\frac{1}{2}} \tag{4.22}$$

$$= \frac{\Delta^{\frac{1}{2}}}{2K}\left[\frac{1}{K^2}\left[4K^2-\Delta\left\{K^2(K^2-2)\right\}\left\{K^2(K^2+2)\right\}\right]\right]^{\frac{1}{2}}$$

$$= O\left(\Delta^{\frac{1}{2}}\frac{1}{K}\right), \tag{4.23}$$

where we have used our assumptions that $K^2(K^2-2)$, $K^2(K^2+2)$ and K^2 are $O(1)$; and $\Delta << 1$, to determine that the function in the square brackets is $O(1)$. Thus, the growth rate, kc_I, is $O\left(\Delta^{\frac{1}{2}}\frac{k}{K}\right)$. We will define $\sqrt{|\sigma|} = kc_I$, which allows for simplification in our later equations. To make the growth rate marginal, we define $\Delta = s^2$.

We will now introduce slow time and large space parameters. Since the growth rate is $O(s)$, we scale time as

$$T = st, \tag{4.24}$$

noting that $\partial_t \rightarrow \partial_t + s\partial_T$, giving us

$$\alpha = \alpha_c + \mu(\tau_o + \tau(T))s^2. \tag{4.25}$$

We also introduce a large space parameter,

$$X = s^2x; \;\; \partial_x \rightarrow \partial_x + s^2\partial_X, \tag{4.26}$$

noting that Reszka (1997) showed that the (shorter) large space scale $\chi = sx$ dropped out.

Substituting (4.24) through (4.26) into (4.17) and (4.18), simplifying, and

sorting by order of s, we obtain

$$\begin{aligned} & h_t + \alpha_c p_x + \alpha_c \Delta h_x \\ & \quad + s\left\{ \left[\partial_T + \nu\right] h + J\left(p + \Delta h, h\right) + \alpha_c^2 \left(h_{xy} + \left(y - \frac{L}{2} \right) \Delta h_x \right) \right\} \\ & \quad + s^2 \Big\{ \alpha_c [h \Delta h_x + 2 h_y h_{xy} - h_x h_{yy} + h_x h_{xx}] \\ & \quad + \mu(\tau_o + \tau)(p + \Delta h)_x + \alpha_c (p_X + \Delta h_X + 2 h_{Xxx}) \Big\} = 0, \end{aligned} \tag{4.27}$$

$$\begin{aligned} & (\Delta p + h)_t + (\alpha_c - 1) p_x + s\{[\partial_T + \nu](\Delta p + h) + J(p, \Delta p + h)\} \\ & \quad + s^2 \{ \mu(\tau_o + \tau) p_x + 2 p_{tXx} + p_X (\alpha_c - 1) \} = 0. \end{aligned} \tag{4.28}$$

We expand h and p in an asymptotic series,

$$(p, h) = (p^{(0)}, h^{(0)}) + s(p^{(1)}, h^{(1)}) + s^2 (p^{(2)}, h^{(2)}) + \ldots, \tag{4.29}$$

where $p^{(0)}$, $h^{(0)}$, $p^{(1)}$, $h^{(1)}$, $p^{(2)}$, $h^{(2)}$, etc. are functions of x, y, t, X and T.

4.2.2 O(1) Problem

Substituting (4.29) into (4.27) and (4.28), the $O(1)$ problem is

$$h_t^{(0)} + \alpha_c p_x^{(0)} + \alpha_c \Delta h_x^{(0)} = 0, \tag{4.30}$$

$$(\Delta p^{(0)} + h^{(0)})_t + (\alpha_c - 1) p_x^{(0)} = 0. \tag{4.31}$$

Assuming $p^{(0)}$ and $h^{(0)}$ have normal mode solutions, our problem is equivalent to the linear case. Thus, our $O(1)$ solutions are:

$$p^{(0)} = A(X,T)\exp(ik\theta)\sin(ly) + c.c., \tag{4.32}$$

$$h^{(0)} = B(X,T)\exp(ik\theta)\sin(ly) + c.c., \tag{4.33}$$

where, as before, $B(X,T) = \mu A(X,T)$, $\theta = x - ct$,

$$c = \frac{1 - \mu K^2}{K^2(2 - \mu K^2)}, \text{ and} \tag{4.34}$$

$\mu = \pm 1$ with the plus sign denoting the phase velocity on the upper branch of the MSC, and the minus sign denoting the phase velocity on the lower branch of the MSC.

4.2.3 O(s) Problem

The $O(s)$ problem is:

$$h_t^{(1)} + \alpha_c p_x^{(1)} + \alpha_c \Delta h_x^{(1)} \tag{4.35}$$
$$= -[\partial_T + \nu]h^{(0)} - \alpha_c^2 \left(h_{xy}^{(0)} + \left(y - \frac{L}{2} \right) \Delta h_x^{(0)} \right),$$

$$(\Delta p^{(1)} + h^{(1)})_t + (\alpha_c - 1)p_x^{(1)} \tag{4.36}$$
$$= -[\partial_T + \nu](h^{(0)} + \Delta p^{(0)}).$$

The solutions to (4.35) and (4.36) are taken to be the sum of a particular solution and a homogeneous solution.

Particular solutions to (4.35) and (4.36) are

$$p^{(1)}_{\text{particular}} = \tilde{p}(y, X, T) \exp(ik\theta) + c.c., \tag{4.37}$$
$$h^{(1)}_{\text{particular}} = \tilde{h}(y, X, T) \exp(ik\theta) + c.c., . \tag{4.38}$$

For our homogeneous solutions, we take

$$p^{(1)}_{\text{homogeneous}} = \Psi(y, X, T), \tag{4.39}$$
$$h^{(1)}_{\text{homogeneous}} = \Phi(y, X, T), \tag{4.40}$$

which trivially satisfy the homogeneous part of (4.36) since Ψ and Φ are independent of x and t.

Using the terminology introduced in Pedlosky (1987), Φ and Ψ will act to balance the zonal flow alterations forced by nonlinear wave fluxes of the wave perturbation (Pedlosky, 1987). Thus, we refer to Φ and Ψ as mean flow correction terms since they account for changes in the mean flow caused by nonlinear terms. We note that, since Ψ and Φ are modifications to the $O(s)$ streamfunction, they are also streamfunctions.

Combining the particular and homogeneous solutions, our second order perturbation functions are assumed to be of the form

$$p^{(1)} = \tilde{p}(y, X, T) \exp(ik\theta) + c.c. + \Psi(y, X, T), \tag{4.41}$$
$$h^{(1)} = \tilde{h}(y, X, T) \exp(ik\theta) + c.c. + \Phi(y, X, T), \tag{4.42}$$

Since the fluid must satisfy the condition of having no normal flow on the channel walls, $p_x^{(1)}$ and $h_x^{(1)}$ must vanish at $y = 0, L$. However, since we have taken $p^{(1)}$ and $h^{(1)}$ to be of the form (4.41) and (4.42) respectively, the boundary conditions reduce to (if $k \neq 0$)

$$\tilde{p} = \tilde{h} = 0 \text{ on } y = 0, L. \tag{4.43}$$

Substitution of (4.41) and (4.42) into (4.35) and (4.36), after division by $i\alpha_c k$ and $-ick$ respectively, gives us

$$\left[\partial_{yy} - k^2 - \frac{c}{\alpha_c}\right]\tilde{h} + \tilde{p} = -\alpha_c \mu A l \cos(ly) \tag{4.44}$$
$$+\alpha_c \left(y - \frac{L}{2}\right) K^2 \mu A \sin(ly) + \frac{i\mu}{\alpha_c k}[\partial_T + \nu] A \sin(ly),$$

$$\left[\partial_{yy} - k^2 - \frac{\alpha_c - 1}{c}\right]\tilde{p} + \tilde{h} = \frac{i}{ck}(K^2 - \mu)[\partial_T + \nu] A \sin(ly). \tag{4.45}$$

Prior to deriving our solvability condition for this system of differential equations, we simplify the operators on $\tilde{h}$ and $\tilde{p}$ in (4.44) and (4.45) respectively by observing that they simplify as:

$$\left[\partial_{yy} - k^2 - \frac{c}{\alpha_c}\right] = \left[\partial_{yy} - k^2 - \frac{\alpha_c - 1}{c}\right] = \left[\partial_{yy} + l^2 - \mu\right]. \tag{4.46}$$

Now we may write the system of differential equations in the matrix form $\mathcal{L}\mathbf{b}(y) = \mathbf{F}(y)$:

$$\begin{bmatrix} \partial_{yy} + l^2 - \mu & 1 \\ 1 & \partial_{yy} + l^2 - \mu \end{bmatrix} \begin{bmatrix} \tilde{h} \\ \tilde{p} \end{bmatrix} \tag{4.47}$$
$$= \begin{bmatrix} -\alpha_c \mu A l \cos(ly) + \alpha_c \left(y - \frac{L}{2}\right) K^2 \mu A \sin(ly) + \frac{i\mu}{\alpha_c k}[\partial_T + \nu] A \sin(ly) \\ \frac{i}{ck}(K^2 - \mu)[\partial_T + \nu] A \sin(ly) \end{bmatrix}.$$

We note that

$$\mathcal{L} = \begin{bmatrix} \partial_{yy} + l^2 - \mu & 1 \\ 1 & \partial_{yy} + l^2 - \mu \end{bmatrix} \tag{4.48}$$

is a self-adjoint operator since

$$\int_0^L \mathbf{d}(y)\mathcal{L}\mathbf{b}(y)dy = \int_0^L \mathbf{b}(y)\mathcal{L}\mathbf{d}(y)dy \tag{4.49}$$

for any smooth test vector-function $\mathbf{d}(y)$ that satisfies the boundary conditions $\mathbf{d}(0, L) = \mathbf{0}$. This can be shown directly using integration by parts.

We will now derive a solvability condition for the system in (4.47). We begin by noting that the homogeneous problem,

$$\mathcal{L}\mathbf{b} = \mathbf{0}, \tag{4.50}$$

with boundary conditions given in (4.43), and where

$$\mathbf{b} = \begin{bmatrix} \tilde{h} \\ \tilde{p} \end{bmatrix} = \mathbf{0} \text{ on } y = 0, L \tag{4.51}$$

has solution

$$\mathbf{b}_o = \begin{bmatrix} A(X,T)\sin(ly) \\ B(X,T)\sin(ly) \end{bmatrix}, \tag{4.52}$$

where $B(X,T) = \mu A(X,T)$, just as in the $O(1)$ case.

Since we have a self-adjoint operator for the homogeneous problem, and a nontrivial homogeneous solution exists, the Fredholm alternative theorem (Haberman, 1998) tells us that the nonhomogeneous problem has solutions if and only if $< \mathbf{b}_o, \mathbf{F} >= 0$ over the domain $y = [0, L]$, where

$$\mathbf{F} = \begin{bmatrix} -\alpha_c \mu A l \cos(ly) + \alpha_c \left(y - \frac{L}{2}\right) K^2 \mu A \sin(ly) + \frac{i\mu}{\alpha_c k}[\partial_T + \nu] A \sin(ly) \\ \frac{i}{ck}(K^2 - \mu)[\partial_T + \nu] A \sin(ly) \end{bmatrix}. \tag{4.53}$$

Thus, the solvability condition on (4.44) and (4.45) is that their homogeneous solutions must be orthogonal to the inhomogeneity (Haberman, 1998), ie.

$$\int_0^L [\mu A \sin(ly) \quad A \sin(ly)] \mathbf{F}(y) = 0, \tag{4.54}$$

which upon expansion becomes

$$\begin{aligned} \int_0^L \Bigg\{ & -\alpha_c \mu l A \cos(ly) + \alpha_c K^2 \left(y - \frac{L}{2}\right) \mu A \sin(ly) \\ & + \frac{i\mu}{\alpha_c k}[\partial_T + \nu] A \sin(ly) \Bigg\} \mu A \sin(ly) dy \\ & + \int_0^L \left\{ \frac{i}{ck}(K^2 - \mu)[\partial_T + \nu] A \sin(ly) \right\} A \sin(ly) dy = 0. \end{aligned} \tag{4.55}$$

The first two terms,

$$\int_0^L \left[-\alpha_c \mu l A \cos(ly) + \alpha_c K^2 \left(y - \frac{L}{2}\right) \mu A \sin(ly)\right] \mu A \sin(ly) dy,$$

vanish as the integrand is odd over the region of integration. The remaining terms,

$$[\partial_T + \nu] A \int_0^L \left[\frac{i}{\alpha_c k} + \frac{i}{ck}(K^2 - \mu)\right] \sin^2(ly) dy,$$

evaluate to zero since $\frac{i}{\alpha_c k} + \frac{i}{ck}(K^2 - \mu) = 0$. Thus, (4.55) vanishes trivially, and the $O(s)$ problem gives us no condition on A, forcing us to examine the $O(s^2)$ problem.

Before moving on to the $O(s^2)$ problem, we must determine $\tilde{h}$ and $\tilde{p}$. Isolating for $\tilde{h}$ in (4.45) gives us:

$$\tilde{h} = -\left[\partial_{yy} + l^2 - \mu\right] \tilde{p} + \frac{i}{ck}(K^2 - \mu)[\partial_T + \nu] A \sin(ly). \tag{4.56}$$

Substituting (4.56) into (4.44), and rearranging, we obtain:

$$\begin{aligned} &\{[\partial_{yy} + l^2 - \mu]^2 - 1\}\tilde{p} \\ &= \frac{i}{ck}(K^2 - \mu)[\partial_T + \nu] A [\partial_{yy} + l^2 - \mu] \sin(ly) \\ &+\alpha_c \mu A l \cos(ly) - \alpha_c \left(y - \frac{L}{2}\right) K^2 \mu A \sin(ly) - \frac{i\mu}{\alpha_c k}[\partial_T + \nu] A \sin(ly), \end{aligned} \tag{4.57}$$

or equivalently,

$$\begin{aligned} &[\partial_{yy} + l^2 - 2\mu][\partial_{yy} + l^2]\tilde{p} \\ &= \alpha_c \mu A l \cos(ly) - \alpha_c \left(y - \frac{L}{2}\right) K^2 \mu A \sin(ly) \\ &+[\partial_T + \nu] A \left\{\frac{i}{ck}(K^2 - \mu)[\partial_{yy} + l^2 - \mu] \sin(ly) - \frac{i\mu}{\alpha_c k} \sin(ly)\right\}. \end{aligned} \tag{4.58}$$

Observing that

$$\begin{aligned} &\frac{i}{ck}(K^2 - \mu)[\partial_{yy} + l^2 - \mu] \sin(ly) - \frac{i\mu}{\alpha_c k} \sin(ly) \\ &= \frac{i}{k}\left\{\frac{1}{c}(K^2 - \mu)[-l^2 \sin(ly) + (l^2 - \mu)\sin(ly)] - \frac{\mu}{\alpha_c} \sin(ly)\right\} \\ &= \frac{i}{k}\left\{-\mu\left[\frac{K^2 - \mu}{c} + \frac{1}{\alpha_c}\right] \sin(ly)\right\} \\ &= 0, \end{aligned} \tag{4.59}$$

and creating a new variable, ξ, we can rewrite (4.58) as the system:

$$[\partial_{yy} + l^2 - 2\mu]\tilde{p} = \xi, \tag{4.60}$$
$$[\partial_{yy} + l^2]\xi = \alpha_c \mu A l \cos(ly) - \alpha_c \left(y - \frac{L}{2}\right) K^2 \mu A \sin(ly),$$

which is identical to the system seen in Reszka (1997). The solution to (4.60) is given by:

$$\tilde{p}(y,T) = \gamma_1 \left(y - \tfrac{L}{2}\right)^2 \cos(ly) + \gamma_2 \left(y - \tfrac{L}{2}\right) \sin(ly) + \gamma_3 \cos(ly) \tag{4.61}$$
$$+ \begin{cases} \gamma_4 \sin(ry) + \gamma_5 \sin(r(y-L) \text{ where } L^2 - 2\mu > 0 \\ \bar{\gamma}_4 \exp(-\bar{r}y) + \bar{\gamma}_5 \exp(\bar{r}(y-L)) \text{ where } L^2 - 2\mu < 0\,, \end{cases}$$

where $r = \sqrt{l^2 - 2\mu}$, $\bar{r} = \sqrt{2\mu - l^2}$, and the coefficients are given by:

$$\gamma_1 = -\frac{K^2}{8l}\alpha_c A,\ \gamma_2 = \left[\frac{\mu K^2 - 1}{4} + \frac{K^2}{8l^2}\right]\alpha_c A,$$
$$\gamma_3 = \left[\frac{K^2 L^2}{32l} + \frac{l(K^2-\mu)}{4}\right]\alpha_c A,\ \gamma_4 = \frac{l(K^2-\mu)(-1)^{n+1}}{4\sin(rL)}\alpha_c A,$$
$$\gamma_5 = \frac{l(K^2-\mu)}{4\sin(rL)}\alpha_c A,$$
$$\bar{\gamma}_4 = \frac{((-1)^n \exp(-\bar{r}L) - 1)(K^2-1)l}{4(1-\exp(-2\bar{r}L))}\alpha_c A,$$
$$\bar{\gamma}_5 = \frac{(\exp(-\bar{r}L) - (-1)^n)(K^2-1)l}{4(1-\exp(-2\bar{r}L))}\alpha_c A,$$

and where $\tilde{h}$ is given by:

$$\tilde{h} = -\left[\partial_{yy} + l^2 - \mu\right]\tilde{p} + \frac{i}{ck}(K^2-\mu)[\partial_T + \nu]A\sin(ly). \tag{4.62}$$

4.2.4 O(s^2) Problem

The $O(s^2)$ problem is:

$$\begin{aligned} & h_t^{(2)} + \alpha_c p_x^{(2)} + \alpha_c \Delta h_x^{(2)} \\ & = -[\partial_T + \nu]h^{(1)} - J(p^{(0)} + \Delta h^{(0)}, h^{(1)}) - J(p^{(1)} + \Delta h^{(1)}, h^{(0)}) \\ & -\alpha_c^2 h_{xy}^{(1)} - \alpha_c^2 \left(y - \frac{L}{2}\right) \Delta h_x^{(1)} - \mu(\tau_o + \tau)(p^{(0)} + \Delta h^{(0)})_x \\ & -\alpha_c (p^{(0)} + \Delta h^{(0)})_X - 2\alpha_c h_{Xxx}^{(0)} - \alpha_c \left(y - \frac{L}{2}\right) J(\Delta h^{(0)}, h^{(0)}) \\ & -\alpha_c (h^{(0)} \Delta h_x^{(0)} + 2h_y^{(0)} h_{xy}^{(0)} - h_x^{(0)} h_{yy}^{(0)} + h_x^{(0)} h_{xx}^{(0)}), \end{aligned} \tag{4.63}$$

$$\begin{aligned} & \Delta p_t^{(2)} + h_t^{(2)} + (\alpha_c - 1) p_x^{(2)} \\ & = -[\partial_T + \nu](h^{(1)} + \Delta p^{(1)}) - J(p^{(1)}, \Delta p^{(0)} + h^{(0)}) \\ & -J(p^{(0)}, \Delta p^{(1)} + h^{(1)}) - 2p_{tXx}^{(0)} - \mu(\tau_o + \tau) p_x^{(0)} - (\alpha_c - 1) p_X^{(0)}. \end{aligned} \tag{4.64}$$

Substituting our solutions for the $O(1)$ and $O(s)$ problems into (4.63) and (4.64),

$$\begin{aligned} & h_t^{(2)} + \alpha_c \Delta h_x^{(2)} + \alpha_c p_x^{(2)} \\ & = \Bigg\{ -[\partial_T + \nu]\tilde{h} + Aik\left[(\mu K^2 - 1)\Phi_y - \mu \Psi_y + \mu \Phi_{yyy}\right] \sin(ly) \\ & -ik\alpha_c^2 \left[\tilde{h}_y + \left(y - \frac{L}{2}\right)(-k^2 \tilde{h} + \tilde{h}_{yy})\right] + A_X \alpha_c [2k^2 \mu - (1 - \mu K^2)] \sin(ly) \\ & -Aik\mu(\tau_0 + \tau)(1 - \mu K^2) \sin(ly) \Bigg\} \exp(ik\theta) + G(\tilde{h}, \tilde{p}) \exp(2ik\theta) + c.c. \\ & -[\partial_T + \nu]\Phi - \frac{l}{c}(K^2 - \mu) \sin(2ly)[\partial_T + 2\nu](|A|^2) + \text{ non-resonant terms}, \end{aligned} \tag{4.65}$$

$$\Delta p_t^{(2)} + h_t^{(2)} + (\alpha_c - 1)p_x^{(2)} \tag{4.66}$$
$$= \Big\{ -(\partial_T + \nu)(\tilde{h} + \tilde{p}_{yy} - k^2\tilde{p}) - ikA(\Psi_{yyy} - \Psi_y + (K^2 - \mu)\Phi_y)\sin(ly)$$
$$-(\alpha_c - 1)A_X \sin(ly) - \mu(\tau_o + \tau)Aik\sin(ly)\Big\}\exp(ik\theta)$$
$$+F(\tilde{h},\tilde{p})\exp(2ik\theta) + c.c.$$
$$-[\partial_T + \nu]\Phi - \frac{l}{c}(k^2 - \mu)\sin(2ly)[\partial_T + 2\nu](|A|^2) - [\partial_T + \nu]\Psi_{yy}$$
$$+ \text{ non-resonant terms},$$

where asterisks denote complex conjugate, and we have used the relations,

$$([\partial_T + \nu]A^*)A + ([\partial_T + \nu]A)A^* = [\partial_T + 2\nu](|A|^2), \tag{4.67}$$
$$2\sin(ly)\cos(ly) = \sin(2ly). \tag{4.68}$$

Also, the terms associated with $\exp(2ik\theta)$ have not been written out, since we will not be using them. These terms do not cause resonance since their frequency is not the underlying frequency, $\omega = |kc_R|$, and thus they will not be responsible for *secular growth* (wave amplitude growth with respect to time).

We note that terms on the right hand side of (4.65) and (4.66), which do not have fast phase oscillation, will cause the particular solution to grow linearly in time. Since we want to inhibit this secular growth, we set the sum of these terms to zero, ie.

$$[\partial_T + \nu]\Phi - \frac{l}{c}(K^2 - \mu)\sin(2ly)[\partial_T + 2\nu](|A|^2) = 0, \tag{4.69}$$
$$[\partial_T + \nu](\Phi + \Psi_{yy}) + \frac{l}{c}(k^2 - \mu)\sin(2ly)[\partial_T + 2\nu](|A|^2) = 0. \tag{4.70}$$

Integrating (4.69), and applying the initial condition $\Phi(T = 0) = 0$, we obtain

$$\Phi(y, X, T) = -\frac{l}{c}(K^2 - \mu)\sin(2ly)\frac{1}{\exp(\nu T)}\int_0^T \exp(\nu s)[2\nu + \partial_s](|A(X,s)|^2)ds. \tag{4.71}$$

We define

$$f(X,T) = \frac{1}{\exp(\nu T)}\int_0^T \exp(\nu s)[2\nu + \partial_s](|A(X,s)|^2)ds, \tag{4.72}$$

so that we may write Φ as a product of a function of y with a function of X and T for simpler integration with respect to y later. Thus,

$$\Phi(y, X, T) = -\frac{l}{c}(K^2 - \mu)\sin(2ly)f(X,T). \tag{4.73}$$

Using (4.69) to simplify (4.70), we obtain

$$-[\partial_T + \nu]\Psi_{yy} = 0, \tag{4.74}$$

or equivalently,

$$[\exp(\nu T)\Psi_{yy}]_T = 0. \tag{4.75}$$

Integrating once, we obtain

$$\Psi_{yy} = \exp(-\nu T)q(y, X), \tag{4.76}$$

where $q(y, X)$ is the integration "constant". Since the mean flow correction is taken to be zero at $T = 0$, we may also take $\Psi_{yy}(T = 0) = 0$, without loss of generality. Applying this to (4.76) gives us $q(y, X) = 0$, and thus $\Psi_{yy} = 0$, implying that Ψ takes the form,

$$\Psi(y, X, T) = ya(X, T) + b(X, T) + d(X), \tag{4.77}$$

where $a(X, T)$, $b(X, T)$, and $d(X)$ are unknown.

We now derive a boundary condition on Ψ_{yT} at $y = 0, L$. The rate of change of the circulation, Γ, in the presence of dissipation, is given by (Pedlosky, 1987),

$$\frac{d\Gamma}{dt} = -\nu\Gamma, \tag{4.78}$$

where Γ is given by

$$\Gamma = \oint_c \mathbf{u}_2 \cdot d\mathbf{r}. \tag{4.79}$$

Writing (4.78) in terms of the lower layer streamfunction, we obtain

$$\frac{d}{dt}\int_{-x_1}^{x_1} p_y^{(0)} dx = -\nu \int_{-x_1}^{x_1} p_y^{(0)} dx + O(\delta^{\frac{1}{2}}), \text{ on } y = 0, L, \tag{4.80}$$

where we note that the domain is periodic in x, and we have taken the integral over a closed curve of length $2x_1$. Expanding (4.80) in an asymptotic series, adding in time scaling, and scaling the dissipation term, we obtain

$$\begin{aligned} &s(\partial_t + s\partial_T)\int_{-x_1}^{x_1} [(A\sin(ly) + s\tilde{p})_y \exp(ik\theta) + s\Psi_y] dx \\ &= -\nu s^2 \int_{-x_1}^{x_1} [(A\sin(ly) + s\tilde{p})_y \exp(ik\theta) + s\Psi_y] dx, \text{ on } y = 0, L. \end{aligned} \tag{4.81}$$

Since all terms with $\exp(ik\theta)$ integrate to zero, and Ψ is independent of x and t, to leading order, we have,

$$s^2\partial_T \int_{-x_1}^{x_1} s\Psi_y \, dx = -\nu s^2 \int_{-x_1}^{x_1} s\Psi_y \, dx, \text{ on } y = 0, L, \tag{4.82}$$

which simplifies to

$$\Psi_{yT} = -\nu\Psi_y, \text{ on } y = 0, L, \tag{4.83}$$

which implies

$$\Psi_y = q(X)\exp(\nu T), \text{ on } y = 0, L. \tag{4.84}$$

Since the mean flow correction is taken to be zero at $T = 0$, we may also take $\Psi_y(T = 0)$ to be zero at $T = 0$, without loss of generality, which implies that $q(X) = 0$. Thus, (4.84) becomes

$$\Psi_y = 0, \text{ on } y = 0, L. \tag{4.85}$$

Applying (4.85) to (4.77) shows us that $a(X, T) = 0$, and (4.77) becomes

$$\Psi(y, X, T) = b(X, T) + d(X), \text{ on } y = 0, L. \tag{4.86}$$

Since $\Psi(T = 0) = 0$, we require $b(X, 0) + d(X) = 0$ on $y = 0, L$. Thus, $d(X) = -b(X, 0)$, and

$$\Psi(y, X, T) = b(X, T) - b(X, 0). \tag{4.87}$$

However, since Ψ is a streamfunction and is only defined up to a constant (with respect to x and y), without loss of generality, we can set

$$\Psi(y, X, T) = 0. \tag{4.88}$$

We now assume the $O(s^2)$ problem to have normal mode solutions

$$p^{(2)} = \hat{p}(y, T)\exp(ik\theta) + c.c., \tag{4.89}$$

$$h^{(2)} = \hat{h}(y, T)\exp(ik\theta) + c.c., \tag{4.90}$$

and consider all terms with coefficient $\exp(\pm ik\theta)$. Upon dividing (4.65) and (4.66) by $ik\alpha_c$ and $-ick$ respectively, and applying (4.69) and (4.74), we obtain

$$\left[\partial_{yy} - k^2 - \frac{c}{\alpha_c}\right]\hat{h} + \hat{p} \tag{4.91}$$
$$= \frac{i}{k\alpha_c}[\partial_T + \nu]\tilde{h} - \left[\frac{1}{\alpha_c}(1-\mu K^2)\Phi_y + \frac{\mu}{\alpha_c}(-\Psi_y + \Phi_{yyy})\right] A\sin(ly)$$
$$-\alpha_c\left[\tilde{h}_y + \left(y - \frac{L}{2}\right)\left(\tilde{h}_{yy} - k^2\tilde{h}\right)\right] - \mu(\tau_o + \tau)\frac{1}{\alpha_c}A(1-\mu K^2)\sin(ly)$$
$$-ikA_X\left[2\mu - \frac{1}{k^2}(1-\mu K^2)\right]\sin(ly).$$

$$\left[\partial_{yy} + \frac{1-\alpha_c}{c} - k^2\right]\hat{p} + \hat{h} \tag{4.92}$$
$$= \frac{-i}{ck}[\partial_T + \nu](\tilde{h} + \tilde{p}_{yy} - k^2\tilde{p}) + \frac{1}{c}[\Psi_{yyy} + \Phi_y + (\mu - K^2)\Psi_y]A\sin(ly)$$
$$-A_X ik\left[2 + \frac{\alpha_c - 1}{ck^2}\right]\sin(ly) + \frac{1}{c}\mu(\tau_o + \tau)A\sin(ly).$$

Substituting in our solutions for Φ and Ψ,

$$\left[\partial_{yy} - k^2 - \frac{c}{\alpha_c}\right]\hat{h} + \hat{p} \tag{4.93}$$
$$= \frac{i}{k\alpha_c}[\partial_T + \nu]\tilde{h} + \left\{\frac{1}{\alpha_c}(1-\mu K^2)\left[\frac{2l^2}{c}(K^2-\mu)\cos(2ly)f(X,T)\right]\right.$$
$$\left.+\frac{\mu}{\alpha_c}\left[\frac{8l^4}{c}(K^2-\mu)\cos(2ly)f(X,T)\right]\right\}A\sin(ly)$$
$$-\alpha_c\left[\tilde{h}_y + \left(y - \frac{L}{2}\right)\left(\tilde{h}_{yy} - k^2\tilde{h}\right)\right] - \mu(\tau_o + \tau)\frac{1}{\alpha_c}A(1-\mu K^2)\sin(ly)$$
$$-ikA_X\left[2\mu - \frac{1}{k^2}(1-\mu K^2)\right]\sin(ly).$$

$$\left[\partial_{yy} + \frac{1-\alpha_c}{c} - k^2\right]\hat{p} + \hat{h} \tag{4.94}$$
$$= \frac{-i}{ck}[\partial_T + \nu](\tilde{h} + \tilde{p}_{yy} - k^2\tilde{p}) - 2\frac{l^2}{c^2}(K^2-\mu)cos(2ly)f(T)A\sin(ly)$$
$$-A_X ik\left[2 + \frac{\alpha_c - 1}{ck^2}\right]\sin(ly) + \frac{1}{c}\mu(\tau_o + \tau)A\sin(ly).$$

We will now derive a solvability condition for the system (4.93) and (4.94). We first write the system in the matrix form $\mathcal{L}\mathbf{b}(y) = \mathbf{F}(y)$, making use of the relation in (4.46):

$$\begin{bmatrix} \partial_{yy} + l^2 - \mu & 1 \\ 1 & \partial_{yy} + l^2 - \mu \end{bmatrix} \begin{bmatrix} \hat{h} \\ \hat{p} \end{bmatrix} = \begin{bmatrix} \text{RHS (4.93)} \\ \text{RHS (4.94)} \end{bmatrix} \tag{4.95}$$

As before, $\mathcal{L}$ is a self-adjoint operator.

We recall from §4.2.3 that the homogeneous problem,

$$\mathcal{L}\mathbf{b} = \mathbf{0}, \tag{4.96}$$

where

$$\mathbf{b} = \begin{bmatrix} \hat{h} \\ \hat{p} \end{bmatrix}, \tag{4.97}$$

and $\mathbf{b}(y) = \mathbf{0}$ on $y = 0, L$, has the solution

$$\mathbf{b}_o = \begin{bmatrix} A(X,T)\sin(ly) \\ \mu A(X,T)\sin(ly) \end{bmatrix}. \tag{4.98}$$

Since we have a self-adjoint operator for the homogeneous problem, and a nontrivial solution to the homogeneous problem exists, the Fredholm alternative theorem (Haberman, 1998) tells us that the nonhomogeneous problem has a solution if and only if $< \mathbf{b}_o, \mathbf{F} >= 0$ over the domain $y = [0, L]$, where

$$\mathbf{F} = \begin{bmatrix} \text{RHS (4.93)} \\ \text{RHS (4.94)} \end{bmatrix}. \tag{4.99}$$

Thus, the solvability condition on (4.93) and (4.94), is that their homogeneous solutions must be orthogonal to the inhomogeneity, ie.

$$\int_0^L (\text{RHS 4.93})\mu A \sin(ly)dy + \int_0^L (\text{RHS 4.94}) A \sin(ly)dy = 0, \tag{4.100}$$

which simplifies to:

$$\int_0^L \Bigg\{ \frac{i}{k}\left(\frac{\mu}{\alpha_c}-\frac{1}{c}\right)[\partial_T+\nu]\tilde{h} \tag{4.101}$$
$$-\frac{2l^2K^4(K^2-2\mu)^2}{K^2-\mu}[K^2(K^2-2\mu)-4l^2(K^2-\mu)]A\cos(2ly)\sin(ly)f(X,T)$$
$$-\mu\alpha_c\left[\tilde{h}_y+\left(y-\frac{L}{2}\right)\left(\tilde{h}_{yy}-k^2\tilde{h}\right)\right]$$
$$-\frac{i}{ck}[\partial_T+\nu]\left(\tilde{p}_{yy}-k^2\tilde{p}\right)+\mu(\tau_o+\tau)\left[\frac{-\mu}{\alpha_c}(1-\mu K^2)+\frac{1}{c}\right]A\sin(ly)$$
$$\left[-4k+\frac{\mu}{k}(1-\mu K^2)-\frac{\alpha_c-1}{ck}\right]iA_X\sin(ly)\Bigg\}A\sin(ly)dy=0.$$

Simplifying and rearranging, (4.101) becomes the *Amplitude Equation*,

$$[\partial_T+\nu]^2A(X,T)=\sigma(T)A(X,T)+iPA_X(X,T)-NA(X,T)Q(X,T), \tag{4.102}$$

where Q is defined by $[\partial_T+\nu]Q(X,T)=[\partial_T+2\nu](|A(X,T)|^2)$,

and where $Q(X,0)=0$, and our parameters are:

$$P=\frac{4\mu k^3(K^2-\mu)}{K^6(K^2-2\mu)^2}, \tag{4.103}$$

$$N=l^2k^2\left(2-\mu K^2+\frac{4\mu l^2}{K^2}(K^2-\mu)\right), \tag{4.104}$$

$$\sigma(T)=\frac{k^2}{K^2}(\tau_o+\tau) \tag{4.105}$$
$$-\alpha_c\frac{2k^2(K^2-\mu)}{LK^6(K^2-2\mu)^2}\int_0^L\left[h_{1y}+\left(y-\frac{L}{2}\right)(h_{1yy}-k^2h_1)\right]\sin(ly)dy,$$

where $h_1=-[\partial_{yy}+l^2-\mu]\left(\frac{\tilde{p}}{A}\right)$.

Note that $\sqrt{|\sigma|}=O(k/K)$ if $O(\alpha_c)$ terms are neglected, which is the order of the growth rate from linear theory. As well, we note that σ is now a function of T due to the addition of time variability in the supercriticality term, with $\sigma(0)$ being equal to the σ of Reszka (1997). Also, if $\tau(T)=0$, we have $\sigma(T)=\sigma(0)$.

4.2.5 The Lorenz Equivalent

In the case where we have no time variability in the perturbations (ie. $\tau(T)$=0), and the perturbation amplitude is real-valued (ie. $A_X = 0$), we can determine some stability properties of our amplitude equation by converting it into a Lorenz system. We will follow the procedure discussed in Klein and Pedlosky (1992). First, we note that the Lorenz equations with variables F,G, and H typically take the form

$$\begin{aligned} \frac{dF}{d\psi} &= -\phi F + \phi G, \\ \frac{dG}{d\psi} &= -FH + RF - G, \\ \frac{dH}{d\psi} &= FG - bH, \end{aligned} \tag{4.106}$$

where ϕ is the Prandtl number, R is the Rayleigh coefficient, and b is a secondary damping coefficient. Transforming these variables using

$$\begin{aligned} \xi\psi &= T, \\ F &= A_o A, \\ H &= \frac{A_o^2}{2\phi} Q, \end{aligned} \tag{4.107}$$

gives us

$$\begin{aligned} A_{TT} + \frac{\phi+1}{\xi} A_T - \frac{\phi(R-1)}{\xi} A + \frac{A_o^2}{2\xi^2} QA = 0, \\ Q_T + \frac{b}{\xi} Q = (A^2)_T + \frac{2\phi}{\xi} A^2. \end{aligned} \tag{4.108}$$

Writing the amplitude equation in the same form as (4.108):

$$\begin{aligned} A_{TT} + 2\nu A_T + (\nu^2 - \sigma^2) A + NAQ = 0, \\ Q_T + \nu Q = (A^2)_T + 2\nu A^2, \end{aligned} \tag{4.109}$$

and matching coefficients, gives us the relations

$$b = \phi = 1, \tag{4.110}$$

and

$$R = 1 + \frac{\sigma^2 - \nu^2}{\nu}. \tag{4.111}$$

The Raleigh number, R, is a measure of forcing in the Lorenz system (Klein and Pedlosky, 1992). It is necessary that $R > 1$ for there to be nontrivial asymptotic solutions to the Lorenz system (Klein and Pedlosky, 1992). We note that $R > 1$ whenever $\sigma^2 > \nu^2$. That is, the damping coefficient cannot be too large.

The steady solutions are linearly stable since $\phi < b+1$ (Klein and Pedlosky, 1992). In addition, when the Prandtl number is one, for arbitrarily large R, the asymptotic solutions to our system are always stable (Klein and Pedlosky, 1992), meaning that chaotic or self-maintained periodic behaviour cannot take place (Pedlosky and Thomson, 2003). This result tells us that the observation of non-trivial time dependence in our solutions is due to the presence of the time-varying component of the perturbations.

Chapter 5

Solutions to the Amplitude Equation

5.1 Introduction

To determine underlying properties and analyse how the Reszka (1997) solution changes with the addition of time variability and dissipation, we omit the slow space term, A_X, in this chapter. Without the slow space term, $A(X,T)$ is real-valued, and we denote it by $R(T)$. Now, (4.102) becomes

$$\begin{aligned} [\partial_T + \nu]^2 R &= \sigma R - NRQ, \\ [\partial_T + \nu]Q &= [\partial_T + 2\nu]R^2. \end{aligned} \tag{5.1}$$

with initial conditions,

$$R(0) = 0, \;\; R_T(0) = \sqrt{|\sigma(0)|}R_o, \;\; Q(0) = 0. \tag{5.2}$$

This particular linear growth rate $\sqrt{|\sigma(0)|}$ was chosen since the solution to

$$R_{TT} = \sigma(0)R, \quad R(0) = 0 \tag{5.3}$$

is

$$\begin{aligned} R(T) &= R_o \sinh(T\sqrt{\sigma(0)}), \quad \sigma > 0, \\ R(T) &= R_o \sin(T\sqrt{|\sigma(0)|}), \quad \sigma < 0. \end{aligned} \tag{5.4}$$

We will review the solution presented in Reszka (1997) for the case where the time variability and dissipation terms are absent. Next, we will compare these solutions to numerical solutions with $\tau_o + \tau$ nonzero, and no dissipation. Then, we take several curves with specific characteristics, and examine the influence of dissipation.

5.2 The case where $\tau(T) = 0$ and $\nu = 0$

In the case where $\tau(T) = 0$ and $\nu = 0$, the amplitude equation can be solved analytically following Reszka (1997). Substituting $\tau(T) = 0$ and $\nu = 0$ into (5.1), we obtain

$$R_{TT} = \sigma(0)R - NR(R^2 - R_o^2), \tag{5.5}$$

with initial conditions

$$R(0) = R_o \text{ and } \frac{\partial}{\partial T}R(0) = \sqrt{|\sigma(0)|}R_o. \tag{5.6}$$

For the remainder of this section, we will use σ to denote $\sigma(0)$.

Multiplying (5.5) by R_T, and integrating, gives us

$$R_T^2 = \sigma R^2 + (|\sigma| - \sigma)R_o^2 - \frac{N}{2}(R^2 - R_o^2)^2. \tag{5.7}$$

Equation (5.7) may be solved by considering four regions (defined by the signs of N and σ):

$$\{\{N < 0, \sigma < 0\}, \{N > 0, \sigma < 0\}, \{N > 0, \sigma > 0\}, \{N < 0, \sigma > 0\}\}, \tag{5.8}$$

which we will denote as Regions I, II, III, and IV respectively. Given values for μ, L, and n, we can determine which region we are in, for any given k, by examining a plot of N and σ versus k. Since the upper and lower branches exhibit similar behaviour in the same regions, we have chosen to examine the lower branch only, and have chosen the parameters $L = 8$ and $n = 1$. A plot of N and σ versus k with those parameters is given in Figure 5.1.

We will demonstrate properties of the solutions in the first three regions by choosing $K^2 = \{0.1, 0.4, 1.4\}$, which correspond to $k \approx \{0.23, 0.50, 1.12\}$,

and are in regions I, II, and III respectively. We continue using the parameters $L = 8$ and $n = 1$, and consider solutions with a supercriticality only, ie. $\tau_o = 1$. We also consider solutions only on the lower branch, since, as described above, there is similar behaviour in both the upper and lower branches of the MSC.

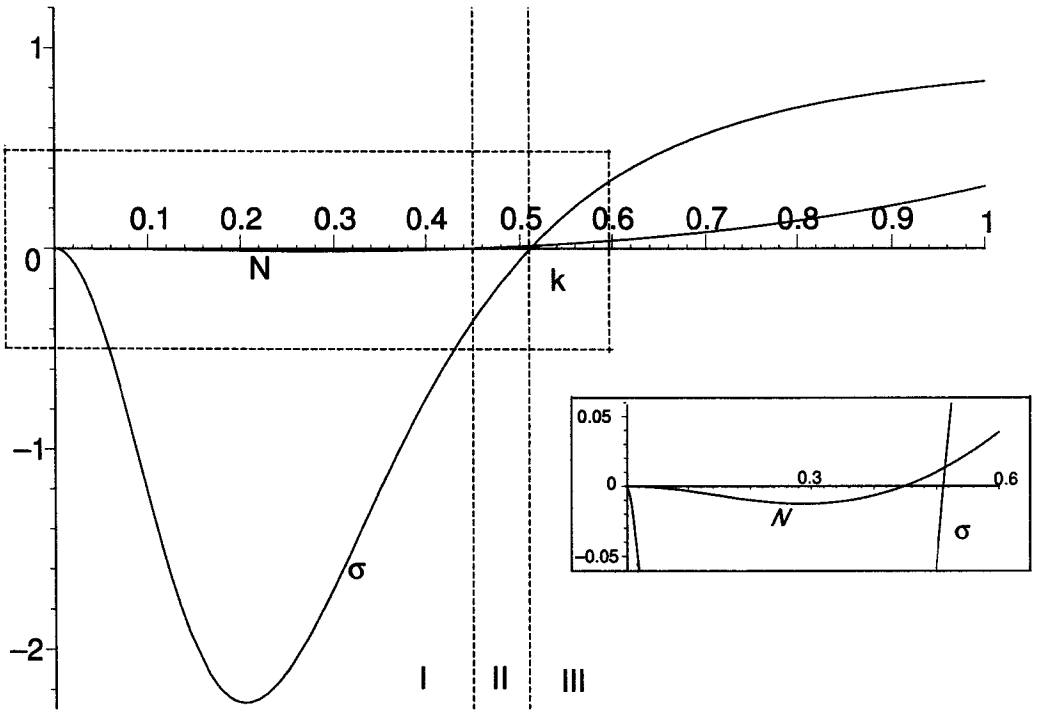

Figure 5.1: N and σ versus k on the lower branch where $L = 8$, and $n = 1$. Inset corresponds to blow up of region in dotted box.

5.2.1 Region I

Substituting $\sigma < 0$ and $N < 0$ into (5.7), and simplifying, we obtain

$$R_T^2 = -\frac{N}{2}\left(R^2 - R_o^2 - \frac{\sigma}{N}\right)^2 - \sigma\left(R_o^2 - \frac{\sigma}{2N}\right). \tag{5.9}$$

Next, we transform the variables using

$$R = \sqrt{\frac{2\sigma}{N}}P, \quad R_o = \sqrt{\frac{2\sigma}{N}}P_o, \quad T = \frac{\kappa}{\sqrt{-\sigma}}, \tag{5.10}$$

which allows (5.9) to be rewritten as

$$\left(\frac{dP}{d\kappa}\right)^2 = \left(P^2 - P_o^2 - \frac{1}{2}\right)^2 + P_o^2 - \frac{1}{4}, \tag{5.11}$$

which can be separated into three cases: $P_o^2 = \frac{1}{4}$, $P_o^2 < \frac{1}{4}$, and $P_o^2 > \frac{1}{4}$.

Case 1: $P_o^2 = \frac{1}{4}$ (i.e. P_o is either $-\frac{1}{2}$ or $\frac{1}{2}$)

Here, (5.11) simplifies to

$$\left(\frac{dP}{d\kappa}\right)^2 = \left(P^2 - \frac{3}{4}\right)^2. \tag{5.12}$$

First, we consider the case of $P_o = \frac{1}{2}$, which gives us $\frac{dP}{d\kappa}(0) = \frac{1}{2} > 0$. It will be shown *a posteriori* that $|P| \leq \frac{\sqrt{3}}{2}$, which allows us to solve for $\frac{dP}{d\kappa}$,

$$\frac{dP}{d\kappa} = \left|P^2 - \frac{3}{4}\right| = \frac{3}{4} - P^2. \tag{5.13}$$

Separation of variables gives us the integral

$$\int_{P_o}^{P} \frac{d\xi}{\xi^2 - \frac{3}{4}} = -\int_0^{\kappa} d\kappa, \tag{5.14}$$

which, upon integrating and substituting in $P_o = \frac{1}{2}$, gives us

$$\kappa = \frac{1}{\sqrt{3}} \ln\left|\frac{(\sqrt{3}+2P)(\sqrt{3}-1)}{(\sqrt{3}-2P)(\sqrt{3}+1)}\right|. \tag{5.15}$$

Now, solving for P as a function of κ,

$$P(\kappa) = \left(\frac{\sqrt{3}}{2}\right)\frac{1-\sqrt{3}+(1+\sqrt{3})\exp(\sqrt{3}\kappa)}{\sqrt{3}-1+(1+\sqrt{3})\exp(\sqrt{3}\kappa)}. \tag{5.16}$$

We note that $P(0) = \frac{1}{2}$ and $|P| \leq \frac{\sqrt{3}}{2}$ as required. Applying the same approach for $P_o = -\frac{1}{2}$, we get

$$P(\kappa) = -\left(\frac{\sqrt{3}}{2}\right)\frac{1-\sqrt{3}+(1+\sqrt{3})\exp(\sqrt{3}\kappa)}{\sqrt{3}-1+(1+\sqrt{3})\exp(\sqrt{3}\kappa)}. \tag{5.17}$$

Case 2: $P_o^2 < \frac{1}{4}$

Since $P_o^2 < \frac{1}{4}$, the constant in (5.11) is negative, and we factor the quadratic as

$$\left(\frac{dP}{d\kappa}\right)^2 = (\beta^2 - P^2)(\zeta^2 - P^2), \tag{5.18}$$

where we have introduced the constants

$$\beta^2 = P_o^2 + \frac{1}{2} + \sqrt{\frac{1}{4} - P_o^2} > 0, \tag{5.19}$$

and

$$\zeta^2 = P_o^2 + \frac{1}{2} - \sqrt{\frac{1}{4} - P_o^2} > 0. \tag{5.20}$$

Without loss of generality, we take β and ζ to be positive quantities. To simplify the equation, we define new variables by

$$P = \beta Q, \quad P_o = \beta Q_o, \tag{5.21}$$

and (5.18) becomes

$$\left(\frac{dQ}{d\kappa}\right)^2 = \beta^2(1-Q^2)(m^2-Q^2), \tag{5.22}$$

where $m = \frac{\zeta}{\beta}$, with $0 < m < 1$.

We will start by solving for the case where $P_o > 0$ (noting that $\frac{dP}{d\kappa}(0) > 0$ here). Examining (5.22), we see that $|Q| < m$ necessarily, allowing us to take the square root of both sides, which gives us

$$\frac{dQ}{d\kappa} = \beta\sqrt{(1-Q^2)(m^2-Q^2)}, \tag{5.23}$$

which can be rewritten as the integral

$$\int_{Q_o}^{Q} \frac{d\xi}{\sqrt{(1-\xi^2)(m^2-\xi^2)}} = \beta\int_0^{\kappa} d\kappa. \tag{5.24}$$

Once put in standard form, we will see that this is an elliptic integral which may be solved for Q with the use of function tables (Milne-Thomson, 1950).

We decompose the left hand side into two parts, and evaluate the right hand side (making use of the fact that $0 < Q < Q_o$ for $P_o > 0$),

$$\int_0^Q \frac{d\xi}{\sqrt{(1-\xi^2)(m^2-\xi^2)}} - \int_0^{Q_o} \frac{d\xi}{\sqrt{(1-\xi^2)(m^2-\xi^2)}} = \beta\kappa. \tag{5.25}$$

Upon rearranging, this becomes

$$\int_0^Q \frac{d\xi}{\sqrt{(1-\xi^2)(m^2-\xi^2)}} = \beta(\kappa - \kappa_o), \tag{5.26}$$

where

$$\kappa_o = -\frac{1}{\beta}\int_0^{Q_o} \frac{d\xi}{\sqrt{(1-\xi^2)(m^2-\xi^2)}}. \tag{5.27}$$

From Milne-Thomson (1950), the left hand side of (5.26) has the solution

$$\int_0^Q \frac{d\xi}{\sqrt{(1-\xi^2)(m^2-\xi^2)}} = \mathrm{sn}^{-1}\left(\frac{Q}{m}\middle| m^2\right), \tag{5.28}$$

where we have made use of the relation $Q < m < 1$, and $\mathrm{sn}(\cdot)$ is the Jacobi elliptic snoidal function. Substituting (5.28) into (5.26), we obtain the relation

$$\mathrm{sn}^{-1}\left(\frac{Q}{m}\middle| m^2\right) = \beta(\kappa - \kappa_o), \tag{5.29}$$

which we then invert, and multiply through by m, to obtain

$$Q = m\ \mathrm{sn}\ (\beta(\kappa - \kappa_o)|m^2). \tag{5.30}$$

Transforming back into our original variables, R and T, we have

$$R = \sqrt{\frac{2\sigma}{N}}\beta m\ \mathrm{sn}\ (\beta(\sqrt{-\sigma}T - \kappa_o)|m^2). \tag{5.31}$$

We have plotted this solution in Figure 5.2, where we have used the parameter values $\mu = -1$, $L = 8$, $\tau_o = 1$, and $K^2 = 0.1$. The curve is periodic and has a period of approximately 4.2.

Solving similarly for the $P_o < 0$ case (making use of the fact that $0 > Q > Q_o$ for $P_o < 0$), we obtain

$$Q = -m\ \mathrm{sn}\ (\beta(\kappa - \kappa_o)|m^2), \tag{5.32}$$

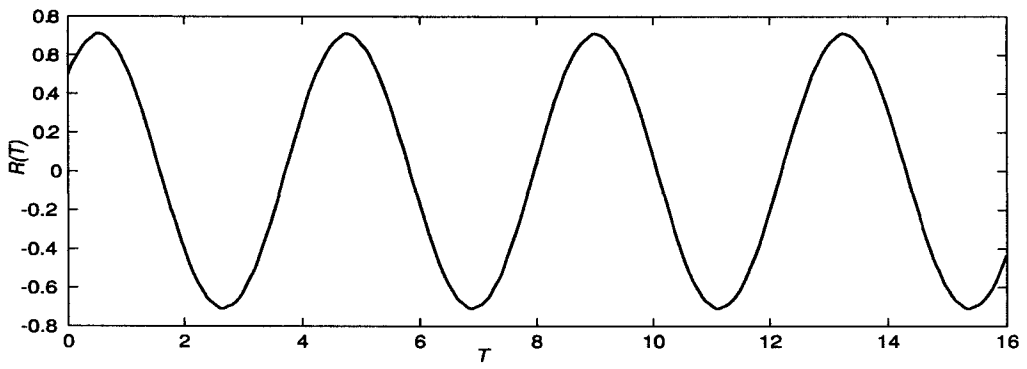

Figure 5.2: R vs. T on the lower branch with $K^2 = 0.1$, $L = 8$, and $\tau_o = 1$ in Region II.

where

$$\kappa_o = \frac{1}{\beta}\int_0^{Q_o} \frac{d\xi}{\sqrt{(1-\xi^2)(m^2-\xi^2)}}\,. \tag{5.33}$$

Case 3: $P_o^2 > \frac{1}{4}$

We will show that the solution is unbounded, and that it becomes arbitrarily large in a finite time, when $P_o^2 > \frac{1}{4}$. Since $P_o^2 - \frac{1}{4}$ is now a strictly positive quantity, so too is the right hand side of equation (5.11). Taking the square root of both sides, we see that P will approach either ∞ or $-\infty$ depending on the sign of $P_\kappa(0)$. We will prove the result for the case $P_\kappa(0) > 0$, noting that the case $P_\kappa(0) < 0$ is proven by the equivalent argument.

Claim: P becomes arbitrarily large in finite time if $P_o^2 > \frac{1}{4}$

Proof: We know that P grows monotonically without bound. The time required for $P \to \infty$ can be written as the integral

$$\kappa^* = \int_{P_o}^{\infty} \frac{dP}{\sqrt{(P^2 - P_o^2 - \frac{1}{2})^2 + P_o^2 - \frac{1}{4}}}\,, \tag{5.34}$$

which may be rewritten as the sum of two integrals,

$$\kappa^* = \int_{P_o}^{P^*} \frac{dP}{\sqrt{(P^2 - P_o^2 - \frac{1}{2})^2 + P_o^2 - \frac{1}{4}}} + \int_{P^*}^{\infty} \frac{dP}{\sqrt{(P^2 - P_o^2 - \frac{1}{2})^2 + P_o^2 - \frac{1}{4}}}\,, \tag{5.35}$$

for any $P^* > \sqrt{P_o^2 + \frac{1}{2}}$.

Examining (5.35), we see that it satisfies

$$\kappa^* < I_1 + I_2, \tag{5.36}$$

where

$$I_1 = \int_{P_o}^{P^*} \frac{dP}{\sqrt{(P^2 - P_o^2 - \frac{1}{2})^2 + P_o^2 - \frac{1}{4}}}, \tag{5.37}$$

with I_1 finite, and

$$I_2 = \int_{P^*}^{\infty} \frac{dP}{\left|P^2 - P_o^2 - \frac{1}{2}\right|}. \tag{5.38}$$

Since $P^2 - P_o^2 - \frac{1}{2} > 0$ for all $P \geq P^*$, we can remove the absolute value signs, and integrate to obtain

$$\begin{aligned} I_2 &= \lim_{l\to\infty} \int_{P^*}^{l} \frac{dP}{P^2 - a^2} \quad \text{where } a^2 = P_o^2 + \frac{1}{2} \\ &= \lim_{l\to\infty} \frac{1}{2a} \ln\left|\frac{l-a}{l+a}\right| - \frac{1}{2a} \ln\left|\frac{P^*-a}{P^*+a}\right| \\ &= \frac{1}{2a}\ln(1) - \frac{1}{2a}\ln\left|\frac{P^*-a}{P^*+a}\right| \\ &= \frac{1}{2a}\ln\left|\frac{P^*+a}{P^*-a}\right| < \infty. \end{aligned} \tag{5.39}$$

Since I_1 and I_2 are both finite, κ^* is also finite. **QED**

5.2.2 Region II

Substituting $\sigma < 0$ and $N > 0$ into (5.7), and simplifying, we obtain

$$R_T^2 = -\frac{N}{2}\left(R^2 - R_o^2 - \frac{\sigma}{N}\right)^2 - \sigma\left(R_o^2 - \frac{\sigma}{2N}\right). \tag{5.40}$$

Next, we transform the variables using

$$R = \sqrt{\frac{-2\sigma}{N}}P, \quad R_o = \sqrt{\frac{-2\sigma}{N}}P_o, \quad T = \frac{\kappa}{\sqrt{-\sigma}}, \tag{5.41}$$

which allows (5.40) to be written as

$$\left(\frac{dP}{d\kappa}\right)^2 = P_o^2 + \frac{1}{4} - \left(P^2 - P_o^2 + \frac{1}{2}\right)^2. \tag{5.42}$$

Since $P_o^2 + \frac{1}{4}$ is strictly positive, (5.42) may be factored as,

$$\left(\frac{dP}{d\kappa}\right)^2 = \left(\sqrt{P_o^2 + \frac{1}{4}} - P^2 + P_o^2 - \frac{1}{2}\right)\left(\sqrt{P_o^2 + \frac{1}{4}} + P^2 - P_o^2 + \frac{1}{2}\right). \tag{5.43}$$

Since $\sqrt{P_o^2 + \frac{1}{4}} + P_o^2 - \frac{1}{2} > 0$, there are three cases, $P_o^2 = 2$, $P_o^2 < 2$, and $P_o^2 > 2$.

Case 1: $P_o^2 = 2$

Here, equation (5.42) simplifies to

$$\left(\frac{dP}{d\kappa}\right)^2 = \frac{9}{4} - \left(P^2 - \frac{3}{2}\right)^2 = P^2(3 - P^2). \tag{5.44}$$

We define new variables

$$P = \sqrt{3}Q, \quad P_o = \sqrt{3}Q_o, \tag{5.45}$$

and apply separation of variables to obtain

$$\int_{Q_o}^{Q} \frac{d\xi}{\sqrt{\xi^2(1-\xi)^2}} = \sqrt{3}\int_0^{\kappa} d\kappa. \tag{5.46}$$

This equation may be solved by making a change of variables

$$\xi = \sin\,\theta\,, \quad d\xi = \cos\,\theta\,d\theta, \tag{5.47}$$

to obtain the solution

$$\begin{aligned} \kappa &= -\frac{1}{\sqrt{3}} \ln|\csc\,\theta - \cot\,\theta| + const \\ &= -\frac{1}{\sqrt{3}} \ln\left|\frac{1+\sqrt{1-\xi^2}}{\xi}\right|_{Q_o}^{Q}, \end{aligned} \tag{5.48}$$

which, after applying

$$Q_o = \frac{1}{\sqrt{3}}\,, \quad P_o = \sqrt{\frac{2}{3}}, \tag{5.49}$$

and taking the exponential of both sides, becomes

$$\exp[-\sqrt{3}\kappa] = \frac{1+\sqrt{1-Q^2}}{Q}\,\frac{\sqrt{2}/\sqrt{3}}{1+\sqrt{1-2/3}}\,. \tag{5.50}$$

Solving for Q, we obtain

$$Q = \sqrt{2}\left(\left(\frac{\sqrt{3}-1}{2}\right)\exp[\sqrt{3}\kappa] + \left(\frac{\sqrt{3}+1}{2}\right)\exp[-\sqrt{3}\kappa]\right)^{-1}. \tag{5.51}$$

Finally, we can find $P(\kappa)$ by application of (5.45).

Case 2: $P_o^2 < 2$

Here, equation (5.42) simplifies to

$$\left(\frac{dP}{d\kappa}\right)^2 = (P^2+\zeta^2)(\beta^2 - P^2), \tag{5.52}$$

with

$$\beta^2 = P_o^2 - \frac{1}{2} + \sqrt{P_o^2 + \frac{1}{4}} > 0, \tag{5.53}$$

and

$$\zeta^2 = -P_o^2 + \frac{1}{2} + \sqrt{P_o^2 + \frac{1}{4}} > 0\,. \tag{5.54}$$

We then substitute the transformation

$$P = \beta Q, \quad P_o = \beta Q_o, \tag{5.55}$$

into (5.52), to get

$$\left(\frac{dQ}{d\kappa}\right)^2 = \beta^2(Q^2+m^2)(1-Q^2), \tag{5.56}$$

where $m = \frac{\zeta}{\beta}$, and $0 < m < 1$. We note that, given the form of (5.56), necessarily we have $0 < Q < 1$.

Transforming (5.56) into integral form, we get the elliptic integral

$$\int_{Q_o}^{Q} \frac{d\xi}{\sqrt{(\xi^2+m^2)(1-\xi^2)}} = \beta\int_0^{\kappa} d\kappa. \tag{5.57}$$

Following the procedure used previously, we rewrite the left hand side as two integrals, and evaluate the right hand side,

$$\int_{Q_o}^{1} \frac{d\xi}{\sqrt{(\xi^2+m^2)(1-\xi^2)}} - \int_{Q}^{1} \frac{d\xi}{\sqrt{(\xi^2+m^2)(1-\xi^2)}} = \beta\kappa, \tag{5.58}$$

which we rearrange to obtain

$$\int_{Q}^{1} \frac{d\xi}{\sqrt{(\xi^2+m^2)(1-\xi^2)}} = -\beta(\kappa - \kappa_o), \tag{5.59}$$

where

$$\kappa_o = \frac{1}{\beta}\int_{Q_o}^{1} \frac{d\xi}{\sqrt{(\xi^2+m^2)(1-\xi^2)}}\,. \tag{5.60}$$

We note that the left hand side of (5.59) can now be solved using integral tables (Milne-Thomson, 1950), where we have used the fact that $0 < Q < 1$, to obtain

$$\int_{Q}^{1} \frac{d\xi}{\sqrt{(\xi^2+m^2)(1-\xi^2)}} = \frac{1}{\sqrt{1+m^2}}\mathrm{cn}^{-1}\left(Q\middle|\frac{1}{1+m^2}\right), \tag{5.61}$$

where cn $(\cdot)$ denotes the Jacobi cnoidal function. Substituting this relation into 5.59, and multiplying through by $\sqrt{1+m^2}$ gives

$$\mathrm{cn}^{-1}\left(Q\middle|\frac{1}{1+m^2}\right) = -\sqrt{1+m^2}\beta(\kappa-\kappa_o). \tag{5.62}$$

Inverting this relation, and noting that the cnoidal function is even about zero, we obtain the solution

$$Q = \mathrm{cn}\left(\sqrt{m^2+1}\beta(\kappa-\kappa_o)\middle|\frac{1}{m^2+1}\right). \tag{5.63}$$

Transforming back into original variables ($R(T)$ and T), we find

$$R(T) = \beta\sqrt{\frac{2\sigma}{N}}\,\mathrm{cn}\left(\sqrt{m^2+1}\beta(\sqrt{-\sigma T}-\kappa_o)\middle|\frac{1}{m^2+1}\right) \tag{5.64}$$

This is plotted in Figure (5.3) with parameter values $\mu = -1$, $K^2 = 0.4$, $\tau_o = 1$, and $L = 8$. This curve is periodic as well with a period of approximately 22.

Case 3: $P_o^2 > 2$

Here, equation (5.42) simplifies to

$$\left(\frac{dP}{d\kappa}\right)^2 = (P^2-\zeta^2)(\beta^2-P^2), \tag{5.65}$$

with

$$\beta^2 = P_o^2 - \frac{1}{2} + \sqrt{P_o^2+\frac{1}{4}} > 0, \tag{5.66}$$

and

$$\zeta^2 = P_o^2 - \frac{1}{2} - \sqrt{P_o^2+\frac{1}{4}} > 0\,. \tag{5.67}$$

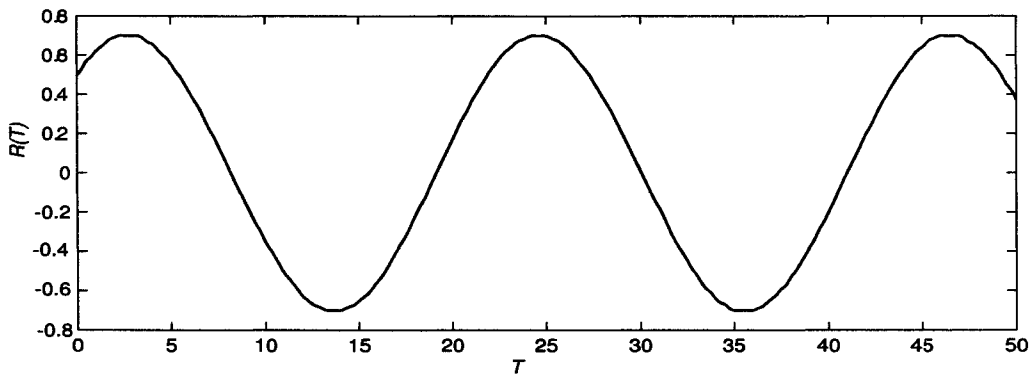

Figure 5.3: R vs. T on the lower branch with $K^2 = 0.4$, $L = 8$, and $\tau_o = 1$ in Region II.

Substituting the transformation

$$P = \beta Q \quad P_o = \beta Q_o, \tag{5.68}$$

we get

$$\left(\frac{dQ}{d\kappa}\right)^2 = \beta^2(Q^2 - m^2)(1 - Q^2), \tag{5.69}$$

where $m = \frac{\zeta}{\beta}$, with $0 < m < 1$. We note that the form of (5.69), combined with the bounds on m, imply that $m < Q < 1$.

Taking the square root of both sides and writing in integral form, we have

$$\int_{Q_o}^{Q} \frac{d\xi}{\sqrt{(\xi^2 - m^2)(1 - \xi^2)}} = \beta \int_0^{\kappa} d\kappa\,. \tag{5.70}$$

We now split the left hand side into two integrals, and evaluate the right hand side, to obtain

$$\int_{Q_o}^{1} \frac{d\xi}{\sqrt{(\xi^2 - m^2)(1 - \xi^2)}} - \int_{Q}^{1} \frac{d\xi}{\sqrt{(\xi^2 - m^2)(1 - \xi^2)}} = \beta\kappa, \tag{5.71}$$

which we then rearrange to get

$$\int_{Q}^{1} \frac{d\xi}{\sqrt{(\xi^2 - m^2)(1 - \xi^2)}} = -\beta(\kappa - \kappa_o), \tag{5.72}$$

where

$$\kappa_o = \frac{1}{\beta} \int_{Q_o}^{1} \frac{d\xi}{\sqrt{(\xi^2 - m^2)(1 - \xi^2)}}\,. \tag{5.73}$$

The left hand side of (5.72) is an elliptic integral whose solution is given by (Milne-Thomson, 1950)

$$\int_Q^1 \frac{d\xi}{\sqrt{(\xi^2 - m^2)(1-\xi^2)}} = \mathrm{dn}^{-1}(Q|1-m^2), \tag{5.74}$$

where $\mathrm{dn}(\cdot)$ denotes the Jacobi dnoidal integral making use of the relation $m < Q < 1$.

Substituting this into (5.72), we obtain

$$\mathrm{dn}^{-1}(Q|1-m^2) = -\beta(\kappa - \kappa_o). \tag{5.75}$$

Inverting, and using the fact that the Jacobi dnoidal function is even about zero, we finally have

$$Q = \mathrm{dn}\left(\beta(\kappa - \kappa_o)|1-m^2\right). \tag{5.76}$$

5.2.3 Region III

Substituting $\sigma > 0$ and $N > 0$ into (5.7), we obtain

$$R_T^2 = \sigma R^2 - \frac{N}{2}(R^2 - R_o^2)^2. \tag{5.77}$$

Applying the transformation

$$R = \sqrt{\frac{2\sigma}{N}}P, \quad R_o = \sqrt{\frac{2\sigma}{N}}P_o, \quad T = \frac{\kappa}{\sqrt{\sigma}}, \tag{5.78}$$

we have

$$\left(\frac{dP}{d\kappa}\right)^2 = -P^4 + (2P_o^2 + 1)P^2 - P_o^4. \tag{5.79}$$

We now rearrange (5.79) to obtain

$$-\frac{P_o^4}{2} = \frac{1}{2}\left(\frac{dP}{d\kappa}\right)^2 + \left(\frac{P^4}{2} - \left(P_o^2 + \frac{1}{2}\right)P^2\right). \tag{5.80}$$

Looking at (5.5), we notice that it has the same form as the equation governing the rectilinear motion of a particle under the action of a restoring force, that is dependent on displacement alone (ie. the harmonic oscillator). Thus, we can consider (5.80) as a decomposition of total energy, E, into kinetic energy

(KE) and potential energy (PE), where $E = -\frac{P_o^4}{2}$, and $KE = \frac{1}{2}\left(\frac{dP}{d\kappa}\right)^2$. Then, we see that $PE = \frac{1}{2}P^4 - \left(P_o^2 + \frac{1}{2}\right)P^2$.

The maximum value of P occurs where the total energy of the system is in potential form. Thus, we can find the maximum value of P by setting the kinetic energy to zero, which results in the relation

$$-P^4 + (2P_o^2 + 1)P^2 - P_o^4 = 0. \tag{5.81}$$

Applying the quadratic formula, we obtain

$$P_{\max}^2, P_{\min}^2 = \left(P_o^2 + \frac{1}{2}\right) \pm \frac{1}{2}\sqrt{4P_o^2 + 1}\,. \tag{5.82}$$

We may write (5.79) in the form

$$\left(\frac{dP}{d\kappa}\right)^2 = -(P^2 - P_{\max}^2)(P^2 - P_{\min}^2). \tag{5.83}$$

To simplify, we rewrite the previous equation by normalizing our amplitude

$$Q = \frac{P}{P_{\max}}\,, \tag{5.84}$$

scaling time

$$\kappa' = P_{\max}\kappa\,, \tag{5.85}$$

and defining a new variable β by

$$\beta = \frac{P_{\min}}{P_{\max}}\,, \tag{5.86}$$

where we see $0 < \beta < 1$, resulting in a new equation,

$$\left(\frac{dQ}{d\kappa'}\right)^2 = (1 - Q^2)(Q^2 - \beta^2). \tag{5.87}$$

We note that, due to the form of this equation, together with the bounds on β, we must have that $\beta < Q < 1$. This equation can be rewritten as

$$\int_0^{\kappa'} d\kappa' = \int_{Q_o}^{Q} \frac{dQ}{\sqrt{(1 - Q^2)(Q^2 - \beta^2)}}, \tag{5.88}$$

to which we apply the same techniques used in our Region II dnoidal solution, to arrive at the solution

$$Q = \mathrm{dn}\,(\kappa' - \kappa_o'|1 - \beta^2), \tag{5.89}$$

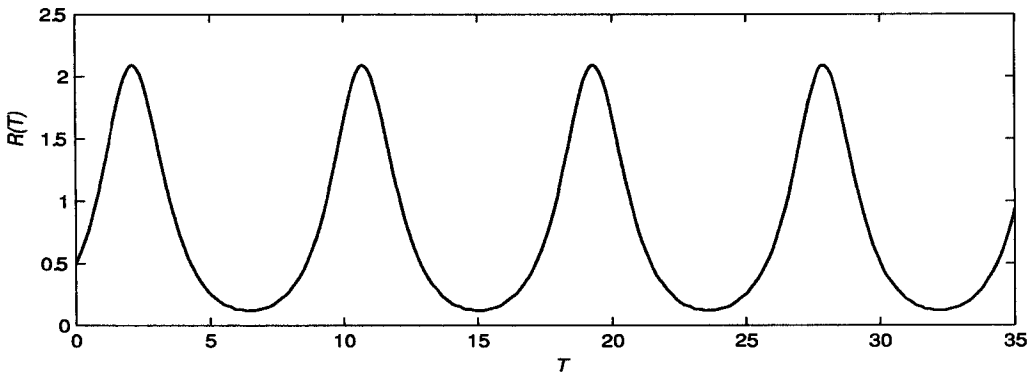

Figure 5.4: R vs. T on the lower branch with $K^2 = 1.4$, $\tau_o = 1$, and $L = 8$ in Region III.

where κ'_o is defined as

$$\kappa'_o = \int_{Q_o}^{1} \frac{dQ}{\sqrt{(1-Q^2)(Q^2-\beta^2)}}\,. \tag{5.90}$$

Transforming back into our original variables, the solution for R is given by

$$R = \sqrt{\frac{2\sigma}{N}} P_{\max} \mathrm{dn}(\kappa' - \kappa'_o | 1-\beta^2), \tag{5.91}$$

which we have plotted in Figure 5.4 with parameter values $K^2 = 1.4$, $\tau_o = 1$, $L = 8$, and $\mu = -1$. The solution is bounded above zero, having a period of approximately 7.5; we also note that the function has softer troughs and sharper peaks when compared to a sinusoidally shaped function.

5.2.4 Region IV

Substituting $\sigma > 0$ and $N < 0$ into (5.7), and simplifying, we obtain

$$R_T^2 = \sigma R^2 - 2\sigma R_o^2 - \frac{N}{2}(R^2 - R_o^2)^2\,. \tag{5.92}$$

Next, we transform the variables using

$$R = \sqrt{-\frac{2\sigma}{N}} P\,, \quad R_o = \sqrt{-\frac{2\sigma}{N}} P_o\,, \quad T = \frac{\kappa}{\sqrt{\sigma}}\,, \tag{5.93}$$

which allows (5.92) to be rewritten as

$$\left(\frac{dP}{d\kappa}\right)^2 = \left(P^2 - P_o^2 + \frac{1}{2}\right)^2 + P_o^2 - \frac{1}{4}. \tag{5.94}$$

When $P_o^2 > \frac{1}{4}$, the right hand side of (5.94) is strictly positive, resulting in P_κ itself being strictly positive. We rewrite (5.94) as

$$\left(\frac{dP}{d\kappa}\right)^2 = P^4 + (1 - 2P_o^2)P^2 + P_o^4. \tag{5.95}$$

Inspecting the equation in its above form, we see that for $0 \leq P_o^2 \leq \frac{1}{4}$, the coefficient of P^2 is positive, and, as a result, $\frac{dP}{d\kappa}$ is strictly positive here as well. Thus, one may conclude that P, and likewise R, grows either positively or negatively without bound. We now prove that this occurs in finite time. We consider only the case where $P \to \infty$, as the other case is proved similarly. Also, we neglect the situation where $P_o^2 = 0$, since, as we see from (5.4), when $P_o^2 = 0$, $R(T)$ is trivially 0 everywhere (for all σ).

Claim: P becomes arbitrarily large in finite time in Region IV.

Proof: We have already established that P grows monotonically and without bound. By applying separation of variables to (5.95), the time required for $P \to \infty$ may be written as the integral

$$\kappa^* = \int_{P_o}^{\infty} \frac{dP}{\sqrt{P^4 + (1 - 2P_o^2)P^2 + P_o^4}}. \tag{5.96}$$

We consider this under two cases. First, we look at $P_o^2 \leq \frac{1}{2}$. In this case, the denominator in the integral is strictly positive, and we have the following relation for κ^*:

$$\kappa^* < \int_{P_o}^{\infty} \frac{dP}{\sqrt{P^4}} = \int_{P_o}^{\infty} \frac{dP}{P^2}, \tag{5.97}$$

which is a finite integral since the exponent on P is greater than one.

Now, looking at the $P_o^2 > \frac{1}{2}$ case, we write (5.96) in the form

$$\kappa^* = \int_{P_o}^{\infty} \frac{dP}{\sqrt{\left(P^2 - P_o^2 + \frac{1}{2}\right)^2 + P_o^2 - \frac{1}{4}}}. \tag{5.98}$$

Since $P_o^2 - \frac{1}{4}$ is strictly greater than zero, we arrive at the inequality

$$\kappa^* < \int_{P_o}^{\infty} \frac{dP}{\left|P^2 - P_o^2 + \frac{1}{2}\right|}. \tag{5.99}$$

As P is monotonically increasing, $P^2 - P_o^2 + \frac{1}{2}$ is strictly greater than zero, and we may omit the absolute value signs. To find a bound on the inequality, we integrate the right hand side directly, and introduce a new variable $a^2 = P_o^2 - 1/2 > 0$,

$$\kappa^* < \int_{P_o}^{\infty} \frac{dP}{P^2 - P_o^2 + \frac{1}{2}} = \int_{P_o}^{\infty} \frac{dP}{P^2 - a^2} \tag{5.100}$$

$$= \lim_{l \to \infty} \left[\frac{1}{2a} \ln \left| \frac{P-a}{P+a} \right| \right]_{P_o}^{l} \tag{5.101}$$

$$= \frac{1}{2a} \left(\ln(1) - \ln \left| \frac{P_o - a}{P_o + a} \right| \right) \tag{5.102}$$

$$= \frac{1}{2a} \ln \left| \frac{P_o + a}{P_o - a} \right| < \infty. \tag{5.103}$$

Therefore, κ^* is finite, and P will become arbitrarily large in finite time. **QED**

5.3 Solutions on the Lower Branch with $\tau_o + \tau$ nonzero and $\nu = 0$

5.3.1 Introduction

Setting $\nu = 0$, (5.1) reduces to

$$R_{TT} = \sigma R - NR(R^2 - R_o^2). \tag{5.104}$$

We recall that $\sigma = \frac{k^2}{K^2}(\tau_o + \tau(T)) + O(\alpha_c)$, and we will consider the case where $\tau(T) = H\cos(\omega T)$. This form of $\tau(T)$ sets up the time dependence of the flow as a periodic oscillation of the current's vertical shear. This is an idealized representation of time dependence which occurs due to phenomena such as seasonal variability and tides (See Pedlosky and Thomson (2003)).

Recalling our earlier discussion in §4.2.1, if the sign of $\tau_o + \tau(T)$ is always positive, we will have a supercriticality, and if it is always negative, we will have a subcriticality; otherwise, we have regions of both sub- and super- criticality. The sign of $\tau_o + \tau = \pm 1 + H\cos(\omega T)$ is strictly dependent on τ_o when $H \leq 1$. That is, for $H \leq 1$, our perturbation is subcritical for $\tau_o = -1$, and supercritical for $\tau_o = 1$. If $H > 1$, $\tau_o + \tau$ goes both positive and negative, switching between sub- and super- critical.

For the nonzero H cases, we have chosen the set $\{0.1, 1, 3\}$. The $H = 0.1$ case gives us very weak time variability. In the $H = 1$ case, our time variability term is of the same order as our time invariant term τ_o. In the $H = 3$ case, our time variability term has a magnitude of 3, which exceeds the magnitude of τ_o, causing both large sub- and super- criticalities. We note that, in the $H = 3$ case, the sign of $\tau_o + \tau$ is still largely determined by the sign of τ_o. This can be seen in Figures 5.5 and 5.6, and is summarized in Table 5.1.

For ω, we consider cases where ω is small, of equal order, or large in relation to the underlying period (with no dissipation or time variability) of R. We denote the underlying period by T_p, and take ω to have the values $\{\pi/(5T_p), 2\pi/T_p, 10\pi/T_p\}$. All solutions are numerical, and are found using the *dsolve* routine in *Maple 8.0*©.

Amplitude of $\tau(T)$	$\tau_o = -1$	$\tau_o = 1$
$H = 0.1$	subcritical	supercritical
$H = 1$	subcritical	supercritical
$H = 3$	both sub- and super- criticalities	both sub- and super- criticalities

Table 5.1: Sub- , or Super-, criticality of τ versus H

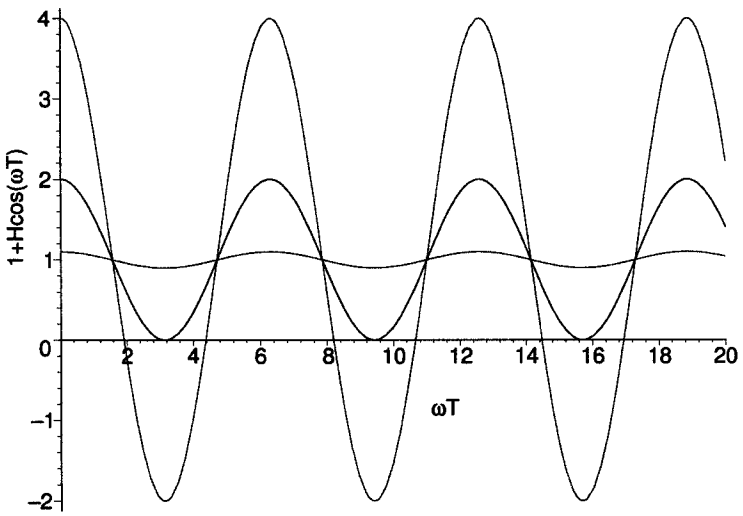

Figure 5.5: $1 + H\cos(\omega T)$ versus ωT for $H \in \{0.1, 1, 3\}$ where greater amplitude corresponds to larger H.

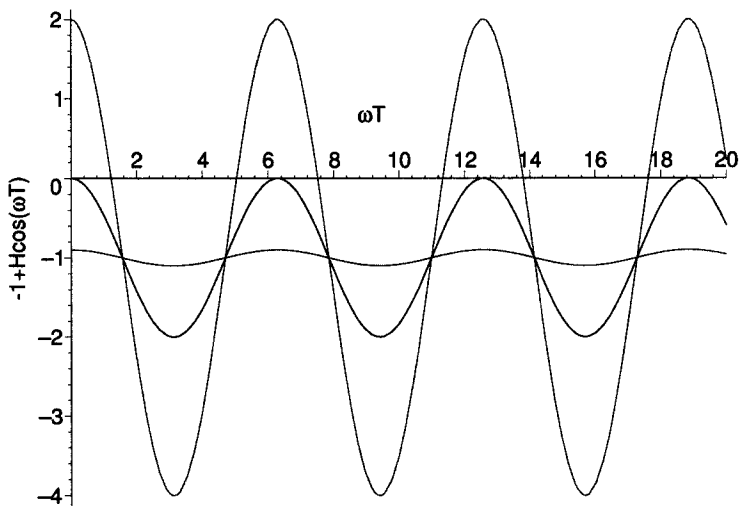

Figure 5.6: $-1 + H\cos(\omega T)$ versus ωT for $H \in \{0.1, 1, 3\}$ where greater amplitude corresponds to larger H.

5.3.2 Stability Properties of the Linear Case

Note that, when $\tau_o = -1$, (5.104) becomes a nonlinear Mathieu equation. Substituting in our chosen form of $\tau(T)$, ignoring terms of $O(\alpha_c)$, and linearizing (by taking $N = 0$), equation (5.104) becomes

$$R_{TT} = \frac{k^2}{K^2}(-1 + H\cos(\omega T))R, \tag{5.105}$$

which is a linear Mathieu equation. This equation has several notable stability properties (as discussed in Bender and Orszag (1978)). Note that if we also have $H = 0$, the solution to (5.105) is simply

$$R(T) = R_o\left[\cos\left(\frac{k\sigma}{K}T\right) + \sin\left(\frac{k\sigma}{K}T\right)\right]. \tag{5.106}$$

Thus, in this case, the solutions simply oscillate in time, which is a result of the neutral stability of the underlying normal mode. However, if instead we take the limit as $H \to 0$, the Mathieu equation has unstable, exponentially growing solutions for the discrete frequency spectrum

$$\omega = \frac{2k\sigma/K}{n}, \text{ for } n \in \mathbb{Z}^+. \tag{5.107}$$

For H further from zero, these discrete values become intervals of finite length, which lengthen as H becomes larger. Thus, for sufficiently large H, almost any value of ω results in instability. This process of destabilization is known as *parametric instability*, and occurs as a result of resonance caused by the interaction of the underlying unforced periodic solution with the periodicity contained in $\tau(T)$.

Thus, we have demonstrated that, in the linear limit, a periodic frontal flow can lead to instability, despite the neutral stability of the time averaged periodic flow.

Region	Subcritical Case: $\tau_o = -1$	Supercritical Case: $\tau_o = 1$
I: $K^2 = 0.1$	3.81	4.24
II: $K^2 = 0.4$	5.49	22.19
III: $K^2 = 1.4$	6.78	9.10

Table 5.2: The Underlying Period

5.3.3 Introducing Subcriticalities and Supercriticalities

We begin by noting the underlying periods, ie. the period where $H = 0$, for our chosen K^2 parameter values, with both a sub- and super- criticality. These can be seen in Table 5.2, and have been calculated using formulas from Milne-Thomson (1950) in conjunction with Maple©. Periods in the case where H is nonzero were calculated using the fast Fourier transform in Matlab©.

In several cases, we will see that the curve is bounded within a *modulational wave packet.* The equation of the modulational curve is called either a *modulating amplitude function* or an *envelope function.* The modulation stems from the addition of slow time variability. Without this modulation, using the chosen parameter values, the curve would continue to grow in magnitude exponentially. Thus, it is the nonlinear terms that stabilize growth in these cases. When the upper and lower curves of the envelope are vertical translations of one another, this is called a *sinuous instability.* When the upper and lower curves of the envelope are mirroring each other, this is called a *varicose instability.*

First, we will compare the effect of introducing sub- and super- criticalities across Regions I through III, for the moderate values $(\omega, H) = (\frac{2\pi}{T_p}, 1)$. These may be seen in Figures 5.7 through 5.9 respectively. In Region I, there is little effect in taking a supercriticality. Both curves are periodic, with the subcritical case having a slightly shorter period of oscillation than the supercritical case, as was the case in the underlying curve. We note that the periods with a moderate ω and H are approximately equal to the underlying periods in this

region in both the sub- and super- critical cases.

In Region II (Figure 5.8), we see that a supercriticality leads to erratic function behaviour, with no distinct periodicity. However, in the case of a subcriticality, the curve remains periodic, but is contained within a modulating wave packet, with the shape of the envelope denoting a varicose instability. The period for the subcritical case is approximately 5.4, with the envelope function having a period of approximately 204.

In Region III (Figure 5.9), for both the sub- and super- critical cases, we see that the peaks and troughs of the function are sharper. Each case exhibits an envelope function. We note a distinct difference between the envelopes. In the supercritical case, the shape of the envelope is sinuous. On the other hand, in the subcritical case, the shape of the envelope is varicose. In the supercritical case, there is a dominant local period of 6.2, and, in the subcritical case, there is a local period of 6.7. The envelope function, however, has a period of approximately 16.7 in the supercritical case, and approximately 33.8 in the subcritical case.

Next, we will examine the case where $H = 3$, which is illustrated in Figure 5.10. As discussed previously, when $H = 3$, the solution exhibits regions of both sub- and super- criticality. Region I displays a varicose envelope function with a period of approximately 180. The local period is approximately 4.3 here. Note, that when looking closely at the curve, it is seen that the amplitude is not strictly increasing or decreasing during the bowing process. Moving on to Regions II and III, we see that the behaviour has become erratic, with no obvious period.

We will now move on to compare the effect of K^2 on the solution where we have chosen a moderate ω of $\frac{2\pi}{T_p}$ and we have a supercriticality. This will be examined for the $H = 0.1$ and $H = 1$ cases, shown in Figures 5.11 and 5.12, respectively. In both of the $H = 0.1$ and $H = 1$ cases, we get a periodic structure in Region I, both having a period of approximately 4.3. In Region II, for $H = 0.1$, we have a periodic function which has a period of approximately 22, and a varicose envelope, having a period of approximately 242. In the

$H = 1$ case, there is erratic behaviour. In Region III, we have erratic behaviour in the $H = 0.1$ case. In the $H = 1$ case, the local period is approximately 6.2, and there is a sinuous envelope with period of approximately 17.

We now fix $K^2 = 1.4$, and $H = 1$, and vary ω. This is seen in Figure 5.13. At $\omega = \frac{2\pi}{T_p}$, there is a local period of 6.2. At the other ω values, we do not see local periodicity. For $\omega = \frac{2\pi}{5T_p}$, there is a sinuous envelope function with an approximate period of 96. At $\omega = \frac{2\pi}{T_p}$, there is a varicose envelope function with an approximate period of 18, and at $\omega = \frac{10\pi}{T_p}$, there is a varicose envelope function with a period of approximately 15, that starts at approximately $T = 32$.

Examining this information on the whole, we now summarize the behaviour of the function $A(T)$. First, we looked at the effect of taking either a sub- or super -criticality in Regions I through III. In Region I, with moderate ω and H values, there was little effect to taking a sub- or super- criticality, and both curves are periodic. In Region II, a supercriticality lead to erratic function behaviour; whereas a subcriticality lead to periodic behaviour, with a varicose envelope function, and fixed local and envelope periods. In Region III, both the sub- and super- critical cases were found to have sharper peaks and troughs. In the subcritical case, there was a varicose envelope function whereas in the supercritical case, there was a sinuous envelope function - both with fixed period.

Next, we looked at the case of large H, where there was both sub- and super- criticality. In Region I, the curve was nearly periodic with a varicose envelope function. Looking closely at its envelope function, we saw that the amplitude was not strictly increasing or decreasing during the bowing process. In regions II and III, the behaviour became erratic, with no obvious period.

We also examined the effect of differing K^2 for the $H = 0.1$ and $H = 1$ cases, where we had chosen a moderate value of ω, and we have a supercriticality. In both cases, in Region I, we obtained a periodic structure. In Region II, with $H = 0.1$, we obtained a periodic structure with a varicose envelope. In Region II, with $H = 1$, we obtained erratic behaviour. In Region III, with

$H = 0.1$, we obtained erratic behaviour; whereas in the $H = 1$ case, the curve was periodic and was contained within a fixed period sinuous envelope.

We examined the effect of differing ω, with fixed K^2, in Region III, and moderate H. For small ω, we observed a sinuous envelope function. For moderate ω, we observed a varicose envelope function and a fixed local period. For large ω, we observed a varicose envelope function with a delayed onset.

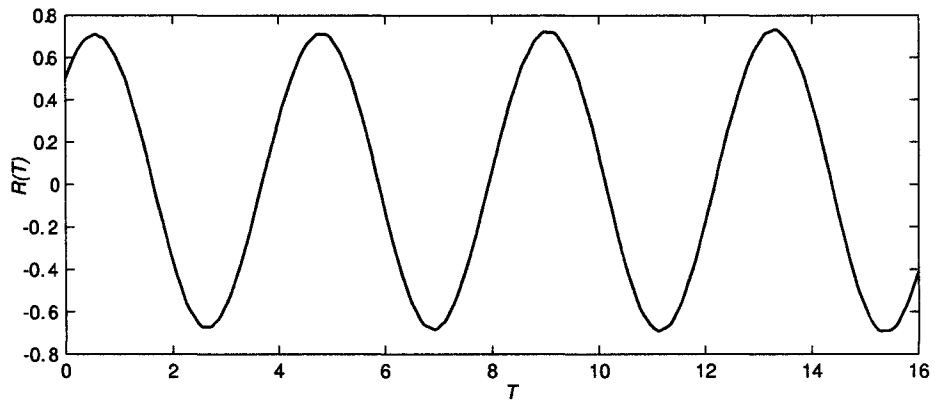

(a) $\tau_o = 1$

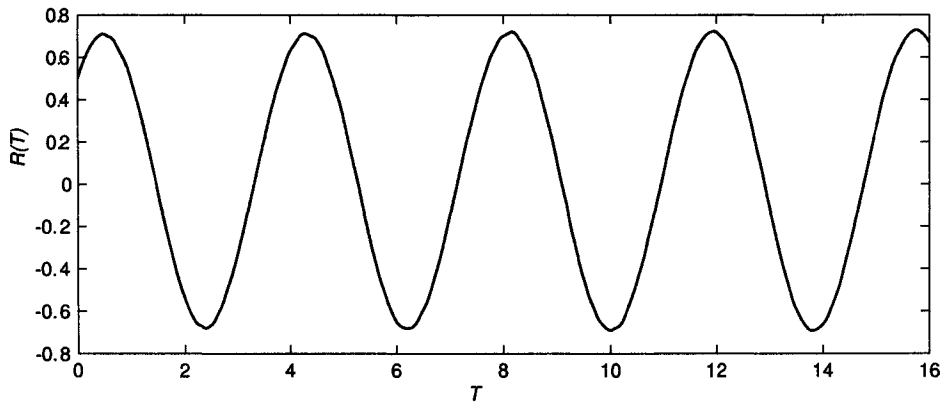

(b) $\tau_o = -1$

Figure 5.7: $R(T)$ versus T on the lower branch with parameters $\tau(T) = \cos(\frac{2\pi T}{T_p})$, $L = 8$, and $K^2 = 0.1$. (a) Here, there is an approximate period of 4.3, and a peak-to-trough amplitude variation of about 1.42. (b) Here, there is an approximate period of 3.8, and a peak-to-trough amplitude variation of 1.42.

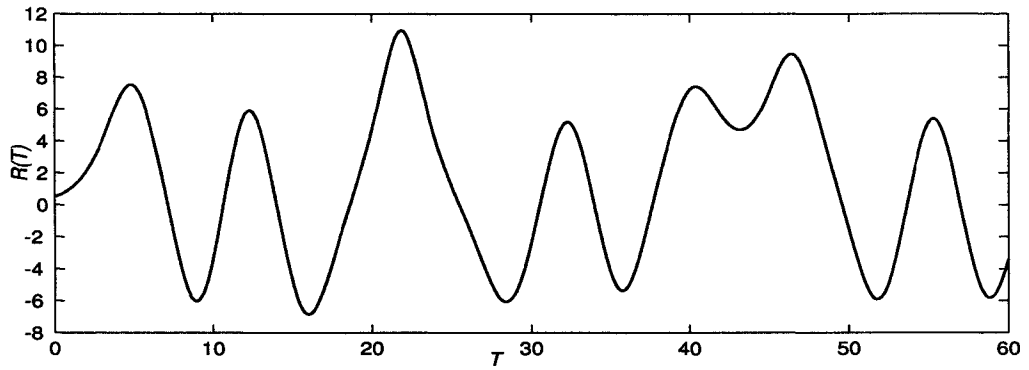

(a) $\tau_o = 1$

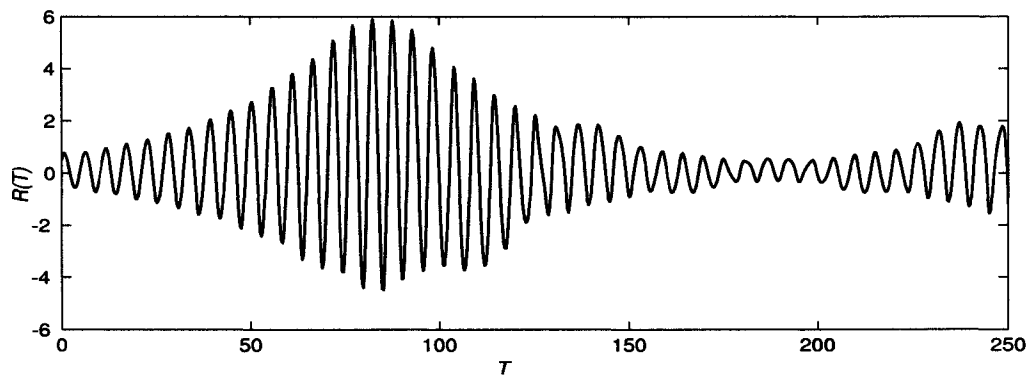

(b) $\tau_o = -1$

Figure 5.8: $R(T)$ versus T on the lower branch with parameters $\tau(T) = \cos(\frac{2\pi T}{T_p})$, $L = 8$, and $K^2 = 0.4$. (a) Here, there is a dominant period of 8.5, and a maximum vertical extent of about 17.8. (b) Here, there is an approximate period of 5.4, and a peak-to-trough amplitude variation of 10.5.

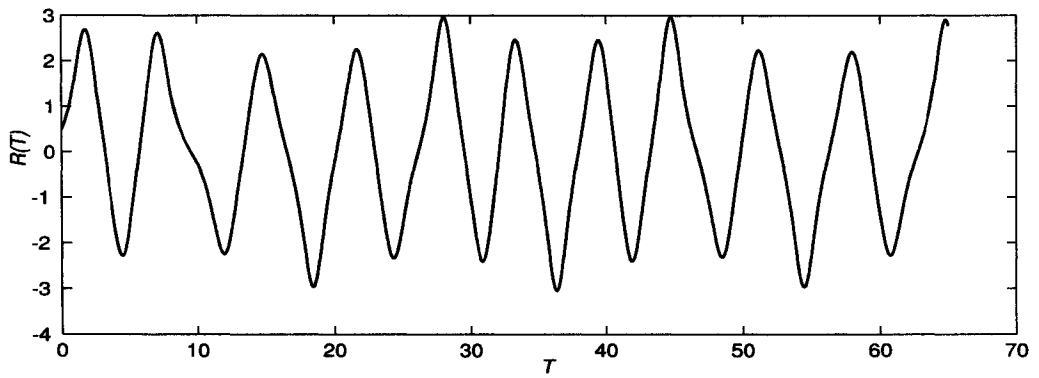

(a) $\tau_o = 1$

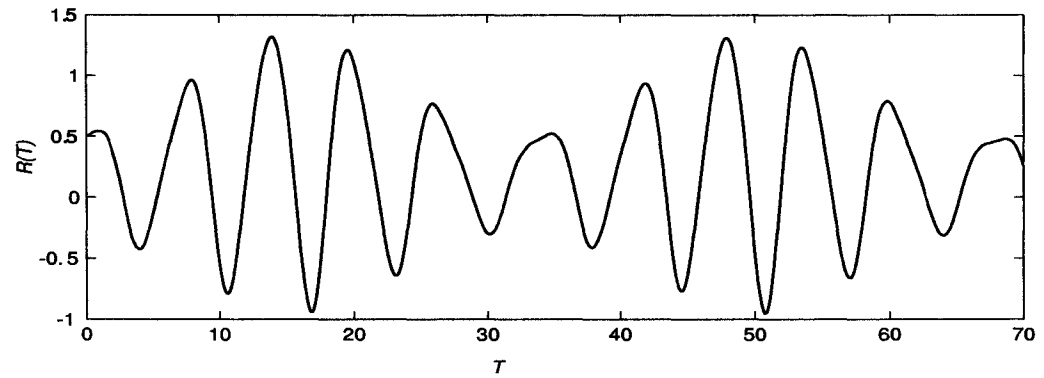

(b) $\tau_o = -1$

Figure 5.9: $R(T)$ versus T on the lower branch with parameters $\tau(T) = \cos(\frac{2\pi T}{T_p})$, $L = 8$, and $K^2 = 1.4$. (a) Here, there is an approximate period of 6.2, and a peak-to-trough amplitude variation of about 6.0. (b) Here, there is an approximate period of 6.7, and a maximum vertical extent of 2.3.

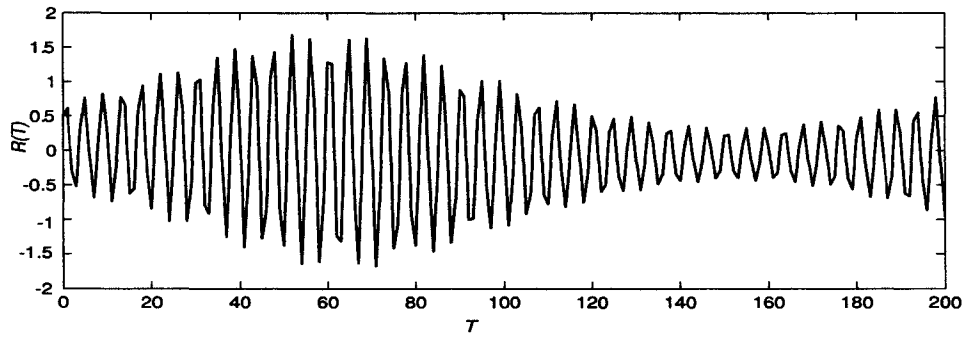

(a) $K^2 = 0.1$

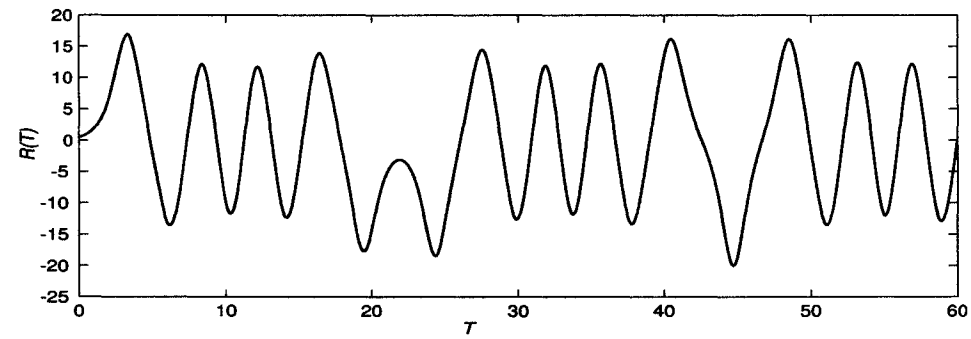

(b) $K^2 = 0.4$

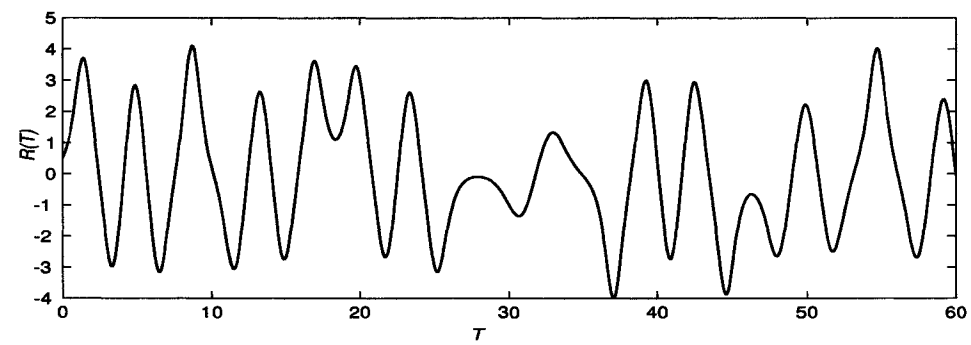

(c) $K^2 = 1.4$

Figure 5.10: $R(T)$ versus T on the lower branch with parameters $\tau(T) = 3\cos(\frac{2\pi T}{T_p})$, $L = 8$, and $\tau_o = 1$, and variable K^2. (a) Here, there is an approximate period of 4.3, and a maximum vertical extent of about 3.4. (b) Here, there is an dominant period of 4.5, and a maximum vertical extent of 36. (c) Here, there is a dominant period of 3.8, and a maximum vertical extent of 8.1.

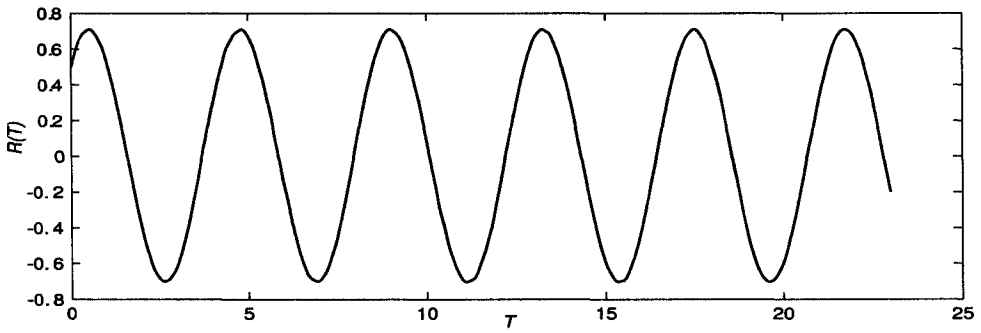

(a) $K^2 = 0.1$

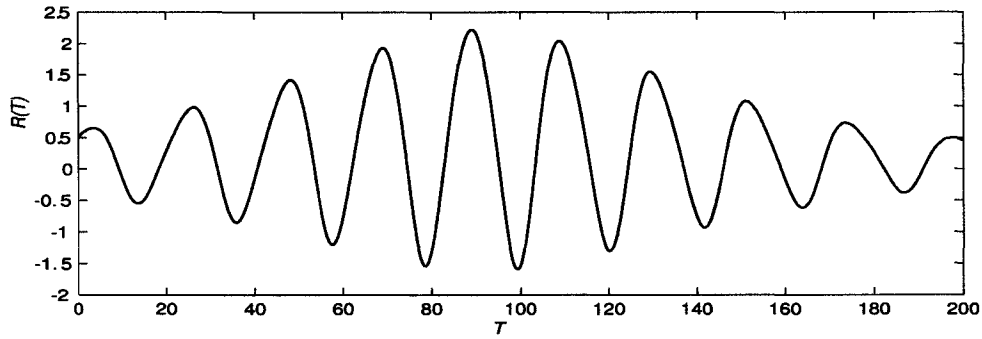

(b) $K^2 = 0.4$

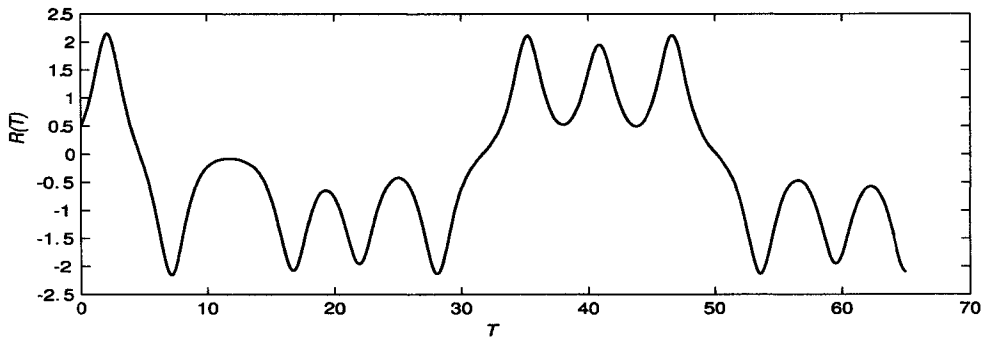

(c) $K^2 = 1.4$

Figure 5.11: $R(T)$ versus T on the lower branch with parameters $\tau(T) = 0.1\cos(\frac{2\pi T}{T_p})$, $\tau_o = 1$, $L = 8$, and variable K^2. (a) Here, there is an approximate period of 4.3, and a peak-to-trough amplitude variation of about 1.4. (b) Here, there is an approximate period of 22, and a maximum vertical extent of 3.8. (c) Here, the function is aperiodic with a maximum vertical extent of 4.3.

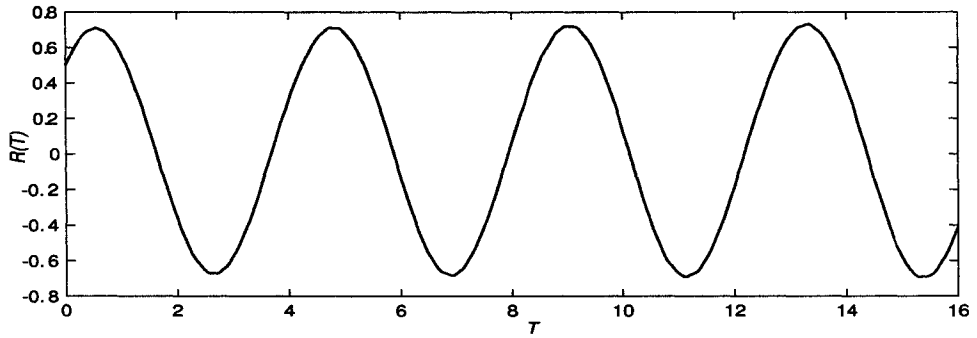

(a) $K^2 = 0.1$

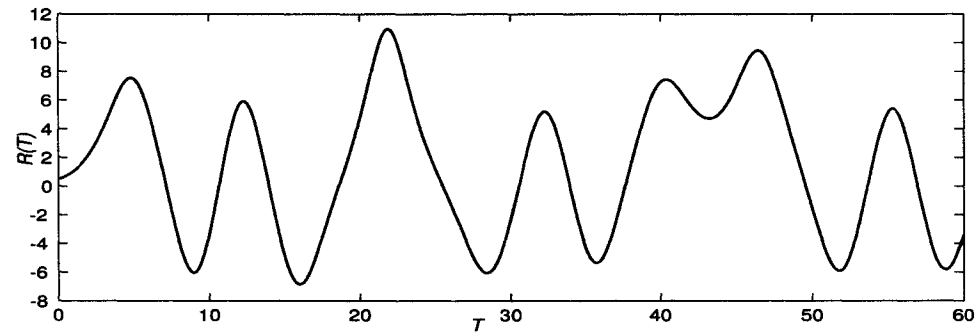

(b) $K^2 = 0.4$

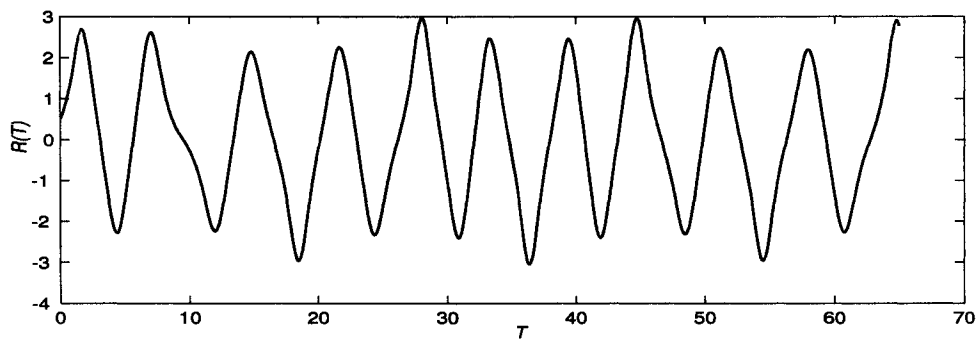

(c) $K^2 = 1.4$

Figure 5.12: $R(T)$ versus T on the lower branch with parameters $\tau(T) = \cos(\frac{2\pi T}{T_p})$, $\tau_o = 1$, $L = 8$, and variable K^2. (a) Here, there is an approximate period of 4.3, and a peak-to-trough amplitude variation of about 1.4. (b) Here, there is a dominant period of 8.5, and a maximum vertical extent of 18. (c) Here, there is an approximate period of 6.2, and a peak-to-trough amplitude variation of 6.0.

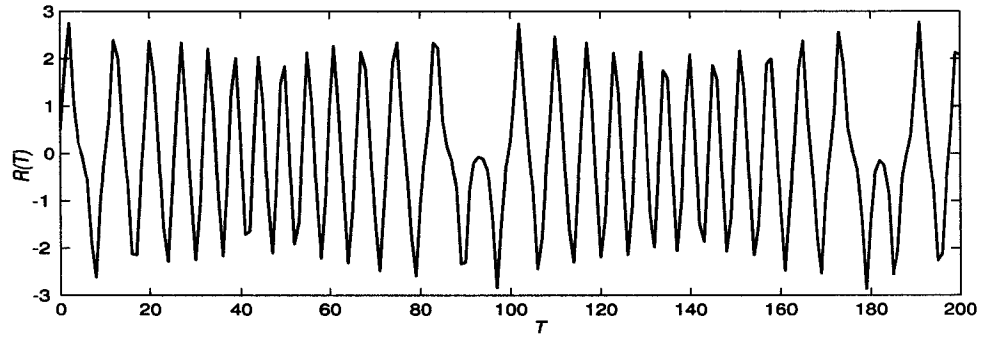

(a) $\omega = 2\pi/(5T_p)$

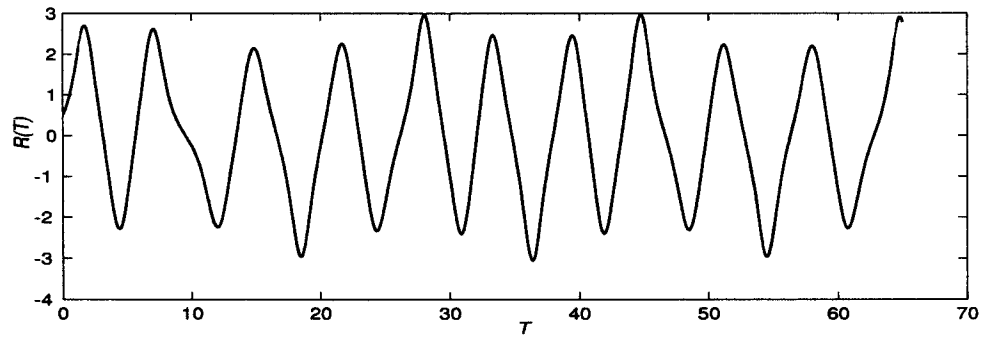

(b) $\omega = 2\pi/T_p$

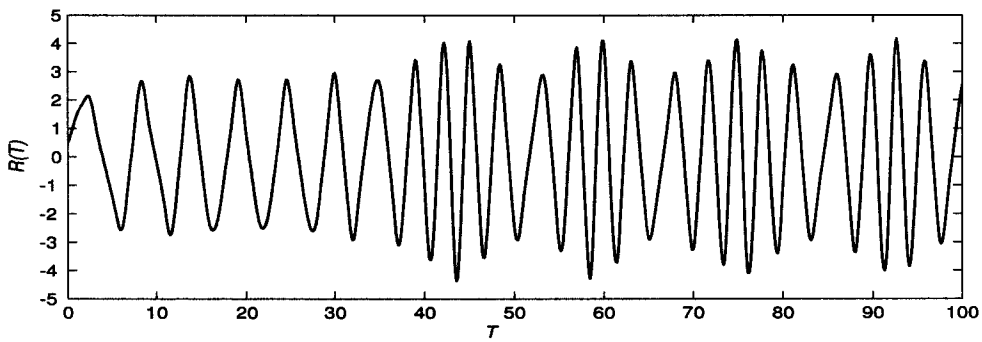

(c) $\omega = 10\pi/T_p$

Figure 5.13: $R(T)$ versus T on the lower branch with parameters $\tau(T) = \cos(\omega T)$, $\tau_o = 1$, $K^2 = 1.4$, $L = 8$, and variable ω. (a) Here, there is a dominant period of 8.1, and a peak-to-trough amplitude variation of about 5.6. (b) Here, there is an approximate period of 6.2, and a peak-to-trough amplitude variation of 6.0. (c) Here, there are dominant periods of 3.6 and 3.0, and a maximum vertical extent of 8.5.

5.4 The Influence of Dissipation

To investigate the influence of dissipation, we will examine the effect of ν on five cases representing a selection of curve shapes. All curves will have the supercritical value $\tau_o = 1$. The first curve in our analysis is the periodic curve arising in Region II, for the case of $\tau(T) = 0$. Figure 5.14 illustrates the results for $\nu = 0$, $\nu = 0.05$, and $\nu = 0.1$. We see that dissipation acts to damp the function to zero smoothly, as expected.

Next, we look at the dnoidal curve in Region III, for the $\tau(T) = 0$ case. This curve has sharp peaks and soft troughs, as shown in Figure 5.15, where we have plotted the curve for the parameters $\nu = 0$, $\nu = 0.1$, $\nu = 0.15$. Moderate dissipation, as shown in 5.15(b), causes $R(T)$ to damp toward 1.0. Enhanced dissipation, as shown in 5.15(c), causes the curve to damp more rapidly to the same value.

We now examine a case in which the original function has both sharp peaks and troughs. In Figure 5.16, we continue with Region III, this time examining the case of nonzero $\tau(T)$, with parameter values $H = 1$ and $\omega = \frac{2\pi}{T_p}$. The dissipation is found to soften these peaks, changing the local period into the period of the envelope function. The amplitude of the curve is also seen to decrease. Upon further increasing of the dissipation, the amplitude continues decreasing, eventually damping to zero.

Next, we look at a case in which $R(T)$ appears to be periodic and is contained within an envelope function. This is seen in Figure 5.17. We see that the curve is damped rapidly upon applying the relatively low dissipation parameter values $\nu = 0.02$ and $\nu = 0.05$.

Our last case is similar to the previous case, except with sharper peaks and troughs, and is shown in Figure 5.18. In 5.18(b) we see that the envelope has been damped. In 5.18(c), using $\nu = 0.15$ (strong damping), we see the function rapidly damps to zero.

We would like to conclude by by making a note about the degree of dissipation required to result significant damping in each solution. For a cnoidal,

or snoidal, curve shape, we found significant damping using $\nu = 0.05$. For the dnoidal curve, a dissipation parameter of $\nu = 0.15$ was required to observe comparable damping. For the curve with sharp peaks and troughs contained within a sinuous envelope, $\nu = 0.07$ was required to observe the same level of damping. For the periodic curve with a varicose envelope, significant damping was found to require a relatively low value of $\nu = 0.05$. Finally, for the function with sharp peaks and troughs contained within a varicose envelope, a relatively high parameter value of $\nu = 0.15$ was needed to yield similar damping.

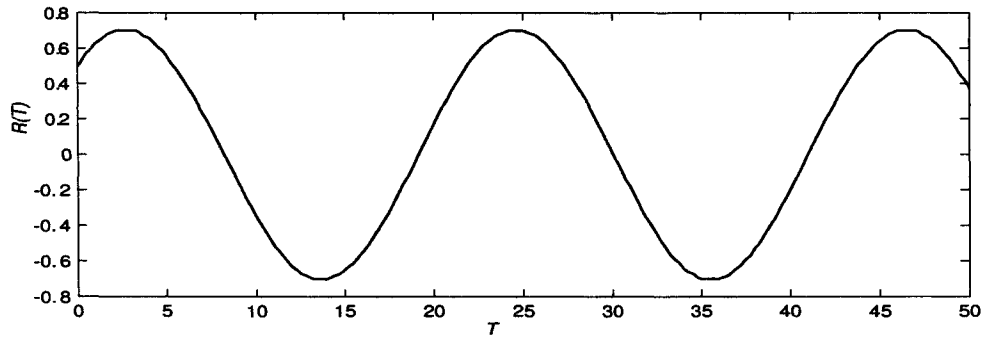

(a) $\nu = 0$

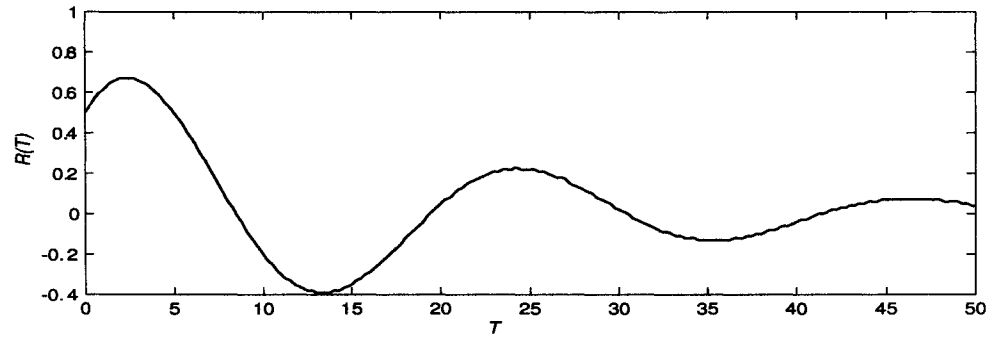

(b) $\nu = 0.05$

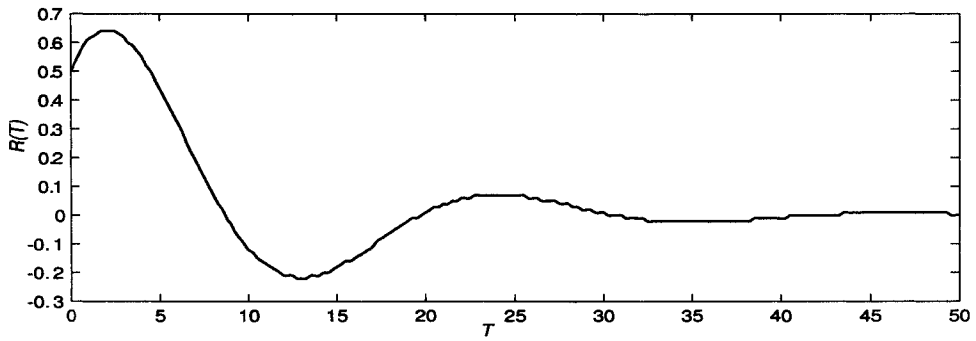

(c) $\nu = 0.1$

Figure 5.14: $R(T)$ versus T on the lower branch with parameters $\tau(T) = 0$, $\tau_o = 1$, $K^2 = 0.4$, $L = 8$, and variable ν. (a) Here there is a period of 22. (b) Here there is a period of approximately 22, and an approximate e-folding time of 19.6. (c) Here there is an approximate period of 23, and an approximate e-folding time of 9.9.

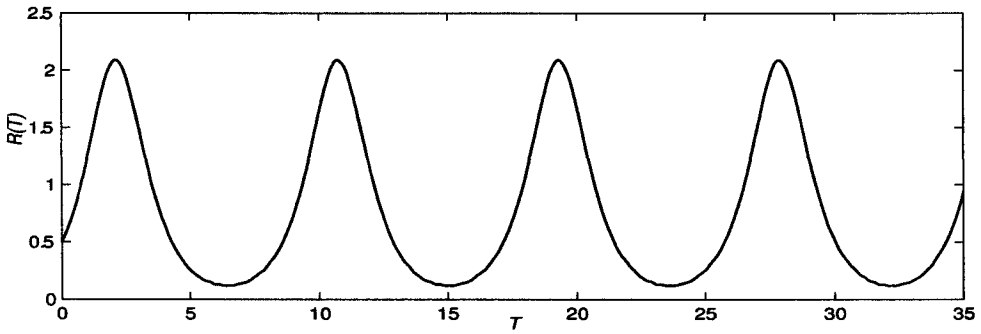

(a) $\nu = 0$

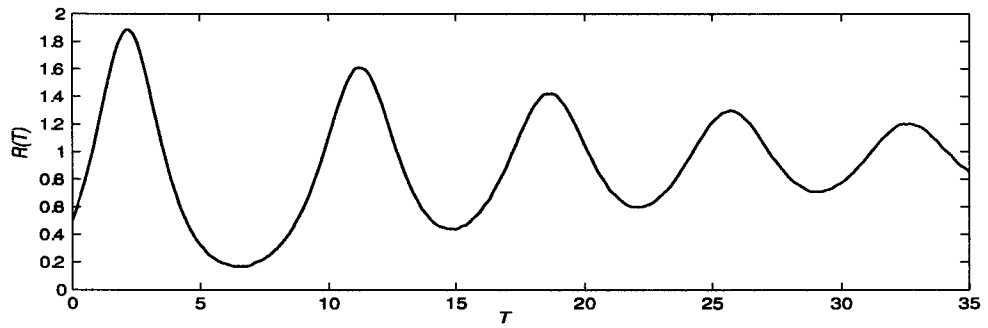

(b) $\nu = 0.1$

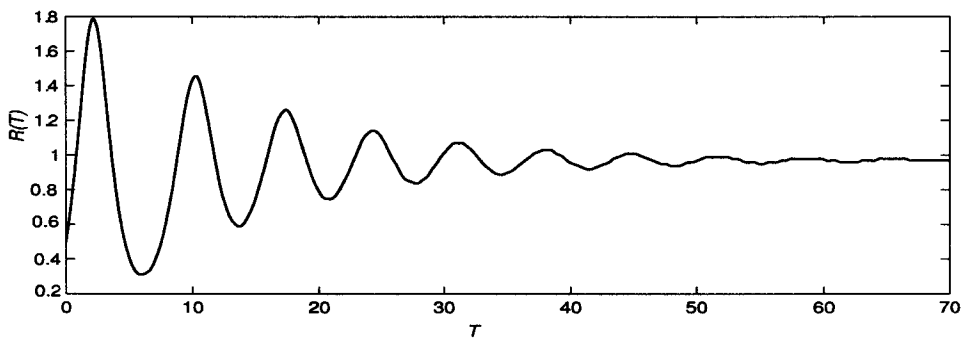

(c) $\nu = 0.15$

Figure 5.15: $R(T)$ versus T on the lower branch with parameters $\tau(T) = 0$, $\tau_o = 1$, $K^2 = 1.4$, $L = 8$, and variable ν. (a) Here there is a period of 9.1. (b) Here there is an approximate period of 7.8, and an approximate e-folding time of 55.6. (c) Here there is an approximate period of 7.7, and an approximate e-folding time of 47.6.

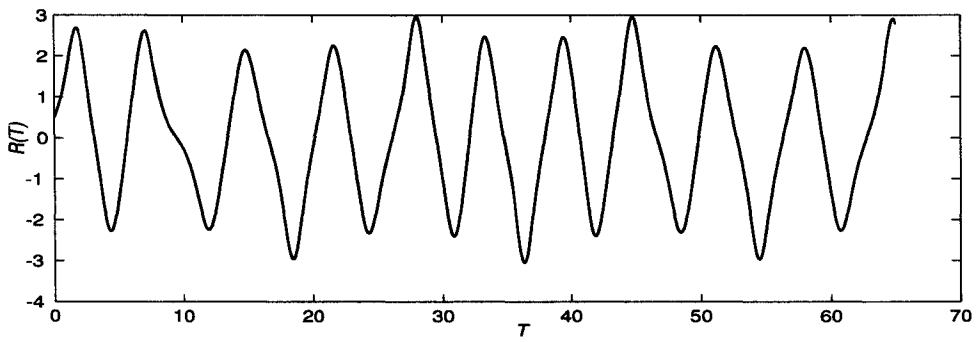

(a) $\nu = 0$

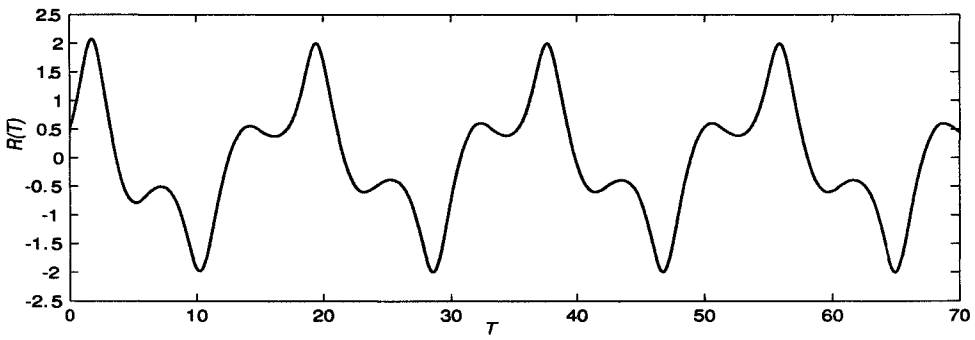

(b) $\nu = 0.3$

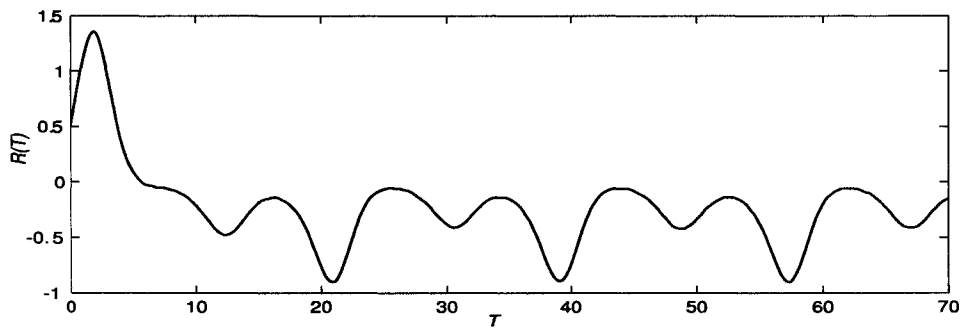

(c) $\nu = 0.7$

Figure 5.16: $R(T)$ versus T on the lower branch with parameters $\tau(T) = \cos(\frac{2\pi T}{T_p})$, $\tau_o = 1$, $L = 8$, $K^2 = 1.4$, and variable ν. (a) Here there is an approximate period of 6.2. (b) Here there is an approximate period of 18. (b) Here the function is aperiodic.

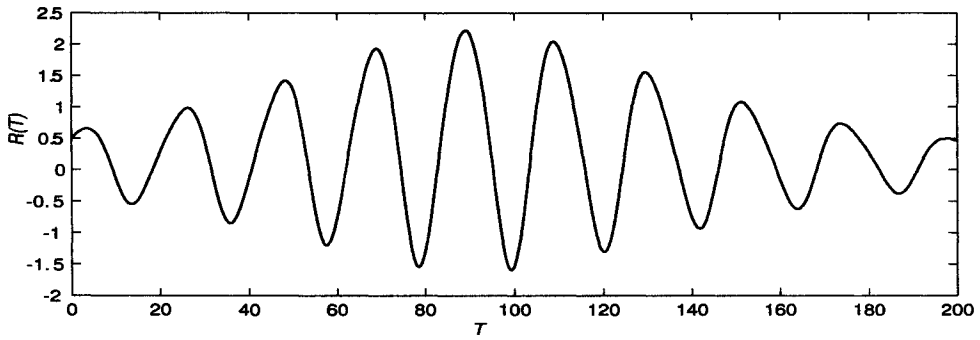

(a) $\nu = 0$

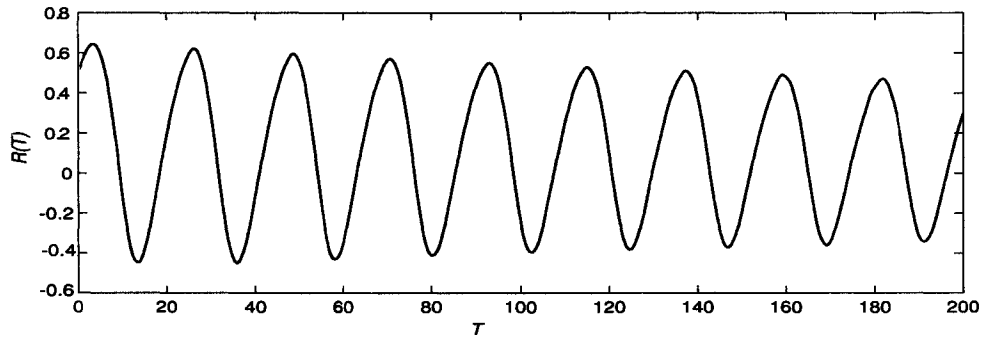

(b) $\nu = 0.02$

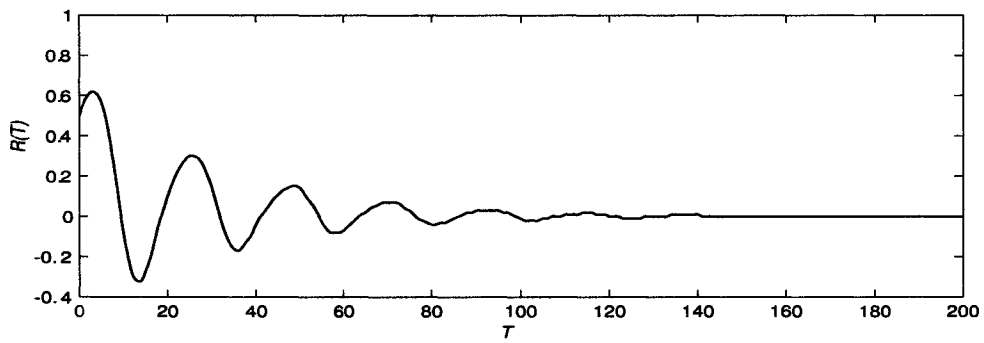

(c) $\nu = 0.05$

Figure 5.17: $R(T)$ versus T on the lower branch with parameters $\tau(T) = 0.1\cos(\frac{2\pi T}{T_p})$, $\tau_o = 1$, $L = 8$, $K^2 = 0.4$, and variable ν. (a) Here, there is an approximate period of 22. (b) Here, there is an approximate period of 22, and an approximate e-folding time of 635. (c) Here, there is an approximate period of 22, and an approximate e-folding time of 11.0.

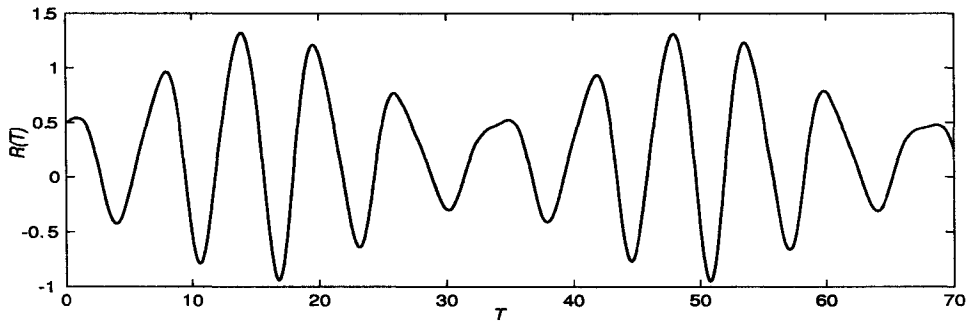

(a) $\nu = 0$

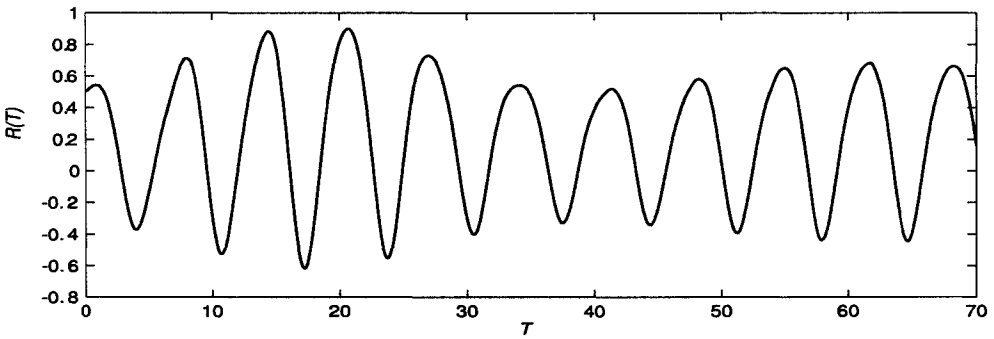

(b) $\nu = 0.05$

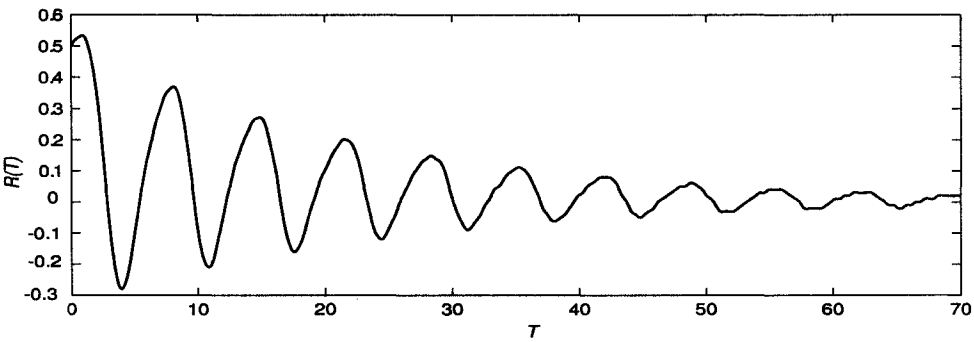

(c) $\nu = 0.15$

Figure 5.18: $R(T)$ versus T on the lower branch with parameters $\tau(T) = \cos(\frac{2\pi T}{T_p})$, $\tau_o = -1$, $L = 8$, $K^2 = 1.4$, and variable ν. (a) Here there is an approximate period of 6.7. (b) Here there is an approximate period of 6.8. (c) Here there is an approximate period of 6.8, and an approximate e-folding time of 19.6.

Chapter 6

Summary and Conclusions

A weakly nonlinear theory for a marginally stable or unstable, time varying frontal geostrophic current on sloping topography with dissipation has been established. We extended the research of Reszka (1997) and Reszka and Swaters (1999) by the inclusion of time variability and dissipation terms, using the methods described in Pedlosky and Thomson (2003). The governing equations were first derived in Swaters (1993), who developed a model to describe the baroclinic dynamics of large amplitude geostrophic (LAG) surface currents and fronts over a sloping continental shelf. The model used in this thesis was a two-layer system of LAG surface currents over a sloping bottom.

We began by deriving the governing equations for a two layer shallow water system. The fluid was taken to be incompressible and inviscid, and we worked in a rotating reference frame. A scale analysis was performed, which allowed us to apply the hydrostatic relation, and remedy the problem of geostrophic degeneracy. Upon simplifying the resulting equations in the one layer case, we expanded our system to two layers, each having a different density. This provided us with mass conservation and continuity equations for each layer, as well as a reduced gravity equation, which related the pressures between both layers.

Next, we nondimensionalized our equations using the scalings of Swaters (1993). After asymptotically expanding our variables about some small para-

meter, we matched terms having the same magnitude, which gave us a series of equations. After performing some algebraic manipulations, we arrived at the governing equations of the Swaters (1993) model. We then repeated the calculation starting with the equations of conservation for potential vorticity in each layer and obtained the same result.

Following this, we derived the linear stability equations by writing the height and pressure variables as a mean part plus a perturbation part. We then set the mean flow in the lower layer to be zero in order to prevent barotropic shear instabilities in the lower layer, which enabled us to focus on the pure baroclinic problem. Also, we assumed the steady solution for the upper layer thickness to be of the form of a simple wedge. We then obtained stability conditions by examining the averaged-energy form of the linearized upper layer equation, following the derivation from Swaters (1993). This allowed us to find a necessary condition for perturbation growth, and a sufficient condition to inhibit that growth.

Next, we performed a normal mode analysis by first assuming the perturbation field to be a superposition of waves. To determine when instability occurs, we noted that perturbations grow in time if the imaginary part of the phase velocity is positive. We substituted our normal mode equations into the linear stability equations and performed an order analysis. This lead us to a pair of coupled ordinary differential equations for our perturbation functions. After subsequent calculations, we arrived at a dispersion relation. We then established a sufficient condition for stability, and therefore, a necessary condition for instability.

We then determined equations for the marginal stability curves. We noted that there were two curves in our case, which we called the Upper and Lower Branches of the Marginal Stability Curve. Having these two marginal stability curves resulted in a unique critical slope and phase velocity value for each of the Upper and Lower Branches. We also determined a high frequency cutoff, which is a cutoff of the total wavenumber above which the flow is always stable.

We studied the evolution of a wedge front which was weakly unstable, ie.

the nonlinear terms were small but nonnegligible. By assuming that the perturbations were initially small, and expanding our equations asymptotically, we were able to derive an amplitude equation describing the slow time evolution of the perturbation amplitude. In deriving our amplitude equation, we followed Pedlosky (1987).

First, we began by introducing dissipation terms, which were chosen to be proportional to the perturbation potential vorticity. We next assumed a wedge front and scaled our variables by the wedge slope parameter. We then introduced a perturbation into the critical slope parameter. Depending on the sign of this perturbation term, we had either a sub- or a super- criticality. In the region of supercriticality, we perturbed the critical slope parameter from the marginal stability curve into the unstable region, giving us marginally unstable solutions, while, in the region of subcriticality, we perturbed into the stable region, giving us marginally stable solutions. In the case where the sign of the perturbation term was both positive and negative, we had regions of super- and sub- criticality.

Modifying the analysis performed by Reszka (1997), we introduced a time variability parameter into the critical slope perturbation. We then rederived the dispersion relation with our new slope parameter. A scale analysis on the complex part of the slope parameter gave us the order of the growth rate. We introduced slow time and large space parameters, and expanded our perturbation functions in asymptotic series. We then derived the the $O(1)$, $O(s)$, and $O(s^2)$ equations from this expansion. Solving these equations by the use of a weakly nonlinear analysis lead us to our amplitude equation, which was a coupled set of ordinary differential equations.

Then, we derived the Lorenz equivalent of our amplitude equation in the case where there is no time variability in the perturbations, with a real-valued perturbation amplitude. This allowed us to show that the observation of nontrivial time dependence in our later solutions was due to the presence of the time-varying component of the perturbations.

Next, we dropped the slow space term. After first deriving the Reszka

(1997) solution, we obtained solutions on the Lower Branch with the addition of time variability, while keeping dissipation zero. We divided our analysis into four regions of parameter space, depending upon the sign of the growth rate and the sign of the nonlinear term, and denoted these Regions I through IV. Region IV was found to have exponentially growing solutions, and thus we restricted further analysis to the first three regions. We restricted our analysis to the Lower Branch, since, on the Upper Branch, the solutions are analogous. We then examined the behaviour of our amplitude function with a sub- or super- criticality, and time variability, by investigating plots of their numerical solutions.

First, we observed the effect of taking either a sub- or super -criticality in Regions I through III. In Region I, with moderate frequency and moderate time variability, there was little effect to taking a sub- or super- criticality, and both curves were periodic. In Region II, a supercriticality lead to erratic function behaviour, whereas a subcriticality lead to a periodic curve contained within a varicose envelope function having fixed local and envelope periods. In Region III, both the sub- and super- critical cases were found to have sharper peaks and troughs when compared to the case with no perturbation in the slope parameter. In the subcritical case, the perturbation amplitude had a varicose envelope function, whereas in the supercritical case, it had a sinuous envelope function, both with fixed period.

We next looked at the case of large time variability with both sub- and super- criticalities. In Region I, the curve was nearly periodic, having a varicose envelope function. Looking closely at this envelope function, we saw that the amplitude was neither strictly increasing or decreasing during the bowing process. In Regions II and III, the behaviour became erratic, with no obvious period.

We also examined the effect of varying the total wavenumber for the small and moderate time variability cases, where we chose a moderate frequency, and we had a supercriticality. In both cases, in Region I, we obtained a periodic structure. In Region II, with small time variability, we obtained

a periodic structure with a varicose envelope. In Region II, with moderate time variability, we obtained erratic behaviour. In Region III, with small time variability, we obtained erratic behaviour; whereas in the moderate time variability case, the solution was locally periodic, and was contained within a fixed period sinuous envelope.

Furthermore, in Region III, we studied the effect of varying frequency, with fixed total wavenumber and moderate time variability. For low frequency, we observed a sinuous envelope function. For moderate frequency, we observed a varicose envelope function with a fixed period. For large frequency, we observed a varicose envelope function with delayed start time.

Next, we chose five cases to explore with dissipation added, representing a selection of curve shapes, and examined plots at various dissipation levels to determine the magnitude of dissipation required for each curve shape to exhibit significant damping. For a cnoidal, or snoidal, curve shape, we found significant damping at a low dissipation level. For the dnoidal curve, a very high dissipation parameter was required to observe significant damping. For the curve with sharp peaks and troughs, and a sinuous envelope, a moderate dissipation parameter was required. For the locally periodic curve with a varicose envelope, significant damping was found to require a relatively low dissipation parameter. Finally, for the function with sharp peaks and troughs, and a varicose envelope, a relatively high dissipation parameter was needed.

The main weakness of the calculation completed in this thesis was the neglecting of the slow space term. A possible future research direction could involve leaving this term in, and performing a soliton calculation to derive an analytical solution to the full amplitude equation.

Bibliography

Bender, C. M., and S. A. Orszag, 1978: *Advanced Mathematical Methods for Scientists and Engineers.* McGraw-Hill, 593 pp.

Benilov, E. S., 1992: A note on the stability of one-layer geostrophic fronts. *Geophys. Astrophys. Fluid Dynam.* **66**, 81–86.

Benilov, E. S., 1995: On the stability of large-amplitude geostrophic flows in a two-layer fluid: the case of 'strong' beta-effect. *J. Fluid Mech.* **284**, 137–158.

Benilov, E. S., and B. Cushman-Roisin, 1994: On the stability of two-layered large-amplitude geostrophic flows with thin upper layer. *Geophys. Astrophys. Fluid Dynam.* **76**, 29–41.

Benilov, E. S., and G. M. Reznik, 1996: The complete classification of large-amplitude geostrophic flows in a two layer fluid. *Geophys. Astrophys. Fluid Dynam.* **82**, 1–22.

Chelton, D. B., and M. G. Schlax, 1996: Global observations on oceanic Rossby waves. *Science* **272**, 234–238.

Cushman-Roisin, B., 1986: Frontal geostrophic dynamics. *J. Phys. Oceanogr.* **16**, 132–143.

Gill, A. E., 1982: *Atmosphere-ocean dynamics.* Academic Press, 662 pp.

Griffiths, R. W., P. D. Killworth, and M. E. Stern, 1982: Ageostrophic instability of ocean currents. *J. Fluid Mech.* **117**, 343–377.

Griffiths, R. W., and P. F. Linden, 1981: The stability of buoyancy driven coastal currents. *Dyn. Atmos. and Oceans* **5**, 281–306.

Ha, S., and G. E. Swaters, 2006: Finite amplitude baroclinic instability of time-varying abyssal currents. *J. Phys. Oceanogr.* **36**, 122–139.

Haberman, R., 1998: *Elementary Applied Partial Differential Equations.* 3rd edition. Prentice-Hall, Inc., 736 pp.

Ikeda, M., and W. J. Emery, 1984: Satellite observations and modeling of meanders in the California current system off Oregan and Northern California. *J. Phys. Oceangr.* **14**, 1434–1450.

Ikeda, M., W. J. Emery, and L. A. Mysak, 1984: Seasonal variability in meanders of the California current system off Vancouver Island. *J. Geophys. Res.* **89**, 3487–3505.

Karsten, R., and G. E. Swaters, 2000: Nonlinear effects in two-layer large-amplitude geostrophic dynamics. part 1. the strong beta case. *J. Fluid Mech.* **412**, 125–160.

Killworth, P. D., 1983: Long wave instability of an isolated front. *Geophys. Astrophys. Fluid Dynam.* **25**, 235–258.

Killworth, P. D., N. Paldor, and M. E. Stern, 1984: Wave propagation and growth on a surface front in a two-layer geostrophic current. *J. Mar. Res.* **42**, 761–785.

Klein, P., and J. Pedlosky, 1992: The role of dissipation mechanics in the nonlinear dynamics of unstable baroclinic waves. *J. Atmos. Sci.* **49**, 29–48.

Milne-Thomson, L. M., 1950: *Jacobian Elliptic Function Tables.* Dover Publications, 123 pp.

Olson, D. B., R. W. Schmitt, M. Kennelly, and T. M. Joyce, 1985: A two layer diagnostic model of the long-term physical evolution of warm core ring 82b. *J. Geophys. Res* **90**, 8813–8822.

Paldor, N., 1983a: Linear stability and stable modes of geostrophic fronts. *Geophys. Astrophys. Fluid Dynam.* **24**, 299–326.

Paldor, N., 1983b: Stability and stable modes of coastal fronts. *Geophys. Astrophys. Fluid Dynam.* **27**, 217–228.

Paldor, N., and M. Ghil, 1990: Finite-wavelength instabilities of a coupled density front. *J. Phys. Oceanogr.* **20**, 114–123.

Paldor, N., and P. D. Killworth, 1987: Instabilities of a two-layer coupled front. *Deep Sea Res.* **34**, 1525–1539.

Pedlosky, J., 1987: *Geophysical Fluid Dynamics.* 2nd edition. Springer-Verlag, 710 pp.

Pedlosky, J., and J. Thomson, 2003: Baroclinic instability of time-dependent currents. *J. Fluid Mech.* **490**, 189–215.

Phillips, N., 1963: Geostrophic motion. *Rev. Geophys.* **1**, 123–176.

Pond, S., and G. L. Pickard, 1983: *Introductory Dynamical Oceanography.* 2nd edition. Pergamon Press, 329 pp.

Reszka, M. K., 1997: *Finite amplitude waves and eddy development on a baroclinically unstable front over a sloping bottom.* Master's thesis, University of Alberta.

Reszka, M. K., and G. E. Swaters, 1999: Eddy formation and interaction in a baroclinic frontal geostrophic model. *J. Phys. Oceanogr.* **29**, 3025–3042.

Rhines, P. B., 1975: Waves and turbulence on a beta-plane. *J. Fluid Mech.* **69**, 417–443.

Robinson, A. R. (editor), 1983: *Eddies in marine science.* Springer.

Roden, G. I., 1975: On North Pacific temperature, salinity, sound velocity and density fronts and their relation to the wind energy flux fields. *J. Phys. Oceanogr.* **5**, 557–571.

Slomp, C. G., and G. E. Swaters, 1997: Finite-amplitude perturbations and modulational instability of a stable geostrophic front. *Geophys. Astrophys. Fluid Dynamics* **86**, 149–172.

Swaters, G. E., 1993: On the baroclinic dynamics, hamiltonian formulation and general stability characteristics of density-driven surface currents and fronts over a sloping continental shelf. *Phil. Trans. R. Soc. Lond.* ***A*** **345**, 295–325.

Appendix A

Symbols

A.0.1 Symbols Introduced in Chapter 2

Dimensional Parameter or Constant	Description
$f = f_o$	Coriolis parameter
g	Gravitational constant
L	Channel width
ρ_1	Lower layer fluid density
ρ_2	Upper layer fluid density
H	Scale for total fluid depth
s^*	Magnitude of bottom slope
$g' = g(\rho_2 - \rho_1)/\rho_2$	Reduced gravity
$\bar{h}$	Scale for upper layer thickness
$R = \sqrt{g'\bar{h}}/f_o$	Rossby radius of deformation
$L = \delta^{-1/4}R$	Horizontal length scale (where seen in scaled variables)
Nondimensional Parameter	**Description**
$\delta = \bar{h}/H$	Scaled thickness parameter
$s = s^*L/\bar{h}$	Scaled bottom slope parameter

Dimensional Variable	Description
x^*	Along channel coordinate
y^*	Across channel coordinate
z^*	Vertical coordinate
t^*	Time
$\mathbf{u}^*(x^*, y^*, z^*, t^*) = (u^*, v^*, w^*)$	Dimensional fluid velocity
$\eta^*(x^*, y^*, t^*)$	Deformation of fluid surface
$h^*(x^*, y^*, t^*)$	Upper layer thickness
$p_1^* = \rho_1 g(H + \eta^* - z^*)$	Upper layer fluid pressure
$p_2^* = \rho_1 g(h^* + \eta^*) + \rho_2 g(H - h^* - z^*)$	Lower layer fluid pressure
$\tilde{p}_2^* = \rho_1 g\eta^* - \rho_2 g' h^*$	Total fluid pressure
Nondimensional Variable	**Description**
$x = x^*/L$	Along channel coordinate
$y = y^*/L$	Across channel coordinate
$t = t^* f_o \delta$	Time
$h = h^*/\bar{h}$	Upper layer thickness
$\mathbf{u}_1 = \mathbf{u}_1^*/(\delta^{1/2} L f_o)$	Layer 1 fluid velocity
$\mathbf{u}_2 = \mathbf{u}_2^*/(\delta L f_o)$	Layer 2 fluid velocity
$p = \tilde{p}_2^*/[\delta(f_o L)^2 \rho_2]$	Total fluid pressure
$\eta = \eta^* g/[\delta^{1/2}(f_o L)^2]$	Deformation of fluid surface
$h = h^*/\bar{h}$	Upper layer thickness

A.0.2 Symbols Introduced in Chapters 3 through 5

Here, all variables are nondimensional. Note that the upper layer thickness and pressure variables are now leading order variables.

Parameter	Description
k	Along-channel wavenumber
$l = n\pi/L$	Cross-channel wavenumber
$K^2 = k^2 + l^2$	Total wavenumber
$\mu = \pm 1$	Positive denotes we are on the upper MSC, negative denotes we are on the lower MSC
$c = [1 - \mu K^2]/[K^2(2 - \mu K^2)]$	Phase velocity
$\alpha_c = \mu/[K^2(2 - \mu K^2)]$	Critical slope
$\tau_o = \pm 1$	Steady part of interfacial slope perturbation
ν	Dissipation parameter
H	Magnitude of time variability
ω	Frequency of time variability
T_p	Period without time variability
Variable	**Description**
$h_o = 1 + \alpha(y - L/2)$	Steady solution for upper layer thickness
h	Upper layer thickness perturbation
p	Pressure perturbation
$T = st$	Slow time
$X = s^2 x$	Large space
$\alpha = \alpha_c + \mu(\tau_o + \tau(T))s^2$	Slope of the interface between layers
$A(X,T)$	Perturbation amplitude
$R(T)$	Real-valued perturbation amplitude
$\tau(T) = H\cos(\omega T)$	Time variability term